

Universidade de Brasília
Faculdade de Medicina
Programa de Pós-graduação em
Patologia Molecular

TESE DE DOUTORADO

**CARACTERIZAÇÃO DA PROTEÍNA
FUNGOGLOBINA E FOSFOPROTEOMA
DURANTE O ESTRESSE HIPÓXICO
EM *PARACOCCIDIOIDES* spp.**



Candidato: Lucas Nojosa Oliveira
Orientadora: Dra. Célia Maria de Almeida Soares

Brasília, DF
2018



UNIVERSIDADE DE BRASÍLIA
FACULDADE DE MEDICINA
PROGRAMA DE PÓS-GRADUAÇÃO EM PATOLOGIA MOLECULAR

Tese de Doutorado

Caracterização da proteína fungoglobina e fosfoproteoma durante o estresse hipóxico em *Paracoccidioides* spp.

Candidato: Lucas Nojosa Oliveira
Orientadora: Prof^a. Dr^a. Célia Maria de Almeida Soares

Brasília, DF
Dezembro de 2018



UNIVERSIDADE DE BRASÍLIA
FACULDADE DE MEDICINA
PROGRAMA DE PÓS-GRADUAÇÃO EM PATOLOGIA MOLECULAR

Tese de Doutorado

Caracterização da proteína fungoglobina e fosfoproteoma durante o estresse hipóxico em *Paracoccidioides* spp.

Tese de Doutorado apresentada ao Programa de Pós-Graduação em Patologia Molecular da Universidade de Brasília para obtenção do Título de Doutor.

Candidato: Lucas Nojosa Oliveira
Orientadora: Dra. Célia Maria de Almeida Soares

Brasília, DF
Dezembro de 2018

Programa de Pós-Graduação em Patologia Molecular da Universidade de Brasília

BANCA EXAMINADORA DA TESE DE DOUTORADO

Candidato: Lucas Nojosa Oliveira

Orientadora: Doutora Célia Maria de Almeida Soares

Membros:

Presidente: Profa. Dra. Célia Maria de Almeida Soares.

Instituto de Ciências Biológicas, Universidade Federal de Goiás.

Membro 1: Prof. Dr. Carlos André Ornelas Ricart.

Instituto de Biologia, Universidade de Brasília.

Membro 2: Profa. Dra. Maristela Pereira.

Instituto de Ciências Biológicas, Universidade Federal de Goiás.

Membro 3: Profa. Dra. Mirelle Garcia Silva Bailão.

Instituto de Ciências Biológicas, Universidade Federal de Goiás.

Membro Suplente: Profa. Dra. Patrícia de Sousa Lima,

Laboratório Interdisciplinar de Biologia, Universidade Estadual de Goiás.

Data: 19 de dezembro de 2018.

*Dedico este trabalho às pessoas mais importantes da minha vida!
Ao meu pai Divino e a minha mãe Eliane, que nunca mediram esforços para minha
formação humana, moral, cristã e intelectual. Vocês são o meu exemplo!
Às minhas irmãs Sarah e Milena que sempre tiveram do meu lado. Obrigado pelo
convívio, pelo carinho, pelo cuidado.
Às minhas sobrinhas Fernanda e Geovana que amo infinito.
A todos familiares e amigos que sempre me apoiaram.
Tudo que sou, sou grato a vocês! Meu amor por vocês é imenso. Agradeço a Deus todos
os dias por ter vocês como família. Amo muito!*

AGRADECIMENTOS

À Deus que me concede a oportunidade de viver a cada dia! Sempre tem me abençoado e me concedido conquistas. Te agradeço pelas alegrias e por guiar meus caminhos. Obrigado pelas pessoas que sempre colocou no meu caminho, e que contribuem para meu crescimento. Obrigado!

À Profa. Dra. Célia Soares pela oportunidade concedida para ser minha orientadora. Admiro sua sabedoria e competência, na criação e coordenação de um grupo de pesquisa forte que produz conhecimento de excelência. Agradeço muito a você por contribuir em meu crescimento e proporcionar essa conquista. Muito obrigado!

Aos meus pais Divino e Eliane que sempre priorizou minha educação, às minhas irmãs Milena e Sarah pela companhia a todo momento, às minhas sobrinhas pelo sorrisos e amor dispensado a aos meus cunhados pelo apoio. Muito obrigado!

Aos professores que também compõe o grupo LBM sempre dispostos a auxiliar: Dra. Maristela Pereira, Dra. Mirelle Garcia, Dr. Clayton Borges, Dr. Alexandre Bailão, Dr. Silva Salem-Izacc e Dr. Juliana Parente. Obrigado!

Às amigas “UnB Together” Dani, Ju e Marielle pela companhia, amizade e contribuição para o trabalho. Vocês são muito especiais e desejo-lhe sucesso em tudo na vida. Obrigado!

Aos fiéis escudeiros Igor, Guilherme Petito, Santiago, Kleber, Raísa, Lívia, Amanda, Amanda Rodrigues, Dila, Karla, Alessandro, Thaynara, Simone Weber e Guilherme Alugo. Agradeço pelo convívio, contribuições e por fazerem parte dessa conquista!

Aos Professores Carlos André e Wagner Fontes e ao Doutor Agenor da Universidade de Brasília que sempre colaborou com seus conhecimentos em proteômica.

Às professoras Patrícia Lima e Luciana Casaletti que sempre me incentivaram, acreditaram no meu potencial e pela amizade. Obrigado!

Aos amigos e companheiros Lucas Weba, Gabi, Mariana P., Christie, Camilla, Ayda, Kezia, Geovana, Lorena, Bianca, Mariana T., André, Vanessa, Andréia, Lana, Laura, Luiz Paulo, Leandro, Marta, Denner, Kassyo, Marcela, Juliano, Aparecido, Dayane, Marcella, Moisés, Karol, Fabiana, Lilian e Laurine. Agradeço pelo convívio.

Aos meus tios e primos (são muitos) que sempre apoiaram meu crescimento, me dando força! Grande abraço. Obrigado por tudo!

Aos meus amigos da Biomedicina-PUCGO, do Grupo de Jovens IASD, de Flores de Goiás por fazerem parte da minha jornada. Vocês são especias!

Às professoras Alessandra Marques, Rejane Sena, Renata Carneiro que me incentivaram desde a época da Faculdade e pela amizade. Obrigado!

À CAPES que me concedeu a bolsa de doutorado e outros financiamentos. Às agências de fomento CNPq, FAPEG e INCT-IPH.

Enfim, a todos que contribuíram, apoiaram e torceram por mim! Vocês fizeram diferença! Valeu!

SUMÁRIO

	Pág.
CAPÍTULO I	8
1. INTRODUÇÃO	9
1.1. <i>Paracoccidioides</i> spp	9
1.2. Paracoccidioidomicose	11
1.3. Hipóxia	14
1.4. Reguladores hipóxico	15
1.5. Sensoriamento em hipóxia	16
1.6. Resposta fúngica à hipóxia	17
1.7. Modificação proteica por fosforilação	18
1.8. Fosfoproteômica	20
2. JUSTIFICATIVA	23
3. OBJETIVOS	24
3.1. Objetivo geral	24
3.2. Objetivos específicos	24
CAPÍTULO II	25
4. Unmasking the new haem-protein related to O ₂ -limitation response in <i>Paracoccidioides</i> species	26
CAPÍTULO III	59
5. iTRAQ-based proteomic and phosphoproteomic analysis of <i>Paracoccidioides brasiliensis</i> in response to hypoxia	60
CAPÍTULO IV	115
6. Conclusão	116
7. Perspectivas	118
8. Referências	119
CAPÍTULO V	134
9. Produções	135

RESUMO

A Paracoccidioidomicose (PCM) é uma doença endêmica na América Latina causada pelos fungos do gênero *Paracoccidioides*. Estes fungos crescem como micélio no ambiente e como levedura no hospedeiro. Em ambos os ambientes há redução dos níveis de oxigênio. O oxigênio é uma molécula fundamental para a biossíntese de ácidos graxos, esteróis, heme e ácido ascórbico, além de ser primordial no processo de respiração celular. Neste trabalho objetivamos caracterizar proteínas e fosfoproteínas relacionadas à adaptação de *Paracoccidioides* spp. durante hipóxia. Inicialmente, verificamos que a fungoglobina, FglA, atua com um sensor dos níveis de oxigênio. A FglA é responsiva a hipóxia aumentando seus níveis transcripcionais e proteicos durante todo a limitação de oxigênio. Em adição, nós verificamos que *P. brasiliensis* tem a capacidade de redirecionar seu metabolismo para a anaerobiose, obtendo energia via fermentação alcoólica. Ainda, verificamos que as funções de ciclo celular e transcrição estão diminuídas provavelmente pelos baixos níveis de fosforilação encontrado. Neste trabalho apresentamos pela primeira vez a caracterização da globina sensora de oxigênio em fungos do complexo *Paracoccidioides*, bem como o perfil proteômico e fosfoproteômico de *P. brasiliensis* durante a limitação de oxigênio. Esperamos que nosso trabalho possa abrir novos caminhos para estudos da biologia dos fungos do gênero *Paracoccidioides*.

ABSTRACT

Paracoccidioidomycosis (PCM) is an endemic disease in Latin America caused by fungi of *Paracoccidioides* genus. These fungi grows as mycelium in the saprophytic environment, and as yeast in the host. In both environments there is a reduction of oxygen levels. Oxygen is a fundamental molecule for the biosynthesis of fatty acids, sterols, haem and ascorbic acid, and in the process of cellular respiration. In this work we aim to characterize proteins and phosphoproteins related to the adaptation of *Paracoccidioides* spp. during hypoxia. Initially, we found that the fungoglobin, FglA, acts with a sensor of the oxygen levels. FglA is responsive to hypoxia by increasing its levels throughout the stress. In addition, we found that *P. brasiliensis* has the ability to redirect its metabolism to anaerobiosis, obtaining energy via alcoholic fermentation. Further, we have found that cell cycle and transcription functions are probably decreased by the low levels of phosphorylation found. In this work we present for the first time the characterization of the oxygen sensing globin in fungi of the *Paracoccidioides* complex, as well as the proteomic and phosphoprotein profile of *P. brasiliensis* during the oxygen limitation. We hope that our work may open new avenues for studies on the biology of fungi of the genus *Paracoccidioides*.

Capítulo I

1. INTRODUÇÃO

1.1. *Paracoccidioides* spp.

Na primeira década do século XX, o médico Adolpho Lutz ao examinar pacientes com lesões orais, deparou-se com um novo agente fúngico que, quando comparado ao fungo *Coccidioides immitis*, apresentou diferenças morfológicas significativas. Deste modo, o achado foi descrito como “uma nova enfermidade pseudococcídica” (Lutz, 1908, 1945). As características morfológicas deste novo agente etiológico foram esclarecidas após o primeiro isolamento e cultivo por Alfonso Splendore, dando a denominação para o fungo de *Zymonema brasiliensis* (Splendore, 1912). Nos anos seguintes Floriano de Almeida soma aos dados já descritos, informações sobre a infecção e a doença sugerindo o gênero *Paracoccidioides brasiliensis* (Almeida, 1930a, 1930b). Por tempos, a doença foi denominada como a Doença de Lutz ou de Lutz-Splendore-Almeida dada tamanha contribuição destes pesquisadores (Benchimol and Sá, 2004; Lacaz et al., 2002). Atualmente a doença é denominada de Paracoccidioidomicose (PCM) (Shikanai-Yasuda et al., 2017). Apesar de ser uma descoberta centenária (Marques, 2008; Soares et al., 2008), a PCM e seus agentes ainda são objetos de muitos estudos que visam elucidar pontos importantes da biologia fúngica e do estabelecimento da infecção.

Os fungos do gênero *Paracoccidioides* apresentam dimorfismo térmico no qual, à temperatura ambiente entre 18-23°C, apresentam-se em forma de micélio (forma infectiva) e no hospedeiro em temperaturas de 35-37°C, como leveduras (forma parasitária) (Bagagli et al., 2006; Brummer et al., 1993; San-Blas et al., 2002). A forma miceliana é caracterizada por hifas hialinas septadas, com ramificações apresentando conídios intercalares e/ou terminais e quando em colônias apresentam-se brancas aveludadas tornando-se acastanhadas (Brasil, 2013; Lacaz et al., 2002; Mendes et al., 2017). Já as leveduras possuem forma arredondadas com múltiplos brotamentos originados de célula-mãe com aspecto de “roda de leme”, enquanto as colônias apresentam-se enrugadas, de coloração creme (Brasil, 2013; Lacaz et al., 2002; Mendes et al., 2017). Os fungos do complexo *Paracoccidioides* também podem apresentar-se na forma de conídios. Os conídios são formas de resistência e sua formação é induzida em condições de estresses, principalmente abióticos (Bustamante-Simon et al., 1985). Essas estruturas também podem causar infecção nos hospedeiros mamíferos (McEwen et al., 1987).

O ciclo de vida provável do fungo *Paracoccidioides* spp. foi descrito por Bagagli e colaboradores (2008). Sabe-se que o principal habitat dos fungos *Paracoccidioides* spp. é o solo (De Albornoz, 1971; Terçarioli et al., 2007; Theodoro et al., 2005) e a partir do manuseio do solo, conídios ou propágulos micelianos presentes neste ambiente podem se tornar dispersos no ar (Arantes et al., 2013) e serem inalados por mamíferos. Ao atingirem o parênquima pulmonar, os propágulos infectantes podem ser eliminados pelo sistema imunitário do hospedeiro ou transitarem para a forma de levedura estabelecendo a infecção (Benard, 2008). Acredita-se que todos os fungos do gênero *Paracoccidioides* possam causar doença em humanos (Shikanai-Yasuda et al., 2017; Teixeira et al., 2013). Além do homem, estes patógenos já foram isolados de tatus (Bagagli et al., 2003; Corredor et al., 2005; Matute et al., 2006b; Sano et al., 1998), cachorros (Ferreira et al., 1990; Rodrigues de Farias et al., 2011; Theodoro et al., 2012), preguiça (Trejo-Chávez et al., 2011) e de pinguins (Garcia et al., 1993).

O gênero *Paracoccidioides* é classificado como pertencente ao filo *Ascomycota*, ordem *Onygenales* e família *Ajellomycetaceae* juntamente com os gêneros *Blastomyces*, *Emmonsia* e *Histoplasma* (Bagagli et al., 2008; Untereiner et al., 2004). Quanto a caracterização das espécies dentro do gênero *Paracoccidioides*, muito se discutiu ao longo dos anos e vem sendo aprimorada em paralelo ao avanço das técnicas moleculares. Inúmeros trabalhos comparativos analizando as semelhanças e divergências genômicas dentre os isolados de *Paracoccidioides* spp. foram realizados (Carrero et al., 2008; Matute et al., 2006a; Muñoz et al., 2016; Soares et al., 1995; Teixeira et al., 2009, 2014; Turissini et al., 2017).

Inicialmente, um estudo do perfil polimórfico de vários isolados de *P. brasiliensis*, realizado por Soares e colaboradores (1995), verificaram que haviam diferenças genéticas consideráveis entre as amostras analisadas. Desta forma, os autores separaram os isolados em dois grupos. As semelhanças entre os isolados de cada grupo foram $\geq 90\%$ (Soares et al., 1995). Esses achados sugeriram a presença de diferenças filogenéticas entre os isolados e serviram de pontapé inicial para uma investigação mais profunda a fim de esclarecer as espécies do gênero *Paracoccidioides*.

Apesar da importante evidência citada acima, somente após 11 anos, Matute e colaboradores (2006) publicaram um estudo avaliando 8 regiões gênicas de 65 diferentes

isolados de *P. brasiliensis*. Os pesquisadores verificaram a existência de três diferentes espécies filogenéticas: S1 (espécie 1), PS2 (espécie filogenética 2), e PS3 (espécie filogenética 3). Além de agrupadas pela semelhança de seus conteúdos genéticos, os grupos ainda possuíam distribuição geográfica particular, sendo que os isolados do grupo S1 estão amplamente distribuídos no Brasil, Argentina, Paraguai, Peru e Venezuela, enquanto os isolados do grupo PS2 são encontrados apenas na região sudeste do Brasil e em áreas da Venezuela, e os isolados do grupo PS3 são restritos à Colômbia (Matute et al., 2006a). Em seguida, Carrero e colaboradores (2008) analisaram novos isolados e observaram divergência entre *Pb01* com os outros isolados, propondo a existência de um quarto grupo filogenético – *Pb01-like*.

Deste modo, até o momento, havia apenas a espécie *P. brasiliensis*, composta por quatro espécies filogenéticas (S1, PS2, PS3 e *Pb01-like*). Buscando elucidar a taxonomia do gênero, um estudo genético amplo foi realizado (Teixeira et al., 2009). A distância filogenética de grupo *Pb01-like*, comparado aos outros, foi notável. Assim, os pesquisadores sugeriram a criação da nova espécie: *Paracoccidioides lutzii* (Salgado-Salazar et al., 2010; Teixeira et al., 2009; Theodoro et al., 2012). Complementando a classificação vigente, a espécie PS4 foi então criada após novos estudos (Muñoz et al., 2016; Teixeira et al., 2014). Com os dados dispostos acima, Turissini e colaboradores (2017) sugeriram a mudança na nomenclatura. Ao invés de classificar a espécie *P. brasiliensis* em subgrupos filogenéticos, cada um deles se transformou em uma espécie dentro do gênero *Paracoccidioides*. Assim, atualmente existem 5 espécies bem definidas do gênero *Paracoccidioides*: *P. brasiliensis*, *P. lutzii*, *P. americana*, *P. venezuelensis* e *P. restrepensis*.

1.2. Paracoccidioidomicose

A PCM é uma doença inflamatória granulomatosa (Fortes et al., 2010), causada pela infecção e permanência dos fungos do gênero *Paracoccidioides* no hospedeiro (Marques, 2012). Primariamente, a infecção se instala nos pulmões causando uma pneumonite, em seguida alcança os linfonodos regionais (Severo et al., 1979). A infecção por *Paracoccidioides* spp. quando não controlada, pode evoluir para a forma disseminada, sendo transportado para outros órgãos através das vias hematogênica e linfática (McEwen et al., 1987; Mendes et al., 2017). Depois do pulmão, os órgãos mais comumente afetados são os

linfonodos, boca, pele, fígado e baço (Mendes et al., 2017; Shikanai-Yasuda et al., 2017). Nem sempre o hospedeiro com a infecção por *Paracoccidioides* spp. pode apresentar a PCM. O hospedeiro pode estar infectado, albergando o agente infeccioso sem manifestação de sinais e sintomas, porém possui teste intradérmico positivo (Montenegro and Franco, 1994). Por outro lado, pacientes podem apresentar a PCM com evolução rápida ou de forma crônica levando anos para apresentarem algum sinal e/ou sintoma (Brasil, 2010; Shikanai-Yasuda et al., 2017).

A forma crônica da PCM é a mais comum, chegando a atingir 76 a 96% dos pacientes. Geralmente, atinge homens entre 30 e 60 anos de idade. A progressão da doença é lenta e pode apresentar-se de forma unifocal ou disseminada. A gravidade da PCM crônica pode ser classificada como leve, moderada e severa, variando de perda de peso leve à insuficiência respiratória e síndromes neurológicas graves. Já a forma aguda ou juvenil atinge cerca de 5 a 25% dos pacientes. Predominante em crianças e adolescentes, apresenta evolução rápida, com disseminação da infecção para múltiplos órgãos. Os sintomas mais frequentes envolvem linfadenomegalia, hepatoesplenomegalia, lesões cutâneas e osteoarticulares. Clinicamente, refere-se a PCM sequelar as alterações anatômicas e funcionais observadas após o tratamento e cura (revisado em Brasil, 2009, 2010; Mendes et al., 2017; Shikanai-Yasuda et al., 2017).

A PCM tem elevada incidência em indivíduos que desempenham atividades laborais relacionadas ao manejo do solo e agricultura (Shikanai-Yasuda et al., 2006, 2017; Terçarioli et al., 2007; Valle et al., 2017). Cerca de 75 a 95% dos pacientes são adultos do sexo masculino (Shikanai-Yasuda et al., 2006). Esse perfil se dá pela maior quantidade de homens em atividades de risco e pela resistência natural feminina, devido ao hormônio β-estradiol nas mulheres, o qual impede a transição do fungo para a forma parasitária (Aristizabal et al., 1998; Salazar et al., 1988; Shankar et al., 2011). Entre outros fatores de risco estão o uso de álcool e tabaco (Santos et al., 2003) e a presença de comorbidades como neoplasias, infecção pelo vírus da imunodeficiência adquirida e tuberculose (Bellissimo-Rodrigues et al., 2011; Brasil, 2009, 2010; Shikanai-Yasuda et al., 2017). A transmissão direta pessoa-pessoa ainda não foi relatada.

O diagnóstico da PCM é clínico e laboratorial. A identificação direta do fungo nos espécimes clínicos é patognomônico para o diagnóstico da PCM (Brasil, 2010, 2013; Lacaz

et al., 2002). Amostras de lesões de mucosa e pele, aspirados de secreção do trato respiratório e linfonodos, além de tecidos obtidos por biópsias são comumente coletados para realização do exame. Exames de cultura do micro-organismo, imagem, testes de sensibilidade, investigações sorológicas, *western blotting*, e métodos moleculares são aplicados para auxiliar no diagnóstico, bem como para acompanhar a evolução da doença (Brasil, 2009, 2010, 2013; Brummer et al., 1993; Mendes et al., 2017; Shikanai-Yasuda et al., 2017). Recentes estudos demonstraram novas moléculas espécie-específica para o diagnóstico diferencial entre as espécies do complexo *Paracoccidioides* (Sylvestre et al., 2018b, 2018a).

O manejo terapêutico da PCM depende da evolução da doença e condições clínicas em que se encontra cada paciente, que normalmente responde bem ao tratamento com várias classes de antifúngicos, tais como, azólicos, sulfamídicos e anfotericina B (Shikanai-Yasuda et al., 2017). O Ministério da Saúde do Brasil estabelece o esquema de tratamento da PCM, indicando o uso único ou combinações de itraconazol, sulfametoaxazol, trimetroprim e anfotericina B, dependendo da situação clínica, idade do paciente e a forma da doença (Brasil, 2009). Estabelece ainda que o paciente deve ser assistido durante e após o tratamento, e a cura será definida respeitando critérios clínicos, radiológicos e imunológicos (Brasil, 2009, 2010; Shikanai-Yasuda et al., 2017). Pesquisas objetivando encontrar novas opções terapêuticas estão sendo desenvolvidas com a argentalactona e tiosemicarbazida obtendo resultados promissores (Araújo et al., 2016; Borba et al., 2018; Silva et al., 2018; Silva et al., 2018a, 2018b). A respeito do uso de vacinas, pesquisas tem sido feitas em busca deste composto com capacidade de induzir a imunidade protetora. Os trabalhos mostraram resultados promissores, em modelo animal, com a utilização da proteína gp43 de *Paracoccidioides* spp. e do seu epítopo imunogênico P10 (revisado em Taborda et al., 2004; Travassos and Taborda, 2012). A vacina terapêutica, induzindo a ativação de células dendríticas, também vem sendo estudada (Ferreira et al., 2011; Silvana dos Santos et al., 2011).

O Brasil é o país com as maiores taxas de incidência, hospitalização e morte pela PCM (Martinez, 2017; Restrepo et al., 2001). Apesar disso, infelizmente, a micose não é uma doença de notificação compulsória (Brasil, 2016) fazendo com que os inquéritos epidemiológicos para a PCM não sejam exatos. Estudos desmosntraram que em regiões endêmicas a média de casos é de 9.4/100.000 habitantes/ano, sendo que durante um surto já foram registrados 40 casos/100.000 habitantes/ano (Vieira et al., 2014). Utilizando dados do

DATASUS (Brasil), Coutinho e colaboradores (2002) verificaram que a média anual de mortes por PCM, em todo Brasil, no período de 1980 a 1995, foi de 1.45/milhão de habitantes sendo que as regiões Sudeste, Sul e Centro-Oeste foram as que tiveram maior número de mortes. Já no estado do Paraná, Bittencourt e colaboradores (2005) verificaram que o índice de mortalidade da PCM foi de 3.48/milhão de habitantes no período de 1980 a 1998. Recentemente, no estado do Rio de Janeiro uma alta taxa de incidência, de 8.25/milhão de habitantes foi observada (Valle et al., 2017). Dados de mortalidade por micoses sistêmicas, entre os anos de 1996 a 2006, demonstram que a PCM é a mais frequente causa de morte correspondendo a aproximadamente 50% dos casos e quando em pacientes com SIDA, a PCM é a quinta principal causa de morte causada por fungos (Prado et al., 2009).

1.3. Hipóxia

O oxigênio nem sempre esteve disponível nas quantidades ideais encontradas atualmente. As tensões atmosféricas foram aumentando com a evolução das cianobactérias, organismos fotossintéticos (Semenza, 2007). A partir deste momento os organismos passaram a desenvolver mecanismos para responder aos níveis alterados de oxigênio (Hedges et al., 2004; Taylor and McElwain, 2010). Hoje os organismos aeróbios utilizam o oxigênio para a biossíntese de esteróis, ácidos graxos, grupo heme, NAD (dinucleotídeo de nicotinamida e adenina) e para a respiração celular (Raymond and Segrè, 2006; Summons et al., 2006). Para esses organismos, a disponibilidade de oxigênio é um fator crítico para a sobrevivência. As tensões de oxigênio podem variar de zero (anóxia) a níveis atmosféricos 21% O₂ ou 159 mmHg [pO₂] (normoxia). Intermediário a esses valores temos a condição de hipóxia (Grahl et al., 2012).

Os micro-organismos patogênicos humanos, durante a infecção encontram um ambiente hipóxico. Em tecidos saudáveis, as concentrações de oxigênio podem variar de 1 a 11% sendo considerado fisiologicamente oxigenado – fisióxia (Carreau et al., 2011). O gradiente de oxigênio nos órgãos depende da proximidade da corrente sanguínea, ou pela atividade das células do tecido hospedeiro (Ernst and Tielker, 2009). Em tecidos acometidos por tumores ou feridas, as concentrações de oxigênio estão abaixo de 1%, sendo considerado hipóxia (Arnold et al., 1987; Dewhirst, 1998; Simmen et al., 1994). Além disso, a resposta imune celular forma aglomerados de células imunes ativadas, principalmente macrófagos,

chamados de granulomas. Já é claro que, no granuloma as concentrações de oxigênio estão surpreendentemente diminuídas (Grahil et al., 2011).

Outro ambiente que faz parte do ciclo biológico de vários micro-organismos é o solo. Mesmo nas camadas mais superficiais do solo (até 15 cm) os níveis de oxigênio variam de 2 a 13%, sendo inversamente proporcional aos níveis de dióxido de carbono (Hanslin et al., 2005). A colonização de pilhas de compostagem também submete os micro-organismos a um ambiente hipóxico, chegando a concentrações de oxigênio próximas de 1,5% (Wang et al., 2007). Os fungos do gênero *Paracoccidioides* habitam durante sua fase saprobiótica no solo (De Albornoz, 1971) e durante o parasitismo no hospedeiro mamífero, produz uma doença granulomatosa (Fortes et al., 2010). Deste modo, durante quase todo seu ciclo de vida, *Paracoccidioides* spp. necessita se adaptar ao estresse hipóxico.

1.4. Reguladores hipóxicos

Reguladores moleculares desempenham importantes funções no equilíbrio e controle das respostas celulares. Nos mamíferos o fator induzível por hipoxia - HIF (*Hypoxia Inducible Factor*) é o principal regulador da resposta à hipoxia. Em quantidades normais de oxigênio, prolil-hidroxilases dependentes de O₂, modificam a subunidade HIF-α deste fator. Posteriormente, a subunidade modificada de HIF-α é degradada via proteassoma. Quando os níveis de oxigênio estão baixos, a subunidade HIF-α não é modificada pelas prolil-hidroxilase, ligando-se à subunidade HIF-β, e quando unidas atuam como um fator de transcrição regulando a expressão de centenas de genes em resposta à hipoxia (Greer et al., 2012; Zaremba and Malech, 2005) relacionados ao transporte de glicose e enzimas da via glicolítica (Semenza, 2007), à respiração mitocondrial (Taylor, 2008), eritropoiese, angiogênese e vasodilatação (Guillemin and Krasnow, 1997).

Em fungos, a regulação do mecanismos celulares durante hipoxia ocorre através de proteínas de ligação ao elemento responsivo esterol (SREBPs -*Sterol Regulatory Element Binding Proteins*), as quais apresentam em alguns aspectos, semelhanças com o fator de transcrição de mamíferos. As SREBPs tem sido caracterizadas em vários fungos tais como, *Schizosacharomyces pombe* – *sre1* (Todd et al., 2006), *Cryptococcus neoformans* – *sre1* (Chang et al., 2007), *Aspergillus fumigatus* - *srbA* (Blatzer et al., 2011; Willger et al., 2008), *P. lutzii* - *srbA* (Lima et al., 2015) e em *Histoplasma capsulatum* – *srb1* (Dubois and

Smulian, 2016). As SREBPs possuem um domínio de ligação ao DNA denominado de bHLH (*basic helix loop helix*) que está envolvido na expressão de genes hipóxicos relacionados principalmente à biossíntese de lipídeos, ergosterol, heme e produção de etanol (Chang et al., 2007; Lima et al., 2015; Todd et al., 2006; Willger et al., 2012). Em *Saccharomyces cerevisiae*, *Candida albicans* e *Candida parapsilosis* esse sensoriamento é realizado pelo fator de transcrição *upc2* que não possui identidade de sequência com as proteínas da família SREBP e contém um domínio de ligação ao DNA tipo Gal4. Entretanto, UPC2 é responsável pela resposta ao estresse hipóxico, regulando também genes da biossíntese de esteróis e outros genes hipóxicos (Butler, 2013; Guida et al., 2011; Vik A and Rine, 2001).

Em *P. lutzii* o regulador SREBP foi chamado de SrbA (*PlSrbA*) e suas funções na homeostase de oxigênio, ferro e resistência a antifúngicos foram evidenciados por Lima e colaboradores (2015). Através de complementação gênica em *A. fumigatus*, verificou-se que a *PlSrbA* está diretamente ligada ao crescimento fúngico durante a hipóxia e privação de ferro, compensando o efeito da limitação desses elementos químicos. Adicionalmente, a *PlSrbA* também influencia na sensibilidade fúngica aos fármacos azólicos. Por exemplo, a deleção do gene da *PlSrbA*, tornou as cepas mais suscetíveis aos fármacos (Lima et al., 2015). Em *A. fumigatus* e *C. neoformans* a deleção de SREBP resultou em uma forte atenuação da virulência, além de afetar o crescimento e a resistência aos fármacos nestes fungos (Chang et al., 2007; Chun et al., 2007a; Willger et al., 2008). A deleção do Upc2 em *C. albicans* acarretou em baixa produção de esteróis, reduziu o crescimento do fungo e afetou a formação de pseudo-hifas mais longas (MacPherson et al., 2005; Synnott et al., 2010).

1.5. Sensoriamento em hipóxia

Para sobreviver em condições de hipóxia, mecanismos de sensoriamento dos níveis de oxigênio são utilizados com a finalidade de ativar sistemas complexos de respostas aos baixos níveis dessa molécula. Algumas proteínas globulares possuem a habilidade de se ligarem ao grupo heme (Vinogradov et al., 2007). O grupo heme é o mais abundante ligante às proteínas e é capaz de se ligar ao ferro, que quando em seu estado ferroso (Fe^{2+}) se liga ao oxigênio (Poulos, 2014). Por consequência, essas metaloproteínas globulares atuam no transporte e armazenamento de oxigênio, bem como no sensoriamento dos níveis de O_2 .

(Hoogewijs et al., 2012; Poulos, 2014). Hemeproteínas podem ser um importante conector entre a disponibilidade de oxigênio e o metabolismo do ferro, porque elas contêm ferro e oxigênio concomitantemente (Chung et al., 2012).

A maioria dos fungos possuem flavohemoglobinas e globinas tipo-S (Vinogradov et al., 2007). Fungos do complexo *Paracoccidioides*, assim como os outros fungos da ordem *Onygenales*, dispõem apenas de globinas tipo S (globinas sensoras) limitadas para um único domínio sensor (Hoogewijs et al., 2012) capazes de formar um túnel apolar permitindo a entrada e saída do oxigênio (Nardini et al., 2008; Pesce et al., 2009; Zhang and Phillips, 2003). Uma nova proteína que vem sendo estudada como um sensor às baixas tensões do oxigênio é a fungoglobina denominada FglA (Hillmann et al., 2014). Globina restrita aos fungos, a FglA foi caracterizada como importante regulador do crescimento em *A. fumigatus* e sua resposta transcricional se dá durante períodos iniciais quando submetido ao estresse hipóxico (Hillmann et al., 2014). Linhagens deletadas para os principais reguladores de hipóxia de *A. fumigatus* ($\Delta srbA$), e reguladores da homeostase de ferro, $\Delta sreA$ e $\Delta hapX$, foram utilizadas para monitoramento dos níveis de expressão do gene *fglA* durante hipóxia e privação de ferro. Os resultados demonstraram que, de forma independente de tais reguladores, a expressão do gene *fglA* aumentou nestas condições (Hillmann et al., 2014).

1.6. Resposta fúngica à hipóxia

Estudos transcripcionais e proteômicos em resposta ao baixo nível de oxigênio estão sendo desenvolvidos em várias espécies de fungos. Os resultados revelam que muitos micro-organismos respondem rapidamente ao estresse hipóxico, alterando severamente seu perfil transcricional, proteico, metabólico, sua morfologia, virulência e susceptibilidade à drogas (Blatzer et al., 2011; Chang et al., 2007; Chun et al., 2007b; Lima et al., 2015; Shimizu et al., 2009; Vödisch et al., 2011). É conhecido que os mecanismos de adaptação à hipóxia são variáveis entre os fungos e que esta condição é um fator chave na capacidade de sobrevivência e virulência para alguns fungos patogênicos humanos (Barker et al., 2012; Shimizu et al., 2009; Synnott et al., 2010).

Em *Paracoccidioides lutzii*, Pl01, as respostas ao estresse hipóxico evidenciaram uma intensa modulação em várias vias metabólicas, com o objetivo de compensar este estresse (Lima et al., 2015). Quando em condições de estresse, no primeiro momento (12h),

há uma redução nos níveis proteicos de vias importantes para a sobrevivência fúngica, tais como glicólise, TCA bem como o transporte de elétrons mitocondrial. A produção de acetil-CoA a partir do acetaldeído e da beta-oxidação foram aumentadas. No entanto, após 24h em ambiente estressor, a glicólise e o transporte de elétrons mitocondrial são reestabelecidos, e as vias da gliconeogênese, do GABA (*gamma*-aminobutyric acid) *shunt* e da beta-oxidação estão aumentados, porém proteínas do ciclo de TCA mantém-se pouco expressas. Além disso, precursores de ergosterol e o piruvato estão aumentados (Lima et al., 2015).

Em *C. neoformans*, vários genes envolvidos na captação e metabolismo de carboidrato, metabolismo de ácidos graxos, esterol e heme foram super-expressos. Em contraste, transcritos relacionadas a respiração celular tiveram sua expressão diminuída, em *C. neoformans* a atividade mitocondrial é essencial para o crescimento durante hipóxia (Chun et al., 2007c; Ingavale et al., 2008; Lee et al., 2007). Já em *C. albicans*, em nível transcripcional, os genes envolvidos glicólise, metabolismo de ácidos graxos e de ergosterol foram induzidos, enquanto aqueles envolvidos com a respiração aeróbica foram reprimidos (Askew et al., 2009; Setiadi et al., 2006; Synnott et al., 2010).

Em fungos do gênero *Aspergillus* vários trabalhos avaliaram a expressão de transcritos e proteínas. Em *A. fumigatus*, a hipóxia induz a transcrição de genes envolvidos no metabolismo de esteróis, ferro, parede celular e GABA *shunt*. Uma redução na expressão de transcritos relacionados ao ciclo do TCA, metabolismo de aminoácidos e degradação de RNA foi encontrada. Quando cultivado por longos períodos em hipóxia, *A. fumigatus* aumenta a expressão de proteínas relacionadas a glicólise, ciclo do TCA, respiração, e metabolismo de aminoácidos (Barker et al., 2012; Vödisch et al., 2011). Em *A. nidulans*, houve um aumento nos transcritos e proteínas relacionadas à via glicolítica, GABA *shunt*, metabolismo de ácidos graxos e ergosterol durante a hipóxia. Genes relacionados à transcrição tiveram sua expressão diminuída (Masuo et al., 2010; Shimizu et al., 2009).

1.7. Modificação proteica por fosforilação

A fosforilação proteica é uma das mais significativas modificações pós-traducionais, sendo importante para a estrutura, estabilidade e funcionamento das proteínas (Nelson and Cox, 2014). A fosforilação desempenha um papel chave nos processos celulares como

diferenciação, transdução de sinal, apoptose, degradação de proteínas, ciclo celular, homeostase, comunicação, proliferação e sobrevivência celular (Delom and Chevet, 2006; Jensen and Larsen, 2007; Nelson and Cox, 2014; Thingham et al., 2009), atuando também em nível de sistema cardiovascular, gastrintestinal, musculoesquelética, mecanismos neurológicos, resposta imunológica e regulação endócrina (revisado em Tarrant and Cole, 2009)

As proteínas cinases são responsáveis pela transferência do fosfato proveniente do ATP, para resíduos de aminoácidos específicos nas proteínas, enquanto as fosfatases realizam de retirada do fosfato (Matthews, 1995). Esta modificação pós-traducional é caracterizada por ser um processo transitório e reversível (Thingham et al., 2009). Em eucariotos, a fosforilação ocorre frequentemente nos resíduos de serina (Ser), treonina (Thr), tirosina (Tyr) e histidina (His), sendo que na histidina a fosforilação é altamente lábil (Puttick et al., 2008). Lisina (Lys) e arginina (Arg) também podem ser fosforiladas, porém é incomum (Matthews, 1995). As fosforilações são mais frequentes nos resíduos de serina e treonina, porém a fosforilação de tirosina é mais representativa para a funções celulares (Cohen, 2002).

Os resíduos de aminoácidos que são fosforilados ocorrem em motivos estruturais comuns que são reconhecidos por proteínas cinases específicas. Algumas proteínas cinases são basófilas, preferindo fosforilar resíduos que tenha a adjacência básica e outras tem preferências diversas (Nelson and Cox, 2014). O dobramento da proteína também pode influenciar na aproximação da proteína-cinase, assim como a existência de outros sítios já fosforilados na proteína. Os átomos de oxigênio do grupo fosforil podem formar ligações de hidrogênio, com o grupo amida do esqueleto peptídico, com a cadeia lateral dos resíduos de arginina ou pode repelir resíduos carregados negativamente (Nelson and Cox, 2014). O evento de fosforilação pode afetar a proteína de 3 maneiras: a) promovendo uma mudança conformacional, b) integrando a estrutura do sítio ativo da proteína e c) rompendo interações proteína-proteína (Alberts et al., 2017).

1.8. Fosfoproteômica

O fosfoproteoma é o conjunto de proteínas fosforiladas de um organismo em determinado momento (Mukherji, 2005). As fosfoproteínas possuem baixa abundância e para sua identificação, métodos analíticos tem sido empregados para permitir a conservação do grupo fosfato ligado ao peptídeo. Para isso, uso de tampões fosfo-protetivos, utilização de inibidores de fosfatases e proteases e métodos de fosfoenriquecimentos são utilizados (Gafken and Lampe, 2006; Thingholm et al., 2009).

Os primeiros estudos de fosforilação eram realizados utilizando marcações com isótopos inorgânicos P³². Com o avanço das técnicas de separação, enriquecimento, identificação dos sítios de fosforilação e devido ao risco, a utilização de materiais radiativos entrou em desuso. Técnicas de separação em gel, purificação com anticorpo, cromatografia de afinidade com metal imobilizado (IMAC), captura com polímeros e cromatografia de troca catiônica forte (SCX) são frequentemente utilizadas. Para análises quantitativas é indicada a marcação dos peptídeos com *tags* (SILAC, iTRAQ e AQUA) que são identificados pelos espectrômetros de massas com maior acurácia. Essa marcação sempre deve ser considerada em análises de fosfoproteômica devido aos baixos níveis de abundância dos peptídeos fosforilados (revisado em Gafken and Lampe, 2006).

Destacamos o uso da cromatografia com o dióxido de titânio (TiO₂). Essa técnica consiste em imobilizar um metal a uma resina –fase estacionária. Esse metal deverá possuir uma carga positiva com o intuito de se ligar através das cargas negativas dos grupos fosfatos (Block et al., 2009; von Stechow, 2016). O fosfato se liga ao dióxido de titânio na forma de óxidos covalentes (von Stechow, 2016), conferindo alta sensibilidade, além de que o TiO₂ é compatível com diversos reagentes bioquímicos (Jensen and Larsen, 2007; Wilson-Grady et al., 2008). O iTRAQ é uma cauda isobárica permitindo a marcação de diferentes amostras simultaneamente e permitindo a identificação das amostras em conjunto, isto é, em uma mesma análise de espectrometria de massas (Thingholm et al., 2009). O iTRAQ é um método poderoso para quantificar a fosforilação em escala proteômica (Bantscheff et al., 2008; Mertins et al., 2012).

Mesmo com tamanha relevância, poucos estudos de fosfoproteomas em fungos patogênicos humanos tem sido realizados. Em *A. nidulans*, Ramsubramaniam e colaboradores (2014) conseguiram identificar 647 proteínas fosforiladas das quais a maior

parte foram preditas para se localizarem no núcleo. Das fosfoproteínas identificadas, um grande grupo (23%) foi classificado como reguladores de processos biológicos. Também, fosfoproteínas relacionadas a formação dos polos de crescimento e organização do citoesqueleto foram induzidas. Sabendo que os fungos filamentares crescem por múltiplos polos, os autores ressaltam a importância da fosforilação para o crescimento de *A. nidulans*.

Em *C. neoformans*, 648 fosfoproteínas foram identificadas das quais 45 eram cinases. Os principais processos biológicos foram os de metabolismo, transporte, transdução de sinal e síntese de proteína. Dentro as proteínas cinases, foram identificadas proteínas envolvidas nos processos de biossíntese de melanina e capsula, resistência ao estresse nitrosativo, manutenção da parede celular e termotolerância, e resistência ao fluconazol. Os dados obtidos, sugerem fortemente que a virulência em *C. neoformans* é controlada pela fosforilação (Selvan et al., 2014).

Analizando o fosfoproteoma de *C. albicans*, Willger e colaboradores (2015) identificaram 2.896 proteínas fosforiladas. Semelhantemente a *A. nidulans*, os processos biológicos de crescimento das hifas e polaridade do citoesqueleto foram os mais abundantes. Quando avaliado somente as proteínas fosforiladas em tirosina, os processos de cinases, ligadores ao DNA e transdução de sinal foram os mais enriquecidos (Willger et al., 2015).

Quando se trata de estudos fosfoproteômicos em fungos do complexo *Paracoccidioides*, poucos estudos foram realizados. Em análise *in silico* do genoma disponível de *Paracoccidioides* spp., Fernandes e colaboradores (2005) evidenciaram as principais vias de sinalização em *P. brasiliensis*. Os dados sugerem a presença de 5 cascatas de sinalização mediada por MAPK (do inglês *mitogen-activated protein kinase*). Essas cascatas estão envolvidas nos processos de controle da formação da parede celular, resposta ao feromônio, integridade celular e controle da osmolaridade (Fernandes et al., 2005).

Recentemente, o mapa proteômico das proteínas fosforiladas durante o estresse oxidativo foi realizado em *P. brasiliensis*. Chaves e colaboradores (2017) identificaram 230 proteínas (2.63% do proteoma total) com 440 sítios de fosforilação. Estas proteínas atuam em diferentes vias de sinalização para respostas ao estresse oxidativo. Os autores destacam a identificação da via HOG1 e da histidina cinase atuantes em resposta ao estresse oxidativo.

Estudos vem sendo desenvolvidos por nosso grupo de pesquisa com o objetivo de caracterizar proteínas que desempanham um papel chave na adapatação de *Paracoccidioides* spp. aos mais diferentes estresses. Desta forma, o estudo diferenciado para a caracterização estrutural e bioquímico, bem como da sua função na biologia fungica durante a infecção é de suma importância. Além disso, trabalhos que revelam o perfil proteômico em resposta ao desafios estressores vem sendo desenvolvidos. Em acréscimo, estudos do fosfoproteoma de *Paracoccidioides* spp. durante a sua diferenciação dimórfica (Araújo et al. em submissão), entre suas espécies (Portis et al. em redação) e durante a resposta ao estresse hipóxico (neste estudo) ampliam o arsenal de estudos sobre a biologia de *Paracoccidioides* spp. Com estes trabalhos esperamos colaborar com o entendimento da adaptação e sinalização celular em *Paracoccidioides* spp. durante o estresse hipóxico.

2. JUSTIFICATIVA

A paracoccidoidomicose é uma micose sistêmica causada pelos agentes etiológicos do gênero *Paracoccidioides*, sendo o Brasil o país com maior número de casos confirmados da doença. Esses fungos possuem uma fase saprobiótica no solo e/ou fezes e outra parasitária em hospedeiros mamíferos. É claro que durante seu ciclo de vida *Paracoccidioides* spp. enfrenta privação de oxigênio, seja no solo ou durante a resposta do sistema imune do hospedeiro. Fungos do gênero *Paracoccidioides* resistem ao estresse hipóxico modelando rapidamente seu metabolismo de aeróbio para anaeróbio, fazendo dele um possível micro-organismo anaeróbio facultativo. No entanto, o estudo de moléculas-chave no sensoriamento dos níveis de oxigênio, da resposta metabólica adaptativa e sua regulação por fosforilação durante o estresse hipóxico de leveduras de *Paracoccidioides* spp. ainda necessitam de melhores esclarecimentos. A identificação inicial dessas moléculas traz informações importantes sobre o ciclo de vida do fungo e sua adaptação durante a infecção. Deste modo, essas proteínas possuem a possibilidade serem alvos para drogas terapêuticas fungo-específicas, e futuramente serem utilizadas no tratamento e controle da doença.

3. OBJETIVOS

3.1.Objetivo Geral

Identificar, caracterizar e comparar as proteínas e fosfoproteínas relacionadas ao sensoriamento, regulação e resposta adaptativa em espécies do complexo *Paracoccidioides*, na sua forma parasitária, durante uma condição de estresse hipóxico.

3.2.Objetivos Específicos

- Buscar o gene da fungoglobina nos genomas das espécies de *Paracoccidioides* spp.;
- Analisar a estrutura molecular da proteína fungoglobina através de modelagem molecular;
- Verificar os níveis transpcionais e proteicos da fungoglobina durante a limitação de oxigênio;
- Caracterizar a fungoglobina nativa;
- Identificar e quantificar proteínas e fosfoproteínas de *P. brasiliensis* durante o estresse hipóxico;
- Avaliar os perfil metabólico de *P. brasiliensis* durante a limitação de oxigênio;
- Descrever o perfil fosfoproteômico durante a adaptação de *P. brasiliensis* ao estresse hipóxico;
- Realizar ensaios confirmatórios para a resposta deduzida pela análise proteômica.

Capítulo II Manuscrito 1

4. Unmasking the new haem-protein related to O₂-limitation response in *Paracoccidioides* species.

Lucas Nojosa Oliveira^{a,b}, Marielle Garcia Silva^{a,b}, Raisa Melo de Lima^a, Santiago Aguiar Espellet Soares^a, Mariana Vieira Tomazett^a, Patrícia de Sousa Lima^c, Maristela Pereira^a, Célia Maria de Almeida Soares^{a,*}

^aLaboratório de Biologia Molecular, Instituto de Ciências Biológicas, ICB II, Campus II, Universidade Federal de Goiás, Goiânia, Goiás, Brazil;

^bPrograma de Pós-graduação em Patologia Molecular, Faculdade de Medicina, Universidade de Brasília, 70910-900, Brasília, Distrito Federal, Brazil;

^cLaboratório Interdisciplinar de Biologia, Universidade Estadual de Goiás, Itapuranga, Goiás, Brazil

*Corresponding author

Célia Maria de Almeida Soares
Laboratório de Biologia Molecular
Instituto de Ciências Biológicas II
Câmpus Samambaia
Universidade Federal de Goiás
74690-900, Goiânia, Goiás – Brazil
Tel/Fax: +55 62 3521 1110
E-mail address: cmasoares@gmail.com

Key-words: hypoxia, fungoglobin, FglA, molecular modeling.

Abstract

The oxygen molecule is fundamental to the life of aerobic organisms. During *Paracoccidioides* life cycle, the oxygen supplement is not always available in adequate quantities. When in saprobiosis in the soil or during the host infection, reduced levels of oxygen directly affect general metabolic processes and oxygen-sensing mechanisms play a fundamental role in the survival of the fungus under those conditions. The strongest hypothesis is that this mechanism of sensing oxygen levels in fungi is mediated by a haem-protein, called fungoglobin. However, the characterization of the fungoglobin in *Paracoccidioides* has not been performed thus far. Here we show the predicted structure of the fungoglobin, as well as its levels during hypoxic-mimetic conditions. The fungoglobin is present in members of all species of *Paracoccidioides* and its structure similar to crystallographic templates. Molecular modeling revealed that the biochemical and biophysical characteristics are maintained allowing binding of the haem-group and oxygen, as well. Besides, fungoglobin is a possible drug target as predicted by PockDrug server. In addition, during the *in vitro* hypoxic-mimetic environment the fungoglobin transcript and proteins are overexpressed at the early treatment time, remaining elevated while there is oxygen limitation, returning to its basal levels upon normoxia. Finally, in a lung infection model, the transcript and the cognate protein are up regulated, suggesting its potential role during infection.

Introduction

Fungi of the *Paracoccidioides* genus are responsible for a life-threatening infection in humans, causing a systemic mycosis, paracoccidioidomycosis (PCM)¹. The lung is the gateway to infection. Conidia or mycelial propagules are inhaled. If the conidia or mycelial propagules are not eliminated by the competent host' immune system, they differentiate into yeast cells establishing infection. Depending on the predisposition of the host, the fungal infection may be limited to the lung or progress to a systemic mycosis^{2,3}. The disease is limited to Latin America⁴, and Brazil has the highest PCM indices⁵, with an estimated occurrence of 3,500 new cases per year⁶, being the fifth leading cause of death caused by systemic mycosis⁷.

Oxygen (O_2) is a molecule that, although toxic in large quantities, is elemental to metabolic processes of aerobic respiration, and as substrate for biosynthesis of molecules such as sterols, haem group, fatty acids and ascorbic acid⁸. In healthy tissues, in the human body, physioxia is considered to have O_2 concentrations ranging from 11% to >1%, and oxygen levels $\leq 1\%$, described in tumors and wounds, are typically considered hypoxia⁹⁻¹². It is known that oxygen supplement is reduced in decomposing organic material layers, as well as in the mammalian lungs at the site of infection^{13,14}. In view of this, oxygen-sensing mechanisms are used to activate complex systems of responses to the low levels of the O_2 -molecule. In most human pathogenic fungi, the hypoxia sensitization occurs through Sterol Responsive Element Binding Proteins - SREBPs¹⁵⁻²⁰ or by UPC2 transcription factor²¹⁻²³, both involved in the expression of hypoxic genes mainly related to lipid, ergosterol and haem biosynthesis, ethanol production and to iron metabolism. Despite being considered physiologically an obligate aerobe, fungi of the genus *Paracoccidioides* can face O_2 -limitation in their ecological niche and in the host tissues^{2,24}. To survive in these environments, metabolic and respiratory adaptations are required, and key proteins play an important role in this response²⁰.

Haem (protoporphyrin IX) bound to the iron ion is the most abundant and widely used prosthetic group for metalloporphyrins. The haem group is capable of transporting electrons between proteins during respiration, iron storage, transport and O_2 storing, as well as acting as sensors during oxygen deprivation when bound to globin^{25,26}. Globins have the ability to bind to haem and fungi possess flavohemoglobins and S-type globins²⁷. Remarkably, fungi of the order Onygenales, such as *Paracoccidioides* spp., has only S-type globins (sensor globins) limited to a single domain sensor globin²⁵. Previously, a fungal haem-protein has been studied as a sensor at low oxygen stresses, named fungoglobin (FglA). FglA was characterized as an important growth regulator in *Aspergillus fumigatus* and its transcriptional response occurs during the onset of hypoxic stress²⁸.

Studies related to hypoxia response are being performed in various fungi and the results indicate that there is a rapid adaptation of these microorganisms to conditions of hypoxia, severely altering metabolism, morphology, transcriptional activities and virulence. The fungus *Paracoccidioides lutzii* also adapts to the conditions of low oxygen concentration and its responses have recently been characterized by our group²⁰. During O_2 -limitation, at first, there is a reduction in the glycolysis, TCA and mitochondrial electron transport.

However, after 24 hours in a stressor environment, glycolysis and mitochondrial electron transport are reestablished, and the gluconeogenesis, GABA shunt and beta-oxidation pathways are increased. In contrast, proteins from the TCA cycle remain poorly expressed²⁰. In addition, the main regulator during hypoxia stress, SrbA, was first characterized in *Paracoccidioides* and data revealed an important action in drug resistance and iron metabolism²⁰. However, several aspects of this adaptation should be better elucidated, such as the characterization of others proteins involved in the sensing of low oxygen levels and their importance in the establishment and persistence of infection. The general aim of this work is to identify and characterize key elements in sensory and adaptive response to hypoxia, in particular FglA, in members of the *Paracoccidioides* complex. Unprecedented, this study was able to evidence by molecular dynamics the *Paracoccidioides* FglA structure, as well as its levels of expression during the oxygen limitation. We believe that this molecule may be important in the fungal adaptation to infection, and that it may be used as a target for drugs.

Materials and Methods

Ethics statement and mice

This study was conducted in strict accordance with the ethical principles of animal research adopted by the Brazilian Society of Laboratory Animal Science and a Brazilian Federal Law 11.749 (October, 2008). The project was approved by institutional Ethics Committee on Animal Use of the Universidade Federal de Goiás (reference number 089/17). Male BALB/c mice, aged 6–8 weeks, were purchased from the Animal house of the Instituto de Patologia Tropical e Saúde Pública – UFG, and were kept in the Animal Facilities in Laboratório de Biologia Molecular of the Departamento de Bioquímica e Biologia Molecular, Instituto de Ciências Biológicas, Universidade Federal de Goiás.

In silico analysis

Nucleotide sequence of *fglA* was retrieved from *Paracoccidioides* sp. genome available at National Center for Biotechnology Information database (<https://www.ncbi.nlm.nih.gov/assembly/?term=Paracoccidioides>). In this database are

available the genomes of all five *Paracoccidioides* species (*P. lutzii* - strain 01, *P. brasiliensis* - strain 18, *P. americana* - strain 03, *P. venezuelensis* - strain 300, *P. restrepensis* - strain CNH). Globins sequences of the *A. fumigatus* A1163 database (<http://www.aspergillusgenome.org>), *Ajellomyces dermatitidis* (<https://www.ncbi.nlm.nih.gov/assembly/?term=Ajellomyces%20dermatitidis>) and *Coccidioides immitis* (<https://www.ncbi.nlm.nih.gov/assembly/?term=Coccidioides%20immitis>) were uploaded. Online algorithms used to predict proteins domains were InterPro (<https://www.ebi.ac.uk/interpro/>;²⁹). The WoLF PSORT (<https://www.genscript.com/wolf-psort.html>;³⁰) and TargetP 1.1 server (<http://www.cbs.dtu.dk/services/TargetP/>;³¹) was used to determine the cellular localization. Nuclear and mitochondrial localization signals were determined by NUCPred (<https://nucpred.bioinfo.se/nucpred/>;³²) and MitoProt (<https://ihg.gsf.de/ihg/mitoprot.html>;³³), respectively. Peptide signal for export was predict by SignalP 4.1 (<http://www.cbs.dtu.dk/services/SignalP/>;³⁴). To predict of GPI-anchor predictions was used PredGPI (<http://gpcr.biocomp.unibo.it/predgpi/pred.htm>;³⁵) and for transmembrane domains was TMHMM 2.0 (<http://www.cbs.dtu.dk/services/TMHMM/>;³⁶). Post-translational glycosylation sites were determined by NetNGlyc 1.0 Server (<http://www.cbs.dtu.dk/services/NetNGlyc/>) and NetOGlyc 4.0 Server (<http://www.cbs.dtu.dk/services/NetOGlyc/>;³⁷). To determine the identity of the proteins among species, the Basic Local Alignment Search Tool on NCBI site (BLAST - <https://blast.ncbi.nlm.nih.gov/Blast.cgi>;³⁸) was employed.

Protein molecular modeling

A structural model of the putative fungoglobin of *P. brasiliensis* (GenBank accession number XP_010756372.1) was obtained by *in silico* analysis. Amino acid sequence was submitted to homology modeling in the I-Tasser server^{39,40}. In order to determined of the architecture of FglA a template was search in the Protein Data Bank and the similarities was evaluated by TM-score algorithm. The COFATOR⁴¹ and COACH⁴² algorithms were used to predict functional regions and protein binding sites. For the structural analysis, the PyMOL molecular visualization program (The PyMOL Molecular Graphics System, Version 2.0 Schrödinger, LLC) was used.

Molecular dynamics (MD) simulation was performed by GROMACS 5.1 software⁴³ using the AMBER force field (ff99SB-ILDN). For energy minimization, the limit of 1,000 kJ/mol was used. For the equilibrium of the thermodynamic variables of the system to a simulation of 100 picoseconds of NVT and NPT, with the protein restricted in its positions and the temperature was adjusted by the thermostat at 300 K (26.85°C), and the velocities calculated from Maxwell equations⁴³. In the NPT simulation, where the volume is allowed to vary, the pressure was maintained by the Parrinello-Rahman barostat⁴⁴. After these steps the protein was subjected to the simulation of 100 nanoseconds, temperature of 300 K, pressure of 1 atm and time interval of 2 fentoseconds, without restriction of the conformation. The trajectory was analyzed by root mean square deviation (RMSD) and the root mean square fluctuation (RMSF) through the gromos algorithm. RMSF is used to verify the fluctuation of amino acid residues of the protein over time of the simulation. The g_cluster program (GROMACS package) was used to determine the conformations that were most present during the simulation, with cut-off of 0.5 nm to differentiate the conformational sets based on the RMSD profile. With the cluster analysis, RMSD and RMSF we observed the conformational profile of the protein throughout the simulation⁴³.

For the analysis of the quality of the generated models, we used the MolProbity server from which we extracted the Ramachandran graphs, the general score of the molecule (score molProbity) and the clashscore. With this server it was possible to compare the structure of the protein before and after the MD⁴⁵. To analyze the pockets of the protein, we used the PockDrug server that predicts binding sites and uses physicochemical descriptors to determine the pocket most likely to be druggable⁴⁶.

Strains and culture conditions

Yeast cells of *P. brasiliensis*, strain 18 (ATCC 32069) and *P. lutzii*, strain 01 (ATCC MYA-826) were used in this work. The cells were maintained in BHI solid medium added of 4% (w/v) glucose for 5 days, at 36 °C. When required, strains were grown in liquid BHI for 72 hours, at 36 °C. Hypoxia-mimetic conditions were performed as described in Lima and collaborators²⁰. *P. brasiliensis* was submitted to normoxia/hypoxia and the cells were collected in the time-interval of 5 min to 48 hours. For hypoxic conditions, a gas incubator (Multi-Gas Incubator MCO-19M-UV, Panasonic Biomedical) was used. For these

experiments the oxygen levels were maintained with the set point of 1% O₂, 5% CO₂ and 94% N₂; normoxic conditions were considered general atmospheric levels within the lab (~21% O₂). Depleted iron conditions were obtained according to Parente and contributors⁴⁷ with brief modifications. After grown in liquid BHI at 36 °C for 72 hours, *P. brasiliensis* yeast cells were transferred to MMcM liquid medium containing 50 µM iron chelator bathophenanthroline disulfonate (BPS) or 10 µM ammonium iron(II) sulfate [Fe(NH₄)₂(SO₄)₂] for iron deprivation and control samples, respectively. To prevent protein glycosylation, the fungal cells were cultured in BHI medium containing 50 µM OSMI-1 (Sigma Aldrich) under normoxia and hypoxia for 12 and 24 hour.

Gene sequencing

Genomic DNA extraction was performed according to standard procedures⁴⁸, using yeast cells of *Paracoccidioides* spp. Oligonucleotides were constructed according to the complete deduced sequence of *fglA* gene (sequence of the primers shown in the topic: *Expression and Purification of Recombinant PbFglA*). The gene was amplified by polymerase chain reaction (PCR), using the genomic DNA as template. Specificity was confirmed by visualization of a single PCR product on 1% agarose gel. Then 5 µL of the PCR product was treated with 1 µL of the exonuclease I:shrimp alkaline phosphatase mix (1:9) (GE Healthcare), and incubated at 37 °C for 90 min and subsequent incubation at 80 °C for 20 min. Thereafter, the sequencing reaction was performed with the BigDye™ reagent (Applied Biosystem™) and the system was subjected to capillary electrophoresis in the automated sequencer ABI 3100 Genetic Analyzer (Applied Biosystem™) and the results were analyzed by the software Chromas Lite® 2.1.1 and Clustal X 2.1⁴⁹.

Bronchoalveolar Samples

P. brasiliensis yeast cells recovered from bronchoalveolar lavage of infected mice were obtained as standardized by Pigozzo and collaborators⁵⁰. Male BALB/c mice were infected with 10⁵ cells in 100 µL of 0.9% (w/v) NaCl saline buffer, via intranasal. After 12 hours of infection, the cells were recovered by bronchoalveolar lavage and immediately used

for RNA extraction as described below. Control RNA was obtained by incubation of *Pb18* cells in liquid BHI medium at 37°C for 12 hours.

Quantitative PCR

P. brasiliensis yeast cells were harvested, and total RNA was extracted using TRIzol (TRI reagent, Sigma Aldrich, St. Louis, MO, USA). Total RNA was treated with DNase (RQ1 RNase-free DNase, Promega) followed by *in vitro* reverse transcription (SuperScript III First-Strand Synthesis Super Mix; Invitrogen, Life Technologies). cDNAs were submitted to a quantitative real time-PCR assay (qPCR) with a SYBR Green PCR Master Mix reagent (Applied Biosystems, Foster City, CA) in a StepOnePlus machine (Applied Biosystems Inc.). Oligonucleotides were designed for the *P. brasiliensis* funglobin (*PbfglA*) gene (*PbfglA*-F: 5'-CCATCAATGGCCGTACTATCA-3'; *PbfglA*-R: 5'-GGCTCCATCTTCTCGGTAAA-3'; GenBank accession number XP_010756372.1); and *P. brasiliensis* alpha-tubulin (*Pbtub*-F: 5'-CCCACGAATCCAATCTGTTAT-3'; *Pbtub*-R: 5'-GGAGACAGGTTGCCATGTATT-3'; GenBank accession number XP_010763621.1) was used as endogenous control. The annealing temperature for all oligonucleotides pairs was 62 °C and specificity was confirmed by visualization of a single PCR product on a 1.2 % agarose gel. Relative expression levels of the genes were calculated using the standard curve method for relative quantification ⁵¹. Standard curves were generated by diluting the cDNA solution 1:5. Data were expressed as the mean and standard deviation of the biological triplicates of independent experiments. Statistical analysis was performed using the Student's t-test and p-values ≤0.05 were considered statistically significant.

Expression and purification of recombinant PbFglA

The empty pET-32a vector (Novagen, Madison, WI, USA) was used to construct the pET-32a::*PbfglA* plasmid. Coding sequence of *PbFglA* was amplified with the specific primers *PbFglA*-F (5'-CGGGATCCATGTCAGCCATCAATGG-3') and *PbFglA*-R (5'-GGCGGCCGCTCAATCCAATCCAACTCCGGCTTCT-3') and cloned into the *BamHI-NotI*

site in the pET-32a vector (*Bam*HI and *Not*I sites are underlined). Transformation of *Escherichia coli* BL21 (DE3) was carried out using standard procedures. Freshly colonies were picked and cultured in LB medium supplemented with ampicillin (100 mg/mL). For protein expression, overnight cultured bacteria were first diluted 100-fold in fresh LB medium plus ampicillin and cultured with agitation at 37 °C until O.D₆₀₀ ~0.6. Isopropyl β-D-1-thiogalactopyranoside (IPTG; Sigma-Aldrich, St Louis, MO, USA) solution was then added at final concentration of 0.5 mM to induce protein expression for the next 2 hours. Bacteria were collected and soluble proteins were extracted by lysozyme incubation (500 µg/mL) for 2 hours followed by cells sonication. The solubilized material was recovered by centrifugation at 8,000 x g, for 15 min. Bacterial overexpressed recombinant FglA (rPbFglA) was purified using Ni₂₊NTA affinity chromatography (Sigma Aldrich). Protein concentration was determined by the Bradford method ⁵² and purity, size, and identity of rPbFglA protein were evaluated using a 12% SDS-PAGE and in-gel protein digestion ⁵³ followed by LC-MS/MS ²⁰.

Mice Immunization

We used the purified rPbFglA protein to generate specific anti-rPbFglA polyclonal antibody in male BALB/c mice. Mice were immunized by subcutaneous injection of 10 µg of protein (in 50µL of 1X PBS) with 50 µL of complete Freund's adjuvant at first administration. Subsequent injections were maintained the same sample proportions but was used incomplete Freund's adjuvant. Animal was boosted twice, at 1-weeks intervals, with the same amount of antigen. One week after the last boost, the serum containing polyclonal antibody to rPbFglA was aliquoted and stored at -20°C. Pre-immune serum was obtained.

Immunoblotting

Hypoxic and normoxic proteins extracts of *P. brasiliensis* or rPbFglA protein was loaded (40 µg) on 12% SDS-PAGE. After gel separation, proteins were stained with Coomassie Blue R or transferred to Hybond ECL membrane (GE Healthcare). Subsequently, membranes were incubated with PBS solution, added of 10% (w/v) non-fat milk and 0.1%

(v/v) Tween 20 (PBS-T) for 2h to block non-specific sites. After blocking, membranes were incubated with anti-rPbFglA polyclonal antibodies diluted 1:150 in PBS-T for 2h. Membranes were washed in PBS-T, followed by incubation with phosphatase-conjugated secondary antibody (1:1,000), in dark at room temperature, for 1 h. Labelled detection was carried out using 5-bromo-4-chloro-3-indolylphosphate–nitroblue tetrazolium (BCIP-NBT).

Results and Discussion

Identification of Paracoccidioides spp. fungoglobin

Globins are important haem-proteins able to bind O₂ and thus play an important role in aerobic organism, acting in the processes as respiration, oxidative energy production, decomposition or production of NO, detoxification of reactive oxygen species or intracellular signaling ⁵⁴. Globins also operate as sensors of oxygen levels ²⁵. In the human pathogenic fungus *A. fumigatus* the fungoglobin (*AfFglA*) was identified as sensor of oxygen and is directly linked to the adaptation to hypoxic stress, connected to fungal growth ²⁸. Several proteins play an important role in *Paracoccidioides* response upon hypoxia ²⁰, but the characterization of FglA protein was not yet establish in this genus.

Therefore, we sought to identify a putative globin-hypoxic responsive protein, FglA, in fungi of the *Paracoccidioides* genus. The sequence of *AfFglA* gene (GenBank accession number AFUB_004020) was searched against the genomic databases of *Paracoccidioides* spp. As result, it was possible to identify a homologous gene in *P. brasiliensis* - *Pb18* (GenBank accession number XP_010756372.1), *P. americana* - *Pa03* (GenBank accession number EEH19835.1), *P. venezuelensis* - *Pv300* (GenBank accession number ODH38897.1), *P. restrepensis* - *PrCNH* (GenBank accession number ODH50562.1), but not in *P. lutzii* - *Pl01* (Figure 1A). Then, the deduced amino acid sequences and their domains were characterized. The InterPro search reveals the presence of the protoglobin domains (Pfam family number PF11563) in all analyzed species (Figure 1A). The protoglobin domain consists of a single globin domain conserved in the ancestral Archaea ⁵⁵. It has been noted that domains of the protoglobin family are part of the superfamily of haemoglobins and form specific apolar tunnels that allow O₂ access, thus acting as an oxygen levels sensor ^{55,56}.

Previous phylogenetic analysis of genomes of 165 species of fungi identified putative globins, and revealed the presence of S-globin only in *P. americana* species²⁵. Through detailed analysis, we identified the sequence in four out five species of *Paracoccidioides*. It is known that among Ascomycetes, Onygenales and Pezizomycetes do not have flavohemoglobins. Rather, they present only Sensor-type globins²⁵. By the discovery of the presence of S-globins in *P. brasiliensis*, *P. venezuelensis* and *P. restrei*, protein phylogenetic relationships including these species was carried out with six Onygenales fungi sequences [*P. americana*, *P. brasiliensis*, *P. venezuelensis*, *P. restrei*, *A. dermatitidis* and *C. immitis*] and a Eurotiales - *A. fumigatus* as outgroup (Figure 1B). These results highlight the evolutionary similarities among *Paracoccidioides* species, as well as the globins of fungi belonging to Onygenales order.

Subsequently, in order to verify the presence/absence of the *fglA* gene in *P. lutzii*, oligonucleotides primers were constructed using the complete *P. brasiliensis-fglA* (*PbfglA*) gene as template, and the PCR was performed with *P. lutzii* gDNA as template. As shown in Figure 1C, the presence of the gene was inferred by the presence of a DNA fragment of identical size in *P. lutzii* compared to *P. brasiliensis* (amplicon of 665 base pairs). Thereafter, the PCR products were subjected to DNA sequencing. Analyzis of the electropherograms (Figure 1D) and sequence alignment (Supplementary File 1) demonstrated that the gene is identical between the *Paracoccidioides* species. Furthermore, the deduced *P. lutzii* amino acid sequence possesses the same characteristics presents in the FglA of the other *Paracoccidioides* species (Figure 1E).

To predict subcellular localization, the *Paracoccidioides* FglA amino acid sequence was submitted to several online algorithms, including TargetP, WoLF PSORT, MitoProt, NucPred, TMHMM, PredGPI and SignalP algorithms, all set to default. Target P and WoLF PSORT predicts *PbfglA* to be a cytoplasmic protein, hypothesis strengthened by the absence of signal sequences for the mitochondria, nucleus, and for export, as well as GPI-anchor and transmembrane domains (Supplementary Figure 1A - G). Together, these analyzes suggest the *Paracoccidioides* FglA cytoplasmic localization.

Molecular model of PbFglA

After the basic information was obtained, the *PbFglA* amino acid sequence was used for all subsequent experiments. Initially we aimed to characterize the three-dimensional structure of *PbFglA*. Interesting outcomes were predicted from the PDBID:5ohe crystal of *Anaeromyxobacter* sp. Fw109-5 (Figure 2). Using the 5ohe as template we obtained a TM-score of 0.71 (SD ± 0.12) for the generated structure of *PbFglA*. According to the COFACTOR and COACH algorithms, the modeled protein presented the haem group as the main ligand (70% of confidence) in which was possible to identify the haem attachment site, as shown in Figure 2A. Regarding the Gene Ontology (GO) classification, we obtained information that *PbFglA* participates in the biological process of oxygen transport (GO: 0015671), with molecular functions such as haem binding (GO: 0020037), oxygen (GO: 0019825) and iron (GO: 0005506). The *PbFglA* model had as molecular function the binding to haem and oxygen (88% of confidence), as biological process of oxygen transport (88% of confidence) and 58% of probability of responsiveness to chemical stimuli, suggesting its action as a sensor.

With the initial results using 5hoe crystal, the molecular dynamics was performed with the purpose of correcting possible errors in the predicted structure. The Supplementary Figure 2 evidences the quality of the molecular dynamic. Before of molecular dynamics, the Ramachandram diagram (Supplementary Figure 2A) show with 81.2% of amino acid residues are in favorable regions and 91.1% in allowed region. In contrast, in Supplementary Figure 2B, after molecular dynamics, 92.5% of the residues meet in favorable regions and 98.6% in the allowed regions, substantially improving the prediction of the protein structure. The Supplementary Figure 2C, shows the cluster graph, in which are evidenced the most representative conformational groups at each time-step of the simulation, evidencing 3 main clusters along the molecular dynamics. In Supplementary Figure 2D, the RMSD graph showing the mean deviation of the initial time structure until the final time of the simulation, disregarding the hydrogens. RMSF graphic (Supplementary Figure 2E) showing the residues that were most flexible along the molecular dynamics (peaks in the graph) and highlights in red in the Supplementary Figure 2F of the corresponding regions. In conclusion, the molecular dynamics increased confidence in the prediction of the three-dimensional structural of *PbFglA*.

The molecular dynamics allowed us to obtain an expected *PbFglA* structure as evidenced in Figure 2A. In a detailed analysis of arrangements of amino acids, we can verify

important similarities between 5hoe crystal and *PbFglA* highlighting important characteristics to the structure and its function. As shown in figure 2B, *PbFglA* amino acid residue HIS137 serve as an anchor for binding of the haem group, conserved in 5hoe crystal. This data is supported by structural analyzes of the haemproteins available in the PDB (Protein Data Bank), that revealed cysteine, histidine, phenylalanine, methionine and tyrosine as the most frequent residues for the haem anchorage, additionally to the haem binding to histidine being more frequent⁵⁷ and the presence of histidine as an anchor is an intrinsic feature of globins^{58,59}. In addition, the amino acid residues of the 5ohe crystal VAL98 and ILE95 that correspond to the amino acids VAL133 and ILE136 of the fungoglobin model assist in the stability of the molecule binding to Fe(II), as represented in the figure 2B. Onward, analysis showed the *PbFglA* tyrosine residue TYR60 that acts by interacting with the oxygen molecule (Figure 2C). This residue is important because it allows the uptake, stabilization and permanence of the oxygen connected to the haem molecule. Mutation in this amino acid prevents oxygen uptake^{55,60}. Another important finding was *PbFglA* ARG103, that similarly to 5ohe crystal LEU68, controls the entry and exit of haem group within the globular protein structure (Figure 2D)⁶⁰.

For the purpose of verifying the possibility of this protein being targeted by drugs, we searched for a possible region of drug addiction in the *PbFglA* using the algorithm PockDrug server⁴⁶. As results, we find a pocket with high volume and high quantity of amino acids (Figure 2E). This pocket is the one with the highest hydrophobicity in the protein and has a 70% chance of being drugable. As shown in the Figure 2E, this pocket (in green) coincides with the site of attachment to the haem group (in blue). Screening of active drugs in this pocket is the subject of further research study.

PbFglA recombinant and antibody production

For the purpose of production of the FglA recombinant protein (r*PbFglA*) and polyclonal antibodies, the FglA was expressed in *E. coli* and the recombinant purified proteins were injected on BALB/c mice for production of the anti-r*PbFglA* polyclonal antibodies. The overproduction of the recombinant protein in bacteria and its purification were carried out (Supplementary Figure 3A). Analysis of the MS/MS spectra confirms the expression of *PbFglA* protein (Supplementary File 2). r*PbFglA* was injected into BALB/c

male mice for polyclonal antibodies production (Supplementary Figure 3B). In the initial tests, we found that the molecular weight of native *PbFglA* was higher than that of the predicted protein. In this way, we search for post-translational modifications by online algorithms. As predicted, the *PbFglA* have no N-glycosylation sites, but possess three O-glycosylation sites (Supplementary Figure 4A and B). To verify the glycosylation effect on the molecular mass of the native *PbFglA*, we cultured *P. brasiliensis* in an environment that inhibits general protein O-glycosylation, using the OSMI-1 reagent. The minimum inhibitory concentration demonstrated that there was no cellular toxicity when cultured with OSMI-1 (data not shown). In this sense, immunoblotting outcomes confirm the O-glycosylation and the predicted molecular size with or without glycosylation revealing *PbFglA* protein fractions in the molecular sizes of approximately 60 and 25 kDa, respectively (Supplementary Figure 5A and B).

O₂ influences of PbfglA levels

The main regulator during hypoxia stress in fungi is the transcription factor SrbA initially characterized in *P. lutzii* by Lima and collaborators ²⁰. The SrbA regulator promote their function by binding to promoters of putative regulated genes in target sequences: [A/G][C/T]C[A/G/T]..[C/T][C/T/G]A[C/T] ¹⁵, [A/G]TCA[T/C/G][C/G]CCAC[T/C] ⁶¹ and ATC[G/A][T/G][A/G][C/T][G/C]AT ⁶². Thus, such elements were sought in the promoter of *P. brasiliensis fglA* and only the first sequence was found with five consensus sequences: 5'-ATCTCTTCAT-3', 3'-ACCATCCCAT-5', 3'-ATCAGGCCAC-5', 3'-GTCTCCTCAT-5', 3'-ATCTCCTCAT-5' (Figure 3A). This analysis suggests the action of SrbA transcription factor on *fglA* promoter. Interestingly, Hillman et al. (2014) found in *A. fumigatus* that the overexpression of *fglA* transcript is independent of the presence of SrbA ²⁸ indicating that the *fglA* may have different trigger-regulators for its induction.

To check the expression of the *fglA* under O₂-limitation, yeast cells of *P. brasiliensis* were subjected to normoxic and hypoxic environment, and then the relative expression of the *fglA* gene was performed by the quantitative real-time PCR. The RNAs were extracted under conditions of normoxia and hypoxia during early and late times (30 min, 1 h, 1.5 h, 4 h, 6 h, 9 h and 12 h). As shown in Figure 3B, the results evidenced that *PbfglA* expression is regulated by hypoxia after 1h of treatment and remains upregulated upon oxygen limitation.

In *A. fumigatus* the transcriptional response of *fglA* occurs within the first 15 minutes of hypoxic stress²⁸. This data suggests that *Paracoccidioides* spp. present a later response in comparison to *A. fumigatus*.

Furthermore, the *P. brasiliensis* yeast cells were submitted to re-oxygenation conditions. For this, the *P. brasiliensis* yeast cells were kept up to 4 hours under O₂- limitation and after that, the environment was re-oxygenated by 4 hours. The control cells were those submitted to normoxia along the experiment. As shown in Figure 3C, during the absence of O₂, the *PbfglA* transcript are 1.5 to 2-fold induced (until 240 min). When cells were re-oxygenated, this overexpression remains during the first 2 hours (2-fold, time point 360 min) when it returns to normal oxygen concentrations (~21% O₂), decreasing its expression at levels similar to those found in normoxia. We expected this profile, assuming that *PbfglA* acts as a sensor of oxygen levels, presenting themselves increased or decreased expression according to the availability of this chemical element. Besides, similarly as seen above the transcriptional responses of *Paracoccidioides* return more slowly, differentiating from *A. fumigatus* which restores the transcription level of the *fglA* within 20 minutes²⁸.

In addition, the protein levels of FglA were analyzed by immuno-detection assay using anti-r*PbFglA* polyclonal antibodies. As shown in Figure 3D, expression of FglA is higher when in hypoxia at time points for 12, 24 and 48 hours. This indicates that *Paracoccidioides* has effective response FglA-related with the increased of the protein expression during oxygen deprivation. Together, all data suggest a relevant role of the FglA in the response to hypoxia stress.

PbfglA is iron responsive

Haem/haemproteins may be a major connector between the availability of oxygen and iron metabolism, because they contain iron and oxygen concomitantly. For the purpose of verifying the relationship of *PbfglA* during iron deprivation we carried out *in silico* search to promoter's sequences, and quantitative real time PCR. Regarding to iron homeostasis the main regulators in fungi are HapX⁶³ and SreA⁶⁴ that regulate positively and negatively, respectively, genes involved in uptake, transport and storage of iron. In search of consensus regions in the FglA promoter for HapX (CCAAT) and SreA ([A/T/C]GATA[A/G])⁶⁵

binding sites it was possible to verify four consensus sequences for HapX and two regions for SreA (Figure 4A). This result evidences the possible activity of FglA in iron homeostasis. Therefore, the next step was verifying the *fglA* transcript levels during iron deprivation. As shown in Figure 4B, *PbfglA* was upregulated during the first 6 hours of iron withdrawal, and decreasing its expression in later times. We believe that at later times, other mechanisms specific for iron uptake are more active, such as by hemoglobin uptake⁶⁶, siderophores⁶⁵ or the reductive pathway⁶⁷ already reported in the *Paracoccidioides* genus. In conclusion, we consider FglA is only a mechanism of sensing or accessory for iron metabolism and is not involved with iron uptake.

Expression levels of PbfglA is increased in the murine lung

Paracoccidioides can adapt to various stresses, such as oxidative^{68,69}, nitrosative⁷⁰, osmotic⁷¹, deprivation of nutrients such as glucose⁷², metals^{47,73,74}, and essential elements such as oxygen²⁰, and possibly, during infection in the human host, where it faces all these injury simultaneously. In this sense, it reprograms the entire metabolism to survive this powerful attack. Notably, in the lungs there is a decrease in oxygen levels when compared to atmospheric levels⁹. Thus, we decided to verify whether *fglA* is induced in these hostile surroundings. To evaluate the expression of *fglA* in an *in vivo* model, we infected male mice BALB/c with *P. brasiliensis* viable yeast cells. After 12h of intranasal infection, we performed bronchoalveolar lavage recovering the fungus. As shown in Figure 5, the level of *PbfglA* transcript was increased when in contact with cells of the mice lung. It is known that PCM only progresses after the establishment of infection in the lung, the organ initially affected³. In addition, inside the granuloma there is a decrease in the supply of oxygen, depriving the microorganism of this element¹³ thus activating mechanisms of sensing and adaptation to this stress. This result points to a role of the FglA in adaptation during the fungus infection.

Conclusions

Decreasing oxygen to critical levels induces the *Paracoccidioides* spp. to establish strategies for survival. In this work, we demonstrated that a fungoglobin of *P. brasiliensis*,

PbFglA, is more prominently expressed upon hypoxia, suggesting that *PbFglA* acts as a sensor of oxygen limitation. During murine pulmonary PCM its levels are up-regulated denoting the pathogen adaptation in course of lung infection. In addition, the relationship between *PbFglA* and iron metabolism are initial understood. Although the significance of this protein in oxygen-limitation was evidenced, its role in the fungal biology and PCM disease progression has to be confirmed by genetically *PbFglA* deficient yeasts. Despite this, our work characterize a new fungal-specific protein involved in adaptive response and offers a new potential therapeutic target in PCM.

References

1. Teixeira, M. D. M. et al. *Paracoccidioides lutzii* sp. nov.: biological and clinical implications. *Med. Mycol.* **52**, 1–10 (2013).
2. Bagagli, E., Theodoro, R. C., Bosco, S. M. G. & McEwen, J. G. *Paracoccidioides brasiliensis*: Phylogenetic and ecological aspects. *Mycopathologia* **165**, 197–207 (2008).
3. Brummer, E., Castaneda, E. & Restrepo, A. Paracoccidioidomycosis: An update. *Clin. Microbiol. Rev.* **6**, 89–117 (1993).
4. San-Blas, G., Niño-Vega, G. & Iturriaga, T. *Paracoccidioides brasiliensis* and paracoccidioidomycosis: molecular approaches to morphogenesis, diagnosis, epidemiology, taxonomy and genetics. *Med. Mycol.* **40**, 225–42 (2002).
5. Restrepo, A., McEwen, J. G. & Castañeda, E. The habitat of *Paracoccidioides brasiliensis*: how far from solving the riddle? *Med. Mycol.* **39**, 233–41 (2001).
6. Martinez, R. Paracoccidioidomycosis: the dimension of the problem of a neglected disease. *Rev. Soc. Bras. Med. Trop.* **43**, 480–480 (2010).
7. Prado, M., da Silva, M. B., Laurenti, R., Travassos, L. R. & Taborda, C. P. Mortality due to systemic mycoses as a primary cause of death or in association with AIDS in Brazil: A review from 1996 to 2006. *Mem. Inst. Oswaldo Cruz* **104**, 513–521 (2009).
8. Rocha, S. Gene regulation under low oxygen: holding your breath for transcription. *Trends Biochem. Sci.* **32**, 389–397 (2007).
9. Carreau, A., Hafny-Rahbi, B. El, Matejuk, A., Grillon, C. & Kieda, C. Why is the partial oxygen pressure of human tissues a crucial parameter? Small molecules and hypoxia. *J. Cell. Mol. Med.* **15**, 1239–1253 (2011).
10. Dewhirst, M. W. Concepts of oxygen transport at the microcirculatory level. *Semin. Radiat. Oncol.* **8**, 143–50 (1998).
11. Simmen, H. P., Battaglia, H., Giovanoli, P. & Blaser, J. Analysis of pH, pO₂ and pCO₂ in drainage fluid allows for rapid detection of infectious complications during the follow-up period after abdominal surgery. *Infection* **22**, 386–9 (1994).
12. Arnold, F., West, D. & Kumar, S. Wound healing: the effect of macrophage and tumour derived angiogenesis factors on skin graft vascularization. *Br. J. Exp. Pathol.*

- 68**, 569–74 (1987).
- 13. Grahl, N. *et al.* *In vivo* hypoxia and a fungal alcohol dehydrogenase influence the pathogenesis of invasive pulmonary aspergillosis. *PLoS Pathog.* **7**, (2011).
 - 14. Hanslin, H. M., Sæbø, A. & Bergersen, O. Estimation of oxygen concentration in the soil gas phase beneath compost mulch by means of a simple method. *Urban For. Urban Green.* **4**, 37–40 (2005).
 - 15. Todd, B. L., Stewart, E. V., Burg, J. S., Hughes, A. L. & Espenshade, P. J. Sterol Regulatory Element Binding Protein Is a Principal Regulator of Anaerobic Gene Expression in Fission Yeast. *Mol. Cell. Biol.* **26**, 2817–2831 (2006).
 - 16. Chang, Y. C., Bien, C. M., Lee, H., Espenshade, P. J. & Kwon-Chung, K. J. Sre1p, a regulator of oxygen sensing and sterol homeostasis, is required for virulence in *Cryptococcus neoformans*. *Mol. Microbiol.* **64**, 614–629 (2007).
 - 17. Blatzer, M. *et al.* SREBP Coordinates Iron and Ergosterol Homeostasis to Mediate Triazole Drug and Hypoxia Responses in the Human Fungal Pathogen *Aspergillus fumigatus*. *PLoS Genet.* **7**, e1002374 (2011).
 - 18. Willger, S. D. *et al.* A sterol-regulatory element binding protein is required for cell polarity, hypoxia adaptation, azole drug resistance, and virulence in *Aspergillus fumigatus*. *PLoS Pathog.* **4**, e1000200 (2008).
 - 19. Dubois, J. C. & Smulian, A. G. Sterol Regulatory Element Binding Protein (Srb1) Is Required for Hypoxic Adaptation and Virulence in the Dimorphic Fungus *Histoplasma capsulatum*. 1–19 (2016). doi:10.1371/journal.pone.0163849
 - 20. Lima, P. de S., Chung, D., Bailão, A. M., Cramer, R. A. & Soares, C. M. de A. Characterization of the *Paracoccidioides* Hypoxia Response Reveals New Insights into Pathogenesis Mechanisms of This Important Human Pathogenic Fungus. *PLoS Negl. Trop. Dis.* **9**, 1–25 (2015).
 - 21. Synnott, J. M., Guida, A., Mulhern-Haughey, S., Higgins, D. G. & Butler, G. Regulation of the Hypoxic Response in *Candida albicans*. *Eukaryot. Cell* **9**, 1734–1746 (2010).
 - 22. Hoot, S. J., Oliver, B. G. & White, T. C. *Candida albicans* UPC2 is transcriptionally induced in response to antifungal drugs and anaerobicity through Upc2p-dependent and -independent mechanisms. *Microbiology* **154**, 2748–2756 (2008).
 - 23. Vik A & Rine, J. Upc2p and Ecm22p, dual regulators of sterol biosynthesis in *Saccharomyces cerevisiae*. *Mol. Cell. Biol.* **21**, 6395–405 (2001).
 - 24. Fortes, M. R. P., Miot, H. A., Kurokawa, C. S., Marques, M. E. A. & Marques, S. A. Immunology of paracoccidioidomycosis. *An. Bras. Dermatol.* **86**, 516–24 (2010).
 - 25. Hoogewijs, D., Dewilde, S., Vierstraete, A., Moens, L. & Vinogradov, S. N. A phylogenetic analysis of the globins in Fungi. *PLoS One* **7**, 1–15 (2012).
 - 26. Poulos, T. L. Heme Enzyme Structure and Function. *Chem. Rev.* (2014). doi:dx.doi.org/10.1021/cr400415k
 - 27. Vinogradov, S. N. *et al.* A model of globin evolution. *Gene* **398**, 132–142 (2007).
 - 28. Hillmann, F. *et al.* The novel globin protein fungoglobin is involved in low oxygen adaptation of *Aspergillus fumigatus*. *Mol. Microbiol.* **93**, 539–553 (2014).
 - 29. Finn, R. D. *et al.* InterPro in 2017-beyond protein family and domain annotations.

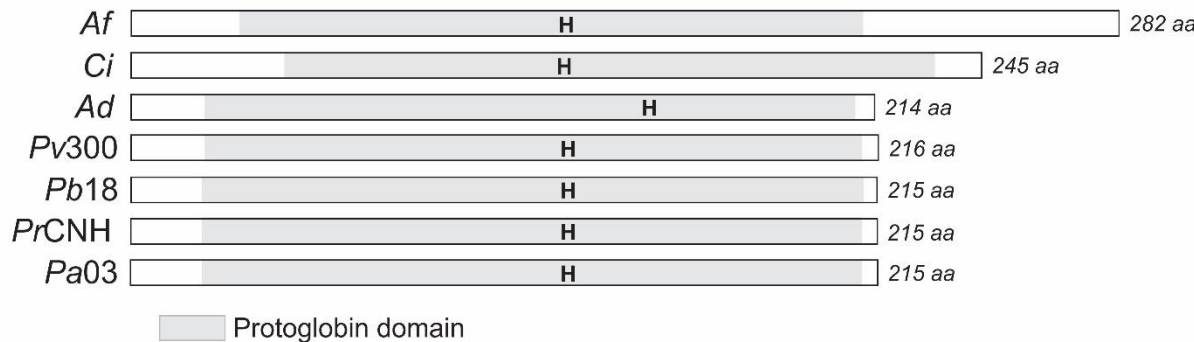
- Nucleic Acids Res.* **45**, D190–D199 (2017).
- 30. Horton, P. *et al.* WoLF PSORT: Protein localization predictor. *Nucleic Acids Res.* **35**, (2007).
 - 31. Emanuelsson, O., Brunak, S., von Heijne, G. & Nielsen, H. Locating proteins in the cell using TargetP, SignalP and related tools. *Nat. Protoc.* **2**, 953–971 (2007).
 - 32. Brameier, M., Krings, A. & MacCallum, R. M. NucPred - Predicting nuclear localization of proteins. *Bioinformatics* **23**, 1159–1160 (2007).
 - 33. Claros, M. G. & Vincens, P. Computational Method to Predict Mitochondrially Imported Proteins and their Targeting Sequences. *Eur. J. Biochem.* **241**, 779–786 (1996).
 - 34. Petersen, T. N., Brunak, S., von Heijne, G. & Nielsen, H. SignalP 4.0: discriminating signal peptides from transmembrane regions. *Nat. Methods* **8**, 785–786 (2011).
 - 35. Pierleoni, A., Martelli, P. & Casadio, R. PredGPI: a GPI-anchor predictor. *BMC Bioinformatics* **9**, 392 (2008).
 - 36. Krogh, A., Larsson, B., von Heijne, G. & Sonnhammer, E. L. . Predicting transmembrane protein topology with a hidden markov model: application to complete genomes11Edited by F. Cohen. *J. Mol. Biol.* **305**, 567–580 (2001).
 - 37. Steentoft, C. *et al.* Precision mapping of the human O-GalNAc glycoproteome through SimpleCell technology. *EMBO J.* **32**, 1478–1488 (2013).
 - 38. Altschul, S. F., Gish, W., Miller, W., Myers, E. W. & Lipman, D. J. Basic local alignment search tool. *J. Mol. Biol.* **215**, 403–10 (1990).
 - 39. Yang, J. & Zhang, Y. Protein structure and function prediction using I-TASSER. *Curr. Protoc. Bioinforma.* 1–24 (2016). doi:10.1002/0471250953.bi0508s52.Protein
 - 40. Yang, J. *et al.* The I-TASSER suite: Protein structure and function prediction. *Nat. Methods* **12**, 7–8 (2014).
 - 41. Zhang, C., Freddolino, P. L. & Zhang, Y. COFACTOR: Improved protein function prediction by combining structure, sequence and protein-protein interaction information. *Nucleic Acids Res.* **45**, W291–W299 (2017).
 - 42. Yang, J., Roy, A. & Zhang, Y. Protein-ligand binding site recognition using complementary binding-specific substructure comparison and sequence profile alignment. *Bioinformatics* **29**, 2588–2595 (2013).
 - 43. Pronk, S. *et al.* GROMACS 4.5: A high-throughput and highly parallel open source molecular simulation toolkit. *Bioinformatics* **29**, 845–854 (2013).
 - 44. Hutter, J. Car-Parrinello molecular dynamics. *Wiley Interdiscip. Rev. Comput. Mol. Sci.* **2**, 604–612 (2012).
 - 45. Chen, V. B. *et al.* MolProbity: All-atom structure validation for macromolecular crystallography. *Acta Crystallogr. Sect. D Biol. Crystallogr.* **66**, 12–21 (2010).
 - 46. Borrel, A., Regad, L., Xhaard, H., Petitjean, M. & Camproux, A.-C. C. PockDrug: A model for predicting pocket druggability that overcomes pocket estimation uncertainties. *J. Chem. Inf. Model.* **55**, 882–895 (2015).
 - 47. Parente, A. F. A. *et al.* Proteomic analysis reveals that iron availability alters the metabolic status of the pathogenic fungus *Paracoccidioides brasiliensis*. *PLoS One* **6**, (2011).

48. Sambrook, J. & Russel, D. W. *Molecular Cloning. A Laboratory Manual.* (Cold Spring Harbor Laboratory Press., 2001).
49. Larkin, M. A. *et al.* Clustal W and Clustal X version 2.0. *Bioinformatics* **23**, 2947–2948 (2007).
50. Pigosso, L. L. *et al.* *Paracoccidioides brasiliensis* presents metabolic reprogramming and secretes a serine proteinase during murine infection. *Virulence* **0**, 1–18 (2017).
51. Bookout, A. L., Cummins, C. L., Mangelsdorf, D. J., Pesola, J. M. & Kramer, M. F. High-Throughput Real-Time Quantitative Reverse Transcription PCR. in *Current Protocols in Molecular Biology Chapter 15*, Unit 15.8 (John Wiley & Sons, Inc., 2006).
52. Bradford, M. M. A rapid and sensitive method for the quantitation of microgram quantities of protein utilizing the principle of protein-dye binding. *Anal. Biochem.* **72**, 248–54 (1976).
53. Rezende, T. C. V *et al.* A quantitative view of the morphological phases of *Paracoccidioides brasiliensis* using proteomics. *J. Proteomics* **75**, 572–587 (2011).
54. Burmester, T. & Hankeln, T. Function and evolution of vertebrate globins. *Acta Physiol.* **211**, 501–514 (2014).
55. Nardini, M. *et al.* Archaeal protoglobin structure indicates new ligand diffusion paths and modulation of haem-reactivity. *EMBO Rep.* **9**, 157–63 (2008).
56. Zhang, W. & Phillips, G. N. Structure of the oxygen sensor in *Bacillus subtilis*: Signal transduction of chemotaxis by control of symmetry. *Structure* **11**, 1097–1110 (2003).
57. Li, T., Bonkovsky, H. L. & Guo, J. Structural analysis of heme proteins: implications for design and prediction. *BMC Struct. Biol.* **11**, 13 (2011).
58. Fraústo da Silvia, J. & Williams, R. *The biological chemistry of the elements.* (Clarendon Press, 1994).
59. Kaim, W. & Schwederski, B. *Bioorganic chemistry: inorganic elements in the chemistry of life.* (Wiley, 1996).
60. Stranava, M. *et al.* Coordination and redox state-dependent structural changes of the heme-based oxygen sensor AfGcHK associated with intraprotein signal transduction. *J. Biol. Chem.* **292**, 20921–20935 (2017).
61. Chung, D. *et al.* ChIP-seq and In Vivo Transcriptome Analyses of the *Aspergillus fumigatus* SREBP SrbA Reveals a New Regulator of the Fungal Hypoxia Response and Virulence. *PLoS Pathog.* **10**, (2014).
62. Linde, J. *et al.* Regulatory interactions for iron homeostasis in *Aspergillus fumigatus* inferred by a Systems Biology approach. *BMC Syst. Biol.* **6**, 6 (2012).
63. Hortschansky, P. *et al.* Interaction of HapX with the CCAAT-binding complex—a novel mechanism of gene regulation by iron. *EMBO J.* **26**, 3157–3168 (2007).
64. Schrettl, M. *et al.* SreA-mediated iron regulation in *Aspergillus fumigatus*. *Mol. Microbiol.* **70**, 27–43 (2008).
65. Silva-Bailão, M. G. *et al.* Hydroxamate production as a high affinity iron acquisition mechanism in *Paracoccidioides* spp. *PLoS One* **9**, (2014).
66. Bailão, E. F. L. C. *et al.* Hemoglobin Uptake by *Paracoccidioides* spp. Is Receptor-Mediated. *PLoS Negl. Trop. Dis.* **8**, 1–20 (2014).

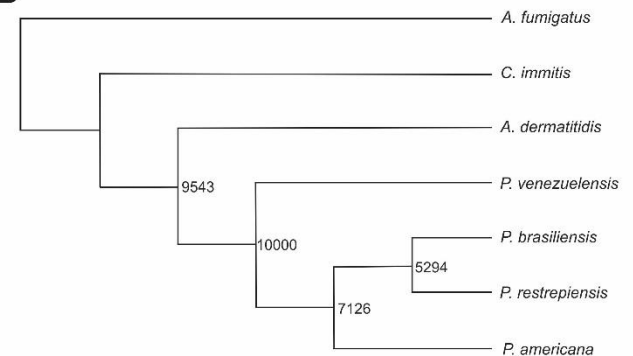
67. Bailão, E. F. L. C. *et al.* *Paracoccidioides* spp. ferrous and ferric iron assimilation pathways. *Front. Microbiol.* **6**, 1–12 (2015).
68. Grossklaus, D. A. *et al.* Response to oxidative stress in *Paracoccidioides* yeast cells as determined by proteomic analysis. *Microbes Infect.* **15**, 347–364 (2013).
69. Chaves, A. F. A. A. *et al.* Phosphosite-specific regulation of the oxidative-stress response of *Paracoccidioides brasiliensis*: a shotgun phosphoproteomic analysis. *Microbes Infect.* **19**, 34–46 (2017).
70. Parente, A. F. A. *et al.* The response of *Paracoccidioides* spp. to nitrosative stress. *Microbes Infect.* **17**, 575–585 (2015).
71. Rodrigues, L. N. da S. *et al.* Osmotic stress adaptation of *Paracoccidioides lutzii*, Pb01, monitored by proteomics. *Fungal Genet. Biol.* **95**, 13–23 (2016).
72. Lima, P. de S. *et al.* Transcriptional and Proteomic Responses to Carbon Starvation in *Paracoccidioides*. *PLoS Negl. Trop. Dis.* **8**, (2014).
73. Parente, A. F. A. *et al.* A proteomic view of the response of *Paracoccidioides* yeast cells to zinc deprivation. *Fungal Biol.* **117**, 399–410 (2013).
74. de Curcio, J. S. *et al.* Identification of membrane proteome of *Paracoccidioides lutzii* and its regulation by zinc. *Futur. Sci. OA* **3**, FSO232 (2017).

FIGURES

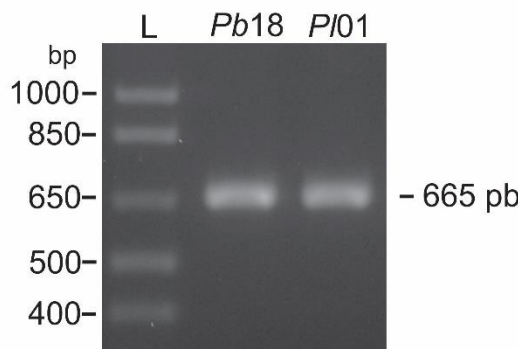
A



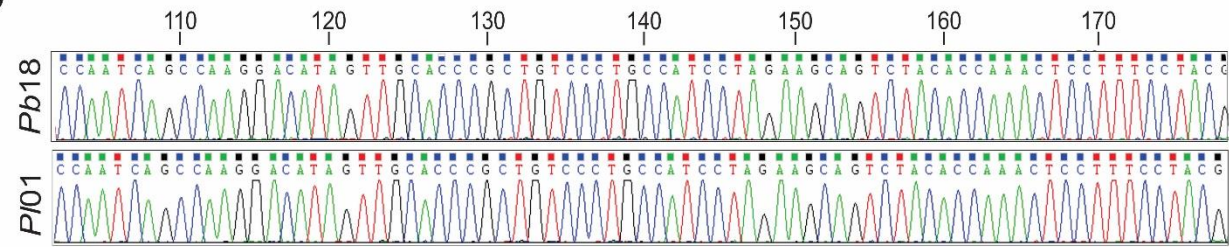
B



C



D



E



Figure 1. Alignment and sequencing of the *fglA* gene. **A)** Sequences from *Paracoccidioides* spp. (*P. venezuelensis*- *Pv*300 - ODH38897.1, *P. brasiliensis* - *Pb*18 - XP_010756372.1, *P. restrepoensis* – *PrCNH* - ODH50562.1, *P. americana* - *Pa*03 - EEH19835.1), *A. dermatitidis* - *Ad* - XP_002625170.1, *C. immitis* - *Ci*- XP_001244432.1 and *A. fumigatus*- *Af* - AFUB_00420 were used. The domains of protoglobin (Pfam family number PF11563) are featured in light gray. “H” indicates a putative histidine residue of haem binding. **B)** Phylogenetic tree using FglA amino acid sequences of *Paracoccidioides* spp., *A. dermatitidis*, *C. immitis* and *A. fumigatus* orthologues for comparison. **C)** Amplification of the *fglA* in *Paracoccidioides* spp. from the genomic DNA. The oligonucleotides resulting in a 665 base pair amplicon. The amplicon was visualized on 1.5% agarose gel. **bp:** base pairs; **L:** ladder marker. **D)** Representative image of the electropherogram of the *fglA* demonstrating the identity between the of *Paracoccidioides* species. **E)** Diagram of the deduced FglA amino acid sequence from *P. lutzii*. The domains of protoglobin (Pfam family number PF11563) are featured in light gray. “H” indicate a putative histidine residue for haem binding.

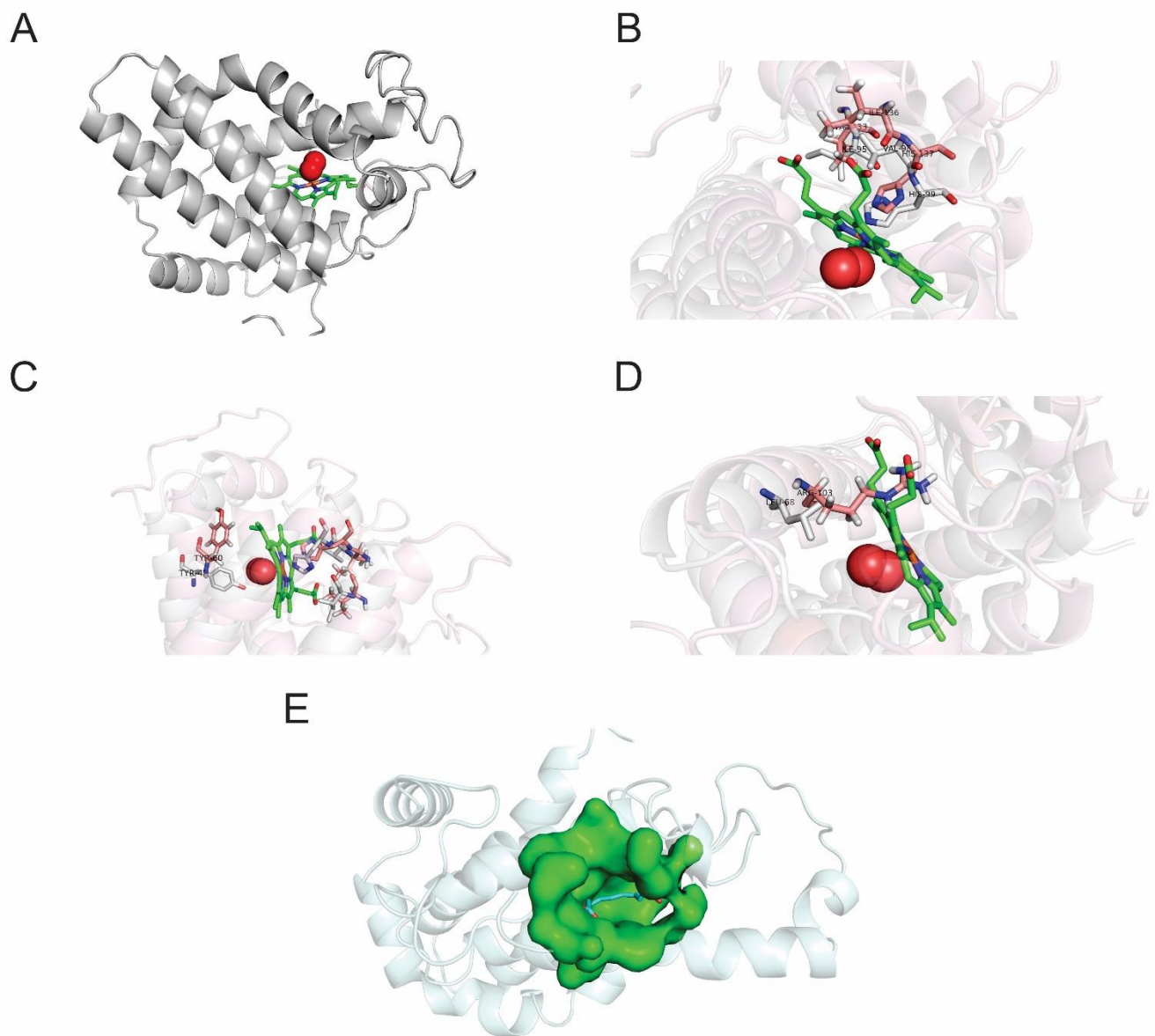


Figure 2. Modelling the predicted *PbFglA*. **A)** *Paracoccidioides* fungoglobin patterned by homology (gray), with the haem group (green) and the oxygen atoms, O₂ (red) in the probable binding site. **B)** Highlighting of the amino acid residues that are involved in the interaction with the haem group. The HIS137 is the key residue in the interaction with the iron of the haem group. **C)** Site of interaction of the haem group, with emphasis on the amino acid TYR45 (5ohe) and TYR60 (*PbFglA*) responsible for the interaction with oxygen. **D)** Amino acids LEU68 (5ohe) and ARG103 (*PbFglA*) control the entry and exit of the haem group. **E)** Region with higher possibility of being linked to drugs (green).

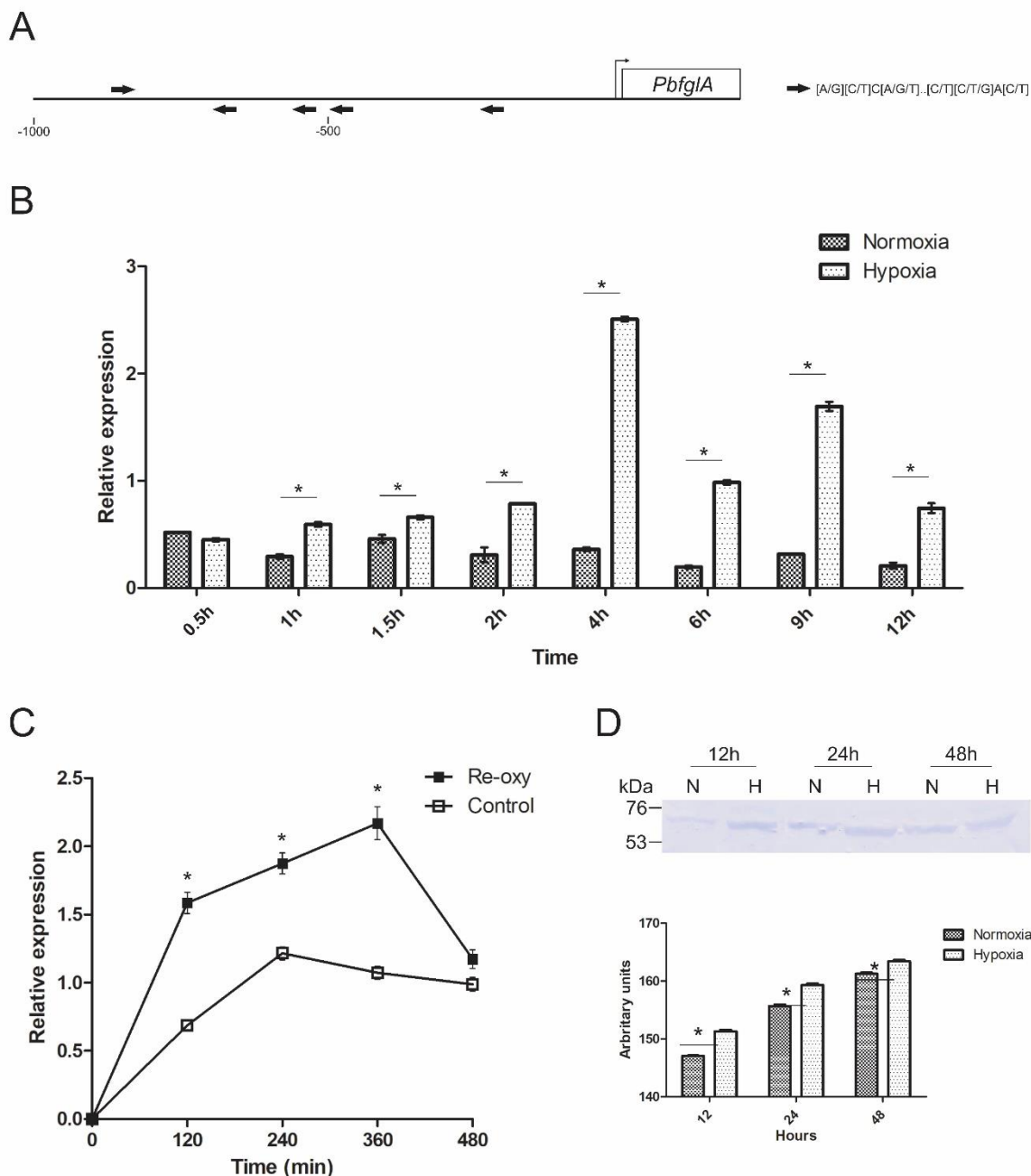


Figure 3. Fungoglobin expression in *P. brasiliensis* under hypoxia. **A)** SrbA consensus regions in the *PbfglA* gene promoter. **B)** Kinetics of the transcript *PbfglA* expression during hypoxia determined by qPCR. **C)** Kinetics of *PbfglA* expression during a re-oxygenation of the environment determined by qPCR. **D)** Proteins levels of *PbFglA* during hypoxia condition determined by immunoblot assay. The native *PbFglA* protein show a molecular mass of approximately 60 kDa. In all panels the Student's *t*-test was used to determine the level of significance, where "*" indicates differentially significant expression ($P \leq 0.01$).

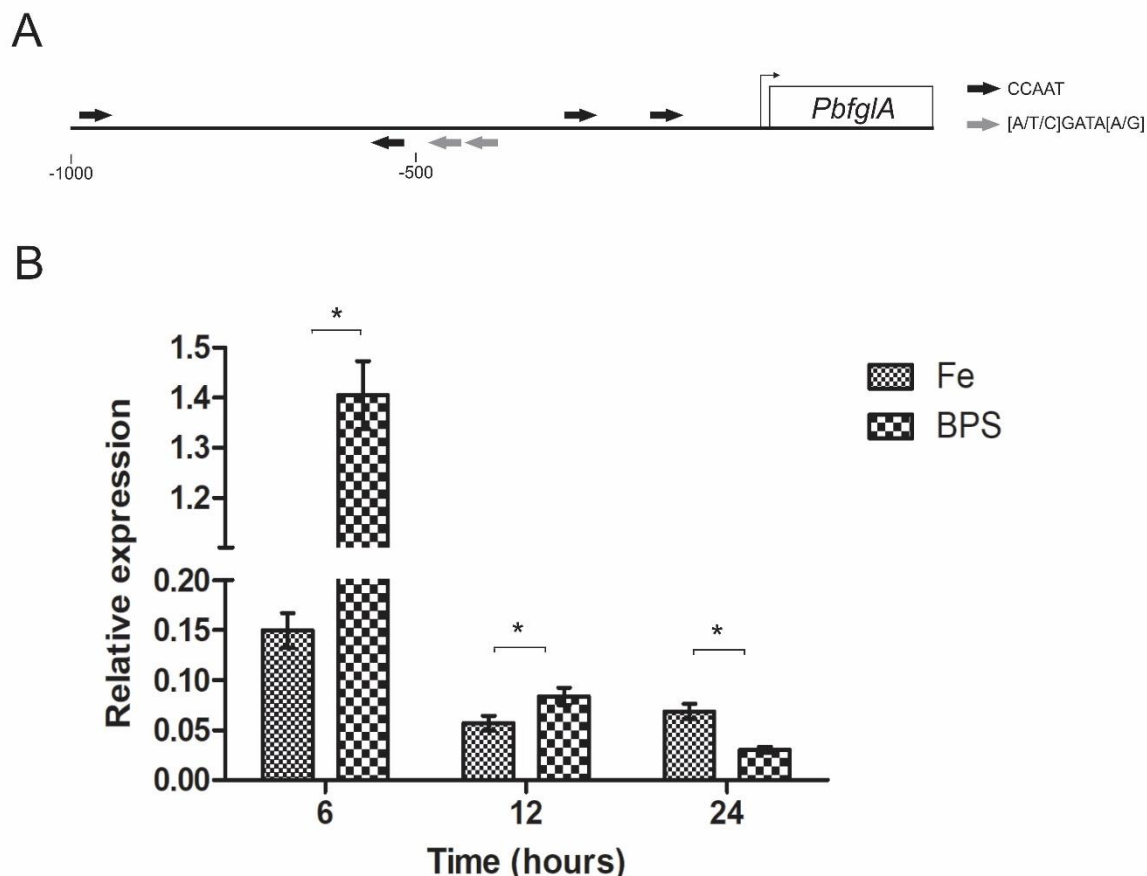


Figure 4. Expression of *fglA* in *P. brasiliensis* upon iron deprivation. A) HapX (black arrow) and SreA (gray arrow) consensus regions in the *PbfglA* gene promoter. **B)** Kinetics of *PbfglA* expression during iron deprivation determined by qPCR. The Student's *t*-test was used to determine the level of significance, where "*" indicates differentially significant expression ($P \leq 0.01$).

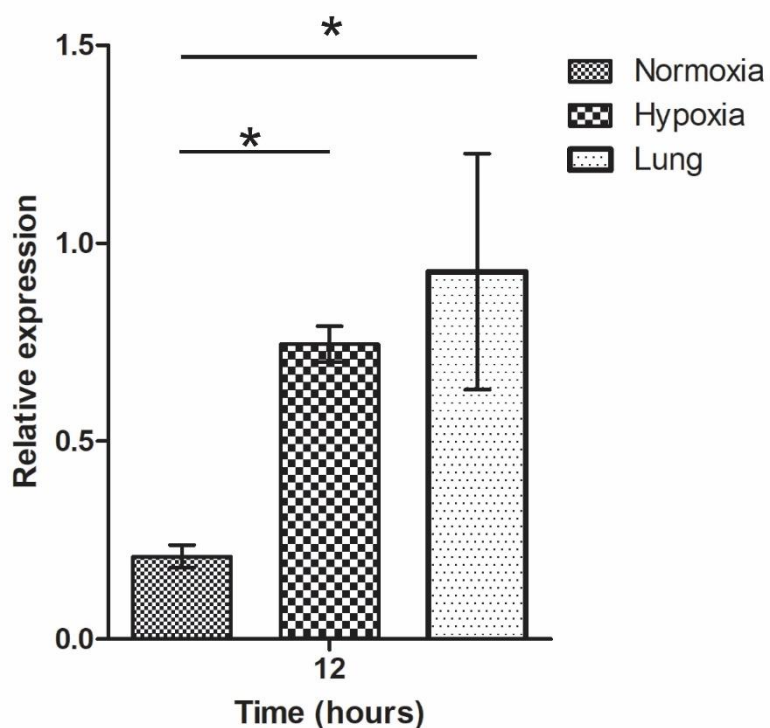
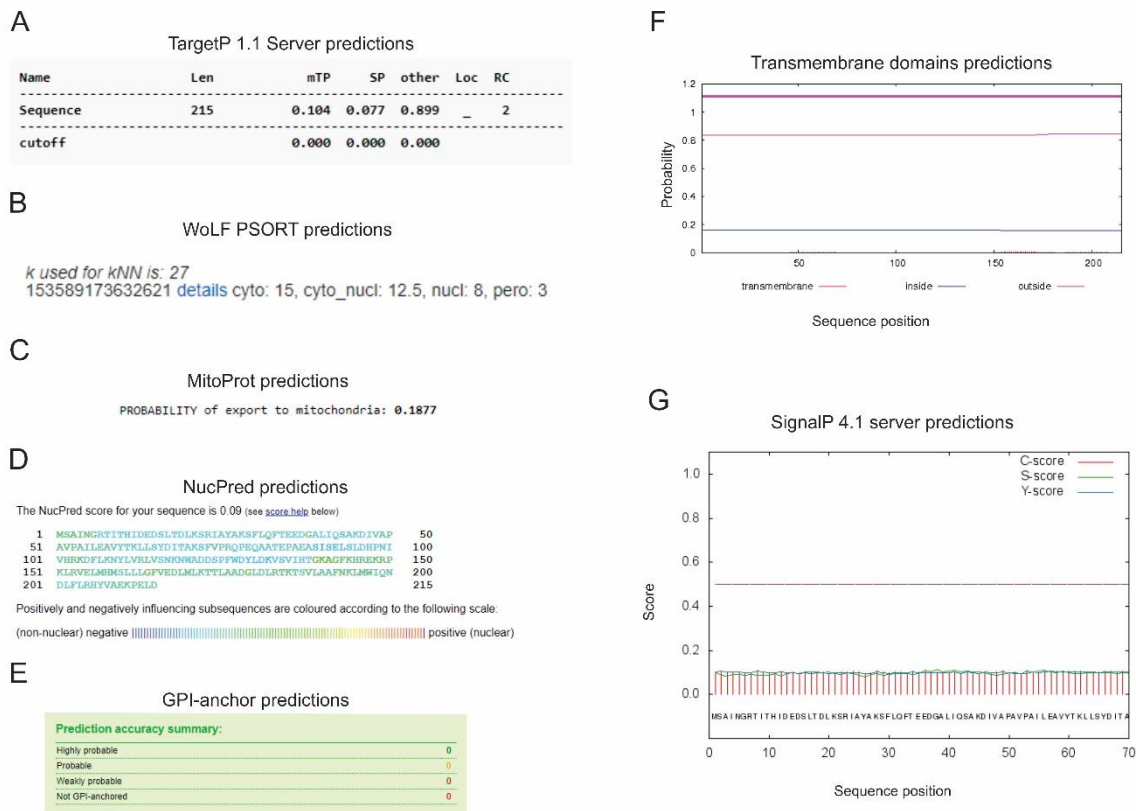
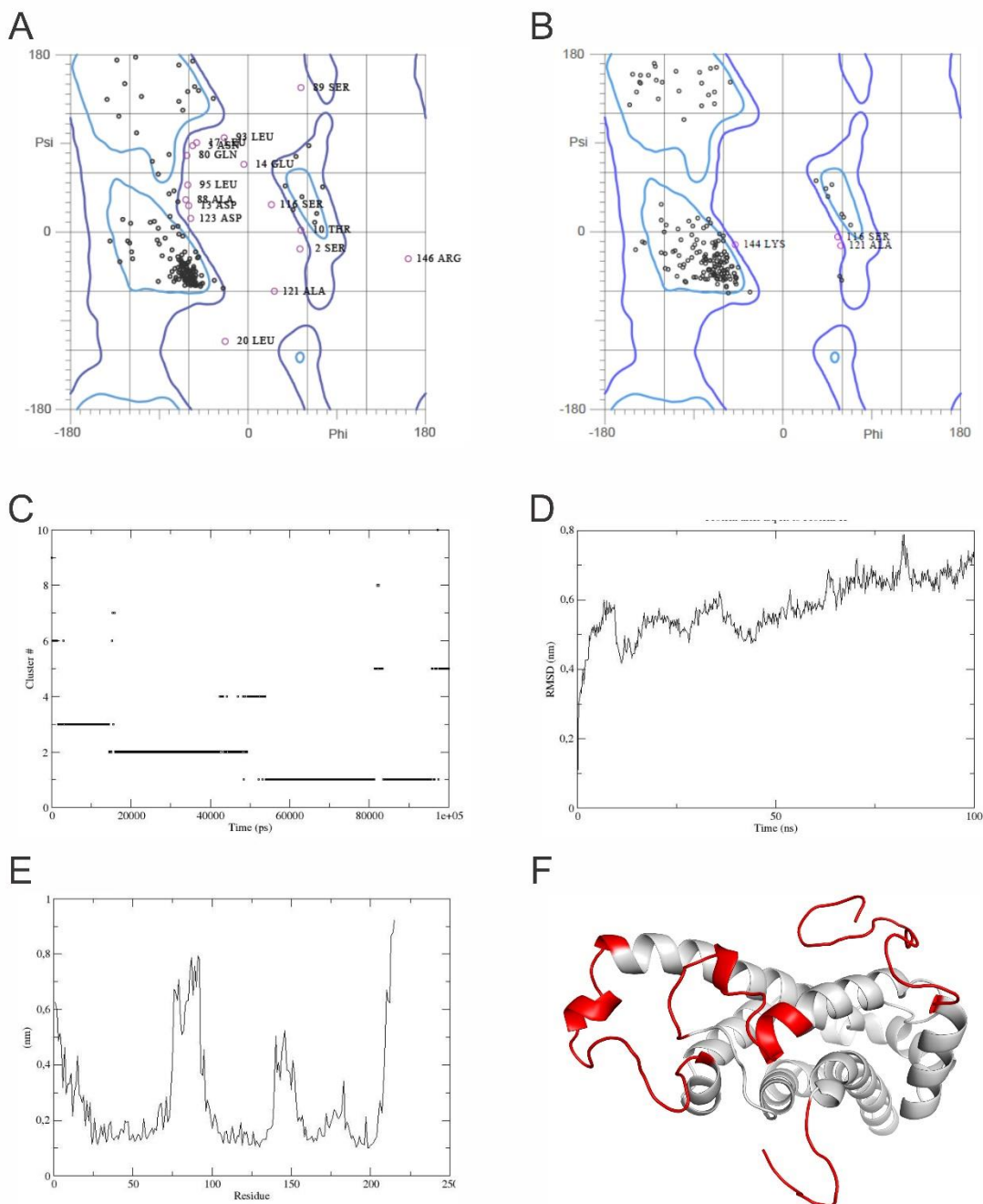


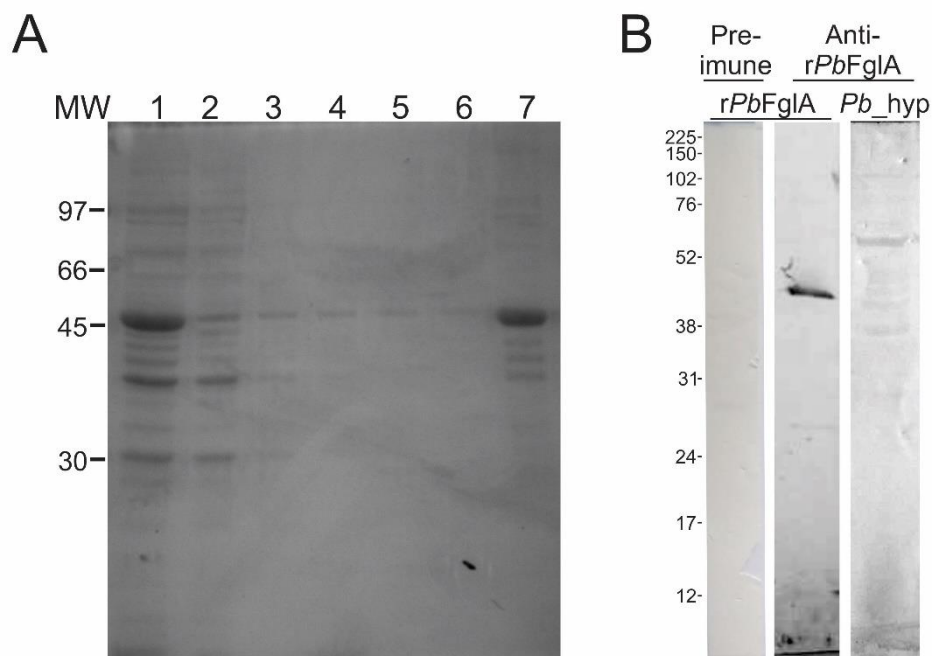
Figure 5. Expression of *fglA* in *P. brasiliensis* yeast cells recovered from lung of infected mice. The *PbfglA* expression during mice pulmonary infection was determined by qPCR. The Student's *t*-test was used to determine the level of significance, where "*" indicates differentially significant expression ($P \leq 0.01$).



Supplementary Figure 1. Prediction analysis of *PbFglA* subcellular localization. The amino acid sequence of *PbFglA* protein was used for analysis. **A)** Prediction of subcellular localization by TargetP 1.1. shows protein length (Len), mitochondrial target peptide (mTP), secretory pathway (SP), localization (Loc) and reliability class (RC). **B)** WoLF PSORT subcellular localization predictions shows score cytoplasm (cyto), cytoplasm and nuclear dual localization (cyto_nucl), nucleus (nucl) and peroxisome (pero). **C)** Mitochondrial localization signal probability. **D)** Nuclear localization signal sequence. **E)** Glycosylphosphatidylinositol anchor predictions. **F)** Transmembrane domains predictions. **G)** Prediction of signal peptide for export.

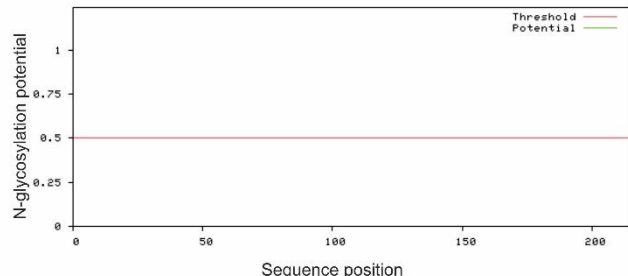


Supplementary Figure 2. Molecular dynamics data. **A)** Ramachandram diagram before molecular dynamics showing the distribution of amino acids. **B)** Ramachandram diagram after molecular dynamics showing the distribution of amino acids. **C)** Cluster chart presents the most representative conformational groups at each time step of the simulation. **D)** RMSD graph showing the mean deviation of the initial time structure until the final time of the simulation. **E)** RMSF graph showing the residues that were more flexible along the molecular dynamics. **F)** Three-dimensional structure of FglA showing the most flexible regions (red).



Supplementary Figure 3. Analysis of the expression and purification of rPbFglA, and production of anti-rPbFglA polyclonal antibody. **A)** SDS-PAGE results of rPbFglA expression by *E. coli* BL21 (DE3) and purified rPbFglA by affinity chromatography. **MW:** molecular weight marker; **Lanes:** 1, cell-free extract; 2, flowthrough; 3-6, wash fractions; 7, eluted fraction using a 400 mM of imidazole. The purified protein has a molecular mass of approximately 46 kDa. **B)** Immunoblot analysis of anti-rPbFglA polyclonal serum. Membranes containing total proteins of BL21 cells after solubilization were incubated with pre-immune serum or anti-rPbFglA polyclonal antibody. The recombinant FglA protein show a molecular mass of approximately 46 kDa. Membrane containing total proteins of *P. brasiliensis*, *Pb18*, upon hypoxia for 12 h (*Pb_hyp*) was incubated with anti-rPbFglA polyclonal antibody. The native *PbFglA* protein show a molecular mass of approximately 60 kDa.

A
N-glycosylation predictions



B
O-glycosylation predictions

#sequence	source	feature	start	end	score	strand	frame	comment
SEQUENCE	netOGlyc-4.0.0.13	CARBOHYD	2	2	0.64181	.	.	#POSITIVE
SEQUENCE	netOGlyc-4.0.0.13	CARBOHYD	8	8	0.569589	.	.	#POSITIVE
SEQUENCE	netOGlyc-4.0.0.13	CARBOHYD	10	10	0.479775	.	.	
SEQUENCE	netOGlyc-4.0.0.13	CARBOHYD	16	16	0.429399	.	.	
SEQUENCE	netOGlyc-4.0.0.13	CARBOHYD	18	18	0.4293872	.	.	
SEQUENCE	netOGlyc-4.0.0.13	CARBOHYD	22	22	0.0891686	.	.	
SEQUENCE	netOGlyc-4.0.0.13	CARBOHYD	29	29	0.0910539	.	.	
SEQUENCE	netOGlyc-4.0.0.13	CARBOHYD	34	34	0.0674745	.	.	
SEQUENCE	netOGlyc-4.0.0.13	CARBOHYD	43	43	0.0799535	.	.	
SEQUENCE	netOGlyc-4.0.0.13	CARBOHYD	61	61	0.0639419	.	.	
SEQUENCE	netOGlyc-4.0.0.13	CARBOHYD	65	65	0.0378076	.	.	
SEQUENCE	netOGlyc-4.0.0.13	CARBOHYD	69	69	0.0899385	.	.	
SEQUENCE	netOGlyc-4.0.0.13	CARBOHYD	72	72	0.251305	.	.	
SEQUENCE	netOGlyc-4.0.0.13	CARBOHYD	83	83	0.758627	.	.	#POSITIVE
SEQUENCE	netOGlyc-4.0.0.13	CARBOHYD	89	89	0.37597	.	.	
SEQUENCE	netOGlyc-4.0.0.13	CARBOHYD	91	91	0.424798	.	.	
SEQUENCE	netOGlyc-4.0.0.13	CARBOHYD	94	94	0.134364	.	.	
SEQUENCE	netOGlyc-4.0.0.13	CARBOHYD	116	116	0.0863541	.	.	
SEQUENCE	netOGlyc-4.0.0.13	CARBOHYD	124	124	0.0419367	.	.	
SEQUENCE	netOGlyc-4.0.0.13	CARBOHYD	134	134	0.175481	.	.	
SEQUENCE	netOGlyc-4.0.0.13	CARBOHYD	138	138	0.0409012	.	.	
SEQUENCE	netOGlyc-4.0.0.13	CARBOHYD	169	169	0.0126901	.	.	
SEQUENCE	netOGlyc-4.0.0.13	CARBOHYD	173	173	0.0295553	.	.	
SEQUENCE	netOGlyc-4.0.0.13	CARBOHYD	174	174	0.399846	.	.	
SEQUENCE	netOGlyc-4.0.0.13	CARBOHYD	184	184	0.0790847	.	.	
SEQUENCE	netOGlyc-4.0.0.13	CARBOHYD	188	188	0.0891984	.	.	
SEQUENCE	netOGlyc-4.0.0.13	CARBOHYD	187	187	0.1469312	.	.	

Supplementary Figure 4. *In silico* analysis of glycosylation post-translational modification. A) N-glycosylation sites predictions. B) O-glycosylation sites predictions.



Supplementary Figure 5. Analysis of the effect of O-glycosylation on molecular weight of native *PbFglA* protein. A) Immunoblotting analysis of anti-rPbFglA polyclonal serum. Membranes containing total extracts cultured in BHI for 12h with a glycosylated native *PbFglA*. B) Immunoblotting analysis of anti-rPbFglA polyclonal serum. Membranes containing total extracts cultured in BHI plus OSMI-1 glycosylated inhibitor for 12 h. The non-glycosylated native *PbFglA* is evidenced. N: normoxia; H: hypoxia.

Supplementary File 1

CLUSTAL 2.1 multiple sequence alignment

^a PABG_02094	ATGTCAGCCATCAATGGCGTACTATCACCCACATCGATGAGGACTCCCTCACAGACCTC 60
^b Seq_Pb18	-----AGGTAAATTACACACATCGATGAGGACTCTCTCACAGACCTC 40
^c Seq_P101	-----TCGTTAGGCCCTCGATGAGGACTCTCTCACAGACCTC 37
	* * *****
PABG_02094	AAATCACGCATTGCCTATGCTAAATCTTCTTACAATTTACCGAAGAAGATGGAGCCCTT 120
Seq_Pb18	AAATCACGCATTGCCTATGCTAAATCTTCTTACAATTTACCGAAGAAGATGGAGCCCTT 100
Seq_P101	AAATCACGCATTGCCTATGCTAAATCTTCTTACAATTTACCGAAGAAGATGGAGCCCTT 97

PABG_02094	ATCCAATCAGCCAAGGACATAAGTTGCACCCGCTGTCCTGCCATCCTAGAACAGTCTAC 180
Seq_Pb18	ATCCAATCAGCCAAGGACATAAGTTGCACCCGCTGTCCTGCCATCCTAGAACAGTCTAC 160
Seq_P101	ATCCAATCAGCCAAGGACATAAGTTGCACCCGCTGTCCTGCCATCCTAGAACAGTCTAC 157

PABG_02094	ACCAAACCTCTTCCTACGATATCACCGCAAATCTTGCCCCGCCAACCGGAGCAG 240
Seq_Pb18	ACCAAACCTCTTCCTACGATATCACCGCAAATCTTGCCCCGCCAACCGGAGCAG 220
Seq_P101	ACCAAACCTCTTCCTACGATATCACCGCAAATCTTGCCCCGCCAACCGGAGCAG 217

PABG_02094	GCTGCTACGGAACCCGCTGAAGCCTCCATCTCGAGCTCTCCCTGATCACCAAATATC 300
Seq_Pb18	GCTGCTACGGAACCCGCTGAAGCCTCCATCTCGAGCTCTCCCTGATCACCAAATATC 280
Seq_P101	GCTGCTACGGAACCCGCTGAAGCCTCCATCTCGAGCTCTCCCTGATCACCAAATATC 277

PABG_02094	GTTCACCGCAAGGACTCTCTCAAAAACATACCTGGTTAGACTAGTCAGCAACAAGAACTGG 360
Seq_Pb18	GTTCACCGCAAGGACTCTCTCAAAAACATACCTGGTTAGACTAGTCAGCAACAAGAACTGG 340
Seq_P101	GTTCACCGCAAGGACTCTCTCAAAAACATACCTGGTTAGACTAGTCAGCAACAAGAACTGG 337

PABG_02094	GCGGATGACAGCCCCTCTGGGATTATCTAGATAAAAGTTAGCGTCATTCACACTGGCAAG 420
Seq_Pb18	GCGGATGACAGCCCCTCTGGGATTATCTAGATAAAAGTTAGCGTCATTCACACTGGCAAG 400
Seq_P101	GCGGATGACAGCCCCTCTGGGATTATCTAGATAAAAGTTAGCGTCATTCACACTGGCAAG 397

PABG_02094	GCCGGTTCAAGCACCGAGAAAAGAGAACCAAGCTCCGTGTCGAGTTATGCATATGTCG 480
Seq_Pb18	GCCGGTTCAAGCACCGAGAAAAGAGAACCAAGCTCCGTGTCGAGTTATGCATATGTCG 460
Seq_P101	GCCGGTTCAAGCACCGAGAAAAGAGAACCAAGCTCCGTGTCGAGTTATGCATATGTCG 457

PABG_02094	CTGCTGCTAGGGTTGTGGAAGATCTGATGCTCAAAACTACATTGGCGGCTGATGGCCTG 540
Seq_Pb18	CTGCTGCTAGGGTTGTGGAAGATCTGATGCTCAAAACTACATTGGCGGCTGATGGCCTG 520
Seq_P101	CTGCTGCTAGGGTTGTGGAAGATCTGATGCTCAAAACTACATTGGCGGCTGATGGCCTG 517

PABG_02094	GATCTCGGACTAAGACGAGCGTTCTCGCTCGTTAATAAGCTGATGTGGATCCAGAAT 600
Seq_Pb18	GATCTCGGACTAAGACGAGCGTTCTCGCTCGTTAATAAGCTGATGTGGATCCAGAAT 580
Seq_P101	GATCTCGGACTAAGACGAGCGTTCTCGCTCGTTAATAAGCTGATGTGGATCCAGAAT 577

PABG_02094	GATCTGTTCTAAGACATTATGTTGCAGAGAACGCCGGAGTTGGATTGA----- 648
Seq_Pb18	GATCTGTTCTAAGACATTATGTTGCAGAGAACGCCGGAGTTGTG-GTGTAACTCGAAGA CA 641
Seq_P101	GATCTGTTCTAAGACATTATGTTGCAGAGAACGCCGGAGTTGTG-G-GTACTCTCGAAGA TA 637

^aPABG_02094 (EEH19835.1): sequence of *Pa03-fglA* gene available from the genomic library;

^bSeq_Pb18 sequence of *Pb18-fglA* gene sequenced in this study; ^cSeq_P101: identification of the *P101-fglA* gene sequenced in this study. “*” indicates an identical nucleotide in the three sequences.

Supplementary File 2

Figure 1. MS/MS spectrum of rFglA identification by mass spectrometry.

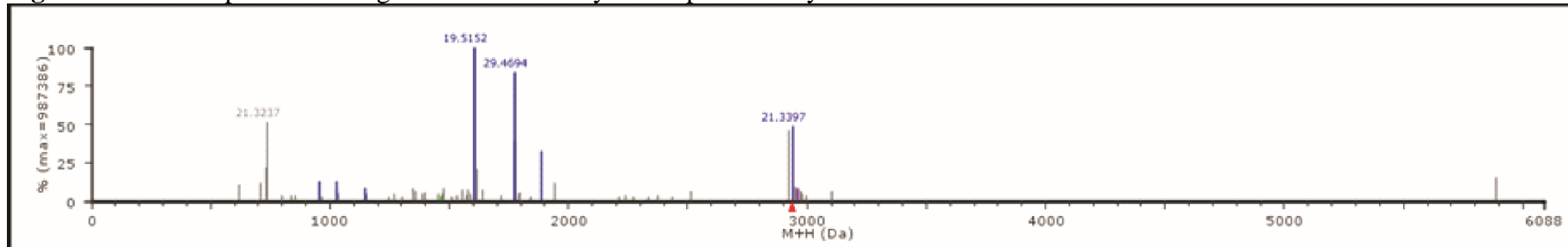


Table 1: Identification of rPbFglA by mass spectrometry.

ID	Description	Length (aa)	Mass	Protein Score	Protein SeqCover (%)	Number of peptides	Peptide Sequence	Peptide Score
PADG_00496/ XP_010756372. 1	hypothetical protein	216	24355,0635	36452,87	66,05	16	TITHIDEDSLTDLK NWADDSPFWDYLDK QPEQAATEPAEASISELSDLHPNIVHR DIVAPAVPAILEAVYTK SFLQFTEEDGALIQSAK TSVLAAFNK LLSYDITAK TTLAADGLDLR QPEQAATEPAEASISELSDLHPNIVHR LMWIQNDLFLR HYVAEKPELD TITHIDEDSLTDLKSR LMWIQNDLFLR LAAFNK EKPELD TTLAADGLD	71824.29 75182.01 109151.3 59927.38 81214.92 9147.442 15054.25 6444.653 144.9853 5315.528 8153.629 150.0182 9666.843 205.9834 126.1243 187.5786

Capítulo III Manuscrito 2

5. iTRAQ-based proteomic and phosphoproteomic analysis of *Paracoccidioides brasiliensis* in response to hypoxia.

Lucas Nojosa Oliveira^{a,b}, Danielle Silva Araújo^{a,b}, Igor Godinho Portis^{a,c}; Agenor de Castro Moreira dos Santos Júnior^{b,d}; Alexandre Siqueira Guedes Coelho^e; Patrícia de Sousa Lima^f, Wagner Fontes^d; Carlos André Ornelas Ricart^d; Célia Maria de Almeida Soares^{a,*}

^aLaboratório de Biologia Molecular, Instituto de Ciências Biológicas, ICB II, Campus II, Universidade Federal de Goiás, 74001-970, Goiânia, Goiás, Brazil;

^bPrograma de Pós-graduação em Patologia Molecular, Faculdade de Medicina, Universidade de Brasília, 70910-900, Brasília, Distrito Federal, Brazil;

^cPrograma de Pós-graduação em Genética e Biologia Molecular, Instituto de Ciências Biológicas, Universidade Federal de Goiás, 74001-970, Goiânia, Goiás, Brazil;

^dDepartamento de Biologia Celular, Instituto de Biologia, Universidade de Brasília, Campus Darcy Ribeiro, Asa Norte, 70910-900, Brasília, DF, Brazil

^eLaboratório de Genética e Genômica de Plantas, Escola de Agronomia, Universidade Federal de Goiás, Goiânia, Brazil

^fLaboratório Interdisciplinar de Biologia, Universidade Estadual de Goiás, Itapuranga, Goiás, Brazil

*Corresponding author

Célia Maria de Almeida Soares
Laboratório de Biologia Molecular
Instituto de Ciências Biológicas II
Câmpus Samambaia
Universidade Federal de Goiás
74690-900, Goiânia, Goiás – Brazil
Tel/Fax: +55 62 3521 1110
E-mail address: cmasoares@gmail.com

Key-words: oxygen, stress response, phosphoproteome, phosphopeptide.

Abstract

When in saprobiosis or during host infection members of the *Paracoccidioides* complex face decreased oxygen levels. The oxygen limitation induces *Paracoccidioides lutzii* to reprogram the central metabolism by shifting the production of electrons by the TCA to the GABA shunt pathway to obtain energy through oxidative phosphorylation. In *Paracoccidioides brasiliensis*, subject of the present work, the response to hypoxia has not been investigated and the regulation of the adaptive process is still unknown. Here we show the *P. brasiliensis* adaptation at the protein and phosphoprotein levels during hypoxia. This approach allowed identification of 232 proteins and 27 phosphoproteins differentially expressed under hypoxia. These results revealed that the methylcitrate cycle is fed by propionyl-CoA from beta-oxidation and oxaloacetate derived amino acids degradation/TCA. The pyruvate formed is directed to alcoholic fermentation. In addition, *P. brasiliensis* yeast cells regulated phosphoproteins are related to the biological processes of cell cycle and transcription. This work contributes to the understanding of the adaptive mechanisms of *P. brasiliensis* under hypoxia and its putative regulation by phosphorylation.

Introduction

It is believed that thousands of people are infected by *Paracoccidioides* spp. These fungi are responsible for a neglected systemic mycosis, called Paracoccidioidomycosis (PCM)¹. This disease is endemic in Latin America, and around 80% of the patients acquire PCM in Brazil², representing approximately 49% of hospital admissions among all mycoses³ and accounting for 51% of deaths due to fungal infections⁴. For the establishment of infection several molecular mechanisms are engineered by the fungus in an attempt to evade the potent defense arsenal of the host's immune system⁵. Yeast cells from *Paracoccidioides* spp. can survive the stresses imposed by the host for years⁶ developing a chronic disease in the majority (74-96%) of the patients⁷.

In the course of the infection in the mammalian host, pathogenic fungi find an environment with reduced oxygen tension, in which they trigger numerous metabolic adaptations, mainly related to energy, guaranteeing their survival⁸. In order to clarify how those adaptations occur, transcriptomic and proteomic data in response to oxygen limitation are being obtained in several species of fungi. In summary, the results show a radical change

in energy production, besides relevant changes in morphology, virulence and susceptibility to drugs⁹⁻¹⁵. In *Paracoccidioides lutzii*, Pl01, responses to hypoxic stress evidenced an intense modulation in several metabolic pathways. At first (12h), there is a reduction in the protein levels of central energy pathways, such as glycolysis, TCA and mitochondrial electron transport⁹. However, after 24 hours in a stressor environment, glycolysis and mitochondrial electron transport are reestablished, and gluconeogenesis, GABA shunt and beta-oxidation pathways are increased⁹.

It is known that the reduction of metabolic rate during hypoxia may directly influence protein phosphorylation owing to the lack of high energy phosphate¹⁶. Protein phosphorylation is one of the most important post-translational phenomena, functioning as a key role in signal transduction. It is known that protein phosphorylation is involved in several important biochemical events, which ensure cell cycle maintenance, cell adhesion, survival, proliferation and differentiation¹⁷⁻²⁰. In eukaryotes, phosphorylation occurs mainly in residues of serine (Ser), threonine (Thr), tyrosine (Tyr) and histidine (His)^{21,22}.

Previous work has shown some aspects of phosphorylation in the *Paracoccidioides* genus. In this respect, *in silico* analysis of the available genome of *Paracoccidioides* spp. revealed the presence of five cascades of mitogen-activated protein kinase (MAPK) signaling²³. The MAPK pathways, for example, can control many important processes, including filamentation, mating, biofilm formation, and stress resistance, through phosphorylation/dephosphorylation cycles²⁴. Sestari *et al.* (2018) evidenced that, when protein kinase A (PKA) is inhibited, the natural dimorphism of *P. lutzii* is prevented suggesting its importance in establishing infection²⁵. Also, phosphorylation is the main regulatory mechanism that controls the activity of *P. brasiliensis* isocitrate lyase (*PbICL*) which is essential for fungal metabolism in non-preferential carbon sources such as acetate and/or fatty acids²⁶. Recently, the proteomic map of phosphorylated proteins during oxidative stress was obtained for *P. brasiliensis* and was possible to identify 230 phosphoproteins acting in different signaling pathways for the elimination of reactive oxygen species (ROS) and the responses to oxidative stress²⁷.

It is clear that different species of fungi when submitted to hypoxia undergo cellular modifications that are determinant for their survival^{9-15,28,29}. Nonetheless, hypoxia-induced phosphoproteins are poorly understood. Since there is no information about how protein

phosphorylation acts in the response to hypoxia, we set out to provide an initial overview of phosphoprotein profile during this stress. The association of proteomic and phosphoproteomic data in hypoxia revealed that *P. brasiliensis* reprograms its energy metabolism, obtaining energy primarily through alcoholic fermentation. Also, remodeling of membrane and cell wall was observed, and maintaining the general cell functions of the cell cycle stacked. Our results highlight the hypoxia-responsive events in *P. brasiliensis*.

Experimental procedures

Growth conditions

P. brasiliensis, strain 18 (ATCC 32069) was used in all experiments. The yeast cells were cultivated for 5 days, at 36 °C in BHI solid medium plus 4% (w/v) glucose. Strains were grown in BHI liquid medium at 36 °C. Normoxic conditions were considered atmospheric levels within the lab (~21% O₂). For hypoxic levels a chamber multi-gas controlled (Multi-Gas Incubator MCO-19M-UV, Panasonic Biomedical) was kept at gas mixture containing 1% O₂, 5% CO₂ and 94% N₂⁹.

Protein extraction

Yeast cells cultivated under normoxia and hypoxia were harvested at time-point of 12 hours. For each experimental condition, biological triplicates were obtained. The protein extraction was performed as described by Villén and collaborators ³⁰. Briefly, the cells were re-suspended in cold Extraction buffer (8 M urea, 75 mM NaCl, 50 mM Tris, pH 8.2, 50 mM β-glycerophosphate, 1 mM sodium orthovanadate, 10 mM sodium pyrophosphate and 1 mM PMSF). After, the cells were disrupted by vigorous mixing with glass beads, processed on ice in a beadbeater apparatus for four cycles of 90 s, in maximum speed. Then, lysates were centrifuged at 15,000 x g for 15 min at 4 °C until no pellet formation and the supernatant was recovered. Proteins concentrations were estimated using a Qubit™ protein assay kit according to the manufactory's instruction (Invitrogen).

In-solution protein digestion

Estimated 150 µg of the protein extract of each condition/replicate was prepared for trypsin digestion as described in Queiroz and collaborators³¹ with slight modifications. Ice-cold acetone was added to the protein suspension and the mixture was vortexed and incubated overnight at -20 °C. After, the samples were centrifuged at 20,000 x g for 15 min at 4 °C and re-suspended in 8 M urea in 0.05 M triethylammonium bicarbonate - TEAB, pH 7.9. Next, proteins were reduced with 0.005 M DTT for 25 min at 55 °C and alkylated with 0.014 M iodoacetamide for 40 min at room temperature in dark. Samples were diluted 5-fold with 0.001 M CaCl₂ in 0.025 M TEAB, pH 7.9. Modified trypsin (Promega, Madison, WI, USA) was added in 1:50 (w/w) substrate ratio. The samples were incubated overnight at 37 °C. The peptide samples were acidified with 0.1% (v/v) TFA and desalted on homemade C18 microcolumns in p200 low-binding tips. Thereafter, all samples were dried in speed vacuum.

Isobaric tag labeling

The peptide mixtures were labeled with iTRAQ (Sciex) according to manufacturer's procedures. Fifty micrograms of the desalted and dried peptides were resuspended in 17 µL of 300 mM TEAB and added to iTRAQ label resuspended in ethanol. The samples were incubated for 2 hours at room temperature. Equimolar amounts of iTRAQ label were mixed in all samples (normoxia labeled with 114; hypoxia with 117).

Phosphopeptide enrichment

In order to enrich phosphopeptides, a part of digested peptides was applied a metal oxide chromatography with TiO₂ phosphoaffinity beads. Briefly, iTRAQ-labeled multiplexed samples were re-suspended in solution of 1 M glycolic acid in 80% (v/v) acetonitrile/5% (v/v) TFA, added 0.6 mg of TiO₂ beads per 100 µg of peptides. The suspension was subjected to shaking (200 rpm) for 20 min, and collected by centrifugation. To the supernatant was added 0.3 mg of TiO₂ beads per 100 µg of peptides and the mixture was subjected to shaking for 20 min; the round was repeated once. The TiO₂ beads from the three incubations were pooled and washed first with 80% (v/v) acetonitrile/1% (v/v) TFA,

and then 10% (v/v) acetonitrile/1% (v/v) TFA to remove non-specific binding. After natural dried, was added to the TiO₂ beads solution of 1.5% (w/v) NH₄OH, pH 11.5 and the mixture was dried in speed vacuum and re-suspended in 1% (v/v) formic acid prior to LC-MS/MS.

LC-MS/MS

iTRAQ labelled peptides were analyzed with three technical repetitions each and separated using a nano-UHPLC Dionex Ultimate 3000 (Thermo Fisher Scientific) coupled with an Orbitrap Elite™ Hybrid Ion Trap-Orbitrap Mass Spectrometer (Thermo Fisher Scientific). Each fraction was loaded onto a pre-column (110 µm x 200 nm) packed in-house with C18 ResiproSilPur of 5 µm with 120 Å pores (Dr. Maisch GmbH, Ammerbuch, Germany). Second chromatography was carried out in column (75 µm x 35 nm) packed in-house with C18 ResiproSilPur of 3 µm with 120 Å pores (Dr. Maisch GmbH, Ammerbuch, Germany) and eluted using a gradient from 100% solvent A [0.1% (v/v) formic acid] to 26% solvent B [0.1% (v/v) formic acid, 95% (v/v) acetonitrile] for 180 min, followed from 26% to 100% solvent B for 5 min and 100% solvent B for 8 min (a total of 193 min at 200 nL/min). After each run, the column was washed with 90% solvent B and re-equilibrated with solvent A. Mass spectra were acquired in positive ion mode applying data-dependent automatic survey MS scan and tandem mass spectra (MS/MS) acquisition modes. Each MS scan in the Orbitrap analyzer (mass range = *m/z* 350–1800, resolution = 120,000) was followed by MS/MS of the fifteen most intense ions in the LTQ. Fragmentation in the LTQ was performed by high-energy collision-induced dissociation (HCD), and selected sequenced ions sequences were dynamically excluded every 15 s.

MS/MS spectra process

Raw data processing was performed using Proteome Discoverer v.1.3 beta (Thermo Scientific). The Raw files were submitted to a database search using Proteome Discoverer with Mascot v.2.3 algorithm against the *P. brasiliensis* database, downloaded using the Database on Demand tool in UniProt/SWISS-PROT (<http://www.uniprot.org/>) and NCBI (www.ncbi.nlm.nih.gov/genome/?term=Paracoccidioides) database. The searches were

performed with the following parameters: MS accuracy - 10 ppm; MS/MS accuracy - 0.05 Da; two missed cleavage sites allowed; carbamidomethylation of cysteine as a fixed modification; and oxidation of methionine, N-terminal iTRAQ tagging, phosphorylation of S, T, and Y residues, and protein N-terminal acetylation as variable modifications. The numbers of proteins, protein groups, and peptides were filtered for false discovery rates less than 1%. A minimum of two peptides per protein was accepted for identification using Proteome Discoverer. The identification lists from technical repetitions were merged, and repeated protein groups were removed. Phosphopeptide identifications with phosphorylation site probability scores less than 75% were removed, as suggested by the software developer.

Data analysis

The data consisted of three replicates containing global proteome and phospho-enriched fractions. To increase the reliability, we applied the following criteria: i) proteins identified with at least 1 unique peptide, ii) with high or medium FDR and, iii) in at least 2 of 3 replicates. The intensity values of each iTRAQ-labeled were log-transformed and applied unpaired Student's *t*-test. Statistical difference was set at p-value ≤ 0.05 and significant difference was set at p-value ≤ 0.01 ³².

Functional categories were determined by search in Blast2GO platform (<http://www.blast2go.com/b2gome>), Pedant on MIPS-Functional Catalogue (<http://pedant.helmholtz-muenchen.de/>) and KEGG database (<http://www.genome.jp/kegg/>). Sequence annotation was assessed using a BlastP algorithm (<http://blast.ncbi.nlm.nih.gov/Blast.cgi>). Finally, consensus motifs were determined using online algorithm Motif-X (<http://motif-x.med.harvard.edu/>;³³) with build of 13 amino acids centered on phosphorylation site. All algorithms are used in default parameters.

Labelling procedures

P. brasiliensis yeast cells cultivated under normoxia and hypoxia were collected at density of 10^6 cells and incubated with 400 μM of MitoTracker Green FM (Sigma-Aldrich), or 1.2 μM of Rhodamine 123 (Sigma-Aldrich) for 30 min at 36°C in order to evaluate

mitochondrial integrity and functionality, respectively. Glucan levels were measured by dying with 100% (v/v) of Aniline Blue (AB, Sigma-Aldrich) for 5 min at room temperature under stirring. Levels of chitin were assessed after dying with 100 µg/mL of Calcofluor White (CFW, Sigma-Aldrich) for 15 min at room temperature. After dye incubation, the samples were washed twice with PBS 1X and the stained suspension was observed using Axio-Scope A1 Microscope (Carl Zeiss AG, Germany). The minimum of 50 cells for each microscope slides, in triplicates, were assessed to measure of the fluorescence intensity (in pixels) through the AxioVision Software (Carl Zeiss AG, Germany), and Student's *t*-test p-values ≤ 0.01 were considered statistically significant.

Enzymatic activities

Cytochrome C Oxidase: to determine the cytochrome c oxidase (CCO) activity, we used the Cytochrome C Oxidase Assay Kit (Sigma Aldrich – CYTOCOX1) as determined by the manufacturer. The CCO activity was evaluated by a colorimetric assay based on observation of the decrease in absorbance of Ferrocytochrome C at 550 nm caused by its oxidation to Ferricytchrome C by CCO. Triplicates were obtained for each condition. The results were considered statistically significant at p-values ≤ 0.01 by Student's *t*-test.

Methylcitrate synthase: the methylcitrate synthase activity was measure as described previously³⁴. The reaction mix contained 50 mM Tris/HCl, pH 8.0; 1 mM DTNB [5,5'-dithiobis-(2-nitrobenzoic acid), Sigma]; 0.2 mM propionyl-CoA (Sigma) and cell-free extracts of normoxia and hypoxia, in a final volume of 1 mL. The reaction was started by the addition on 1 mM oxaloacetate and monitored at 412 nm. One unit of enzyme activity was defined as the amount of enzyme producing 1 µmol CoASH/min/µg de protein. The results were considered statistically significant at p-values ≤ 0.01 by Student's *t*-test.

Biochemical tests

Ethanol: the concentration of intracellular ethanol was measured by the enzymatic detection kit as described in manufacturer's instructions (Ethanol UV-method, R-Biopharm, Darmstadt, Germany). This assay measures the amount of NADH released after the

oxidation of ethanol to acetaldehyde followed by oxidation of acetaldehyde to acetic acid. For proper this, 10^8 *P. brasiliensis* yeast cells were recovered after normoxic and hypoxic incubation and prepared as described in manufacturer's instructions. Triplicates were obtained for each condition. The results were considered statistically significant at p-values ≤ 0.01 by Student's *t*-test.

Reduced thiol: free thiol levels were determined using Ellman's reagent, 5, 5'-dithio-bis-(2-nitrobenzoic acid) (DTNB - Sigma Aldrich). A total of 10^6 *P. brasiliensis* yeast cells were obtained after normoxic and hypoxic incubation and lysed as described by Pigozzo *et al.* (2017). After centrifugation, 100 mL of the supernatant was added to 100 mL of 500 mM phosphate buffer, pH 7.5, followed by the addition of 20 ml of 1 mM DTNB. Absorbance was measured at 412 nm using a plate reader. Triplicates were obtained for each condition. The results were considered statistically significant at p-values ≤ 0.01 by Student's *t*-test.

Immunoblotting

Denatured proteins (40 µg) were loaded on 12% SDS-PAGE and after gel electrophoresis, proteins were stained with Coomassie Blue R or transferred to Hybond ECL membrane (GE Healthcare). Thereafter, membranes were incubated with PBS solution, added of 10% (w/v) non-fat milk and 0.1% (v/v) Tween 20 (PBS-T) for 2h to block non-specific sites. After blocking, membranes were incubated with anti-phosphoSer/Thr (1:1,000; Sigma-Aldrich) and anti-phosphoTyr (1:500; Sigma-Aldrich) polyclonal antibody for 2h. Membranes were washed in PBS-T, followed by incubation with peroxidase conjugated secondary antibody (1:1,000; GE Healthcare), at dark at room temperature, for 1 h. Labelled slots detection was performed using the ECL reagent (GE Healthcare) following a detection Film (Lumi-Film Chemiluminescent, Roche Diagnostics Germany).

Results and Discussion

Overview of metabolic pathways regulated in P. brasiliensis

Proteomic approaches have been largely used in *Paracoccidioides* genus to highlight metabolic changes in stressors conditions^{27,35–37}, in nutrients depletion^{9,38–42} and in infection models^{43,44}. It is clear that oxygen-limitation modulates the proteomic response in *P. lutzii*, *Pb01*⁹ allowing its survival. In this sense, we aimed to characterize the response of *P. brasiliensis* (*Pb18*) during hypoxia. For that we obtained the total extract of yeast cells during normoxia (atmospheric tensions) and hypoxia (1% O₂) at the 12 hours' time-set. First, protein extracts were evaluated on SDS-PAGE. The result shows the high quality of the protein extraction (Supplementary Figure 1). Then, in-solution trypsin digested followed by iTRAQ-labeling peptides was analyzed by liquid chromatography in tandem mass spectrometry (LC-MS/MS). Data revealed 5,997 identified peptides, resulting in 1,190 protein hits containing 5,643 unique peptides. Next, the Student's *t*-test at p-value ≤ 0.01 was used as a threshold to determine the differentially proteins, as described in Yao and co-workers³². As result, *Pb18* presented a total of 76 and 156 significant increased and decreased proteins, respectively, under hypoxia compared with normoxia (control).

Several biological processes were altered as shown in Tables S1 and S2, and Supplementary Figure 2. Proteins with increased or decreased expression during hypoxic stress were categorized according to the Blast2GO platform, Functional Catalogue (FunCat2) and KEEG database. As summarized in Supplementary Figure 2A, proteins involved with metabolism (25%) and energy (24%) categories were more representative as up than down regulated. The energy subcategories such as glycolysis/gluconeogenesis, tricarboxylic acid pathway (TCA), methylcytrate cycle (MCC), fermentation and specific enzymes from energy conservation were up regulated (Table S1). In contrary, only the pentose-phosphate pathway and other enzymes involved with energy conservation were depicted as down regulated in *Pb18* under hypoxia stress (Table S2). Importantly, proteins belonging to cell cycle, transcription, translation, protein fate/degradation and cellular transport were represented much more by down than up regulated proteins, indicating that core cellular processes were directly decreased by hypoxia in *Pb18* (Supplementary Figure 2B). Interestingly, proteins involved with protein synthesis have expressive up and down regulated amounts (Supplementary Figure 2B). A group of proteins involved in cellular communication process was only negatively regulated (Supplementary Figure 2B, Table S2).

Energy and metabolism were the main regulated protein clusters

Hypoxic stress in *P. brasiliensis*, *Pb18*, provoked a relevant remodeling of energy metabolism. Concerning carbohydrate metabolism, stress induces a specific protein related to gluconeogenesis upon 12 h of hypoxia (Figure 1, Table S1). The enzyme phosphoenolpyruvate carboxykinase (PADG_08503) participates only in gluconeogenesis. In cytoplasm, it catalyzes the conversion of oxaloacetate to phosphoenolpyruvate⁴⁵, essential in gluconeogenesis. As down regulated, the 6-phosphogluconolactonase enzyme (PADG_07771) from pentose phosphate shunt, reinforces the idea of the carbon flux flowing to glucose production (Table S2, Figure 1). We suggest that the produced glucose can be directed to form cell wall structural elements.

Regarding beta-oxidation pathway, three specific enzymes were up regulated and results in the production of acetyl-CoA and propionyl-CoA (Figure 1). The enzymes acyl-CoA dehydrogenase (PADG_06805), enoyl-CoA hydratase (PADG_01209) participate in mitochondrial and peroxisomal beta-oxidation. Interesting, a specific peroxisomal 3-ketoacyl-CoA thiolase (PADG_03194) was up regulated (Figure 1, Table S1). This suggests that peroxisome beta-oxidation is activated. In accordance with *Pb01*, the abundance of some enzymes involved in acetyl-CoA production was up regulated in 12 h of hypoxia compared to normoxia⁹. Acetyl-CoA can be used in various metabolic processes and its fate will be discussed below. On the other hand, propionyl-CoA is oxidized with the oxaloacetate for the activation of the methylcitrate cycle, producing pyruvate⁴⁶.

Pyruvate is a key intermediate in several metabolic pathways. Our data showed that this molecule is probably used for ethanol and acetyl-CoA synthesis (Figure 1). To better understand how pyruvate is being consumed there is a need to understand how the pyruvate is being produced since glycolysis is not activated. Our results showed that there are some enzymes up regulated from two important pathways used for anaplerosis of several compounds from mitochondria, the cycle of the tricarboxylic acid (TCA) and methylcitrate cycle (MCC) (Figure 1). A total of four enzymes were found from TCA cycle: succinyl-CoA synthetase (PADG_02266), succinate dehydrogenase (PADG_08013), fumarate reductase - NADH (PADG_02592) and malate dehydrogenase (PADG_07210) (Table S1). Even more, fumarate reductase is, in anaerobic conditions, an enzyme that produces fumarate from succinate⁴⁷, independently from the electron transport chain⁴⁸. All of these TCA enzymes support the oxaloacetate synthesis, which feeds gluconeogenesis as cited above or, interesting, activate the methylcitrate cycle. To confirm the activation of the MCC, the

specific activity of methylcitrate synthase (MCS) was checked. This assay revealed that the MCS is more active during oxygen-limitation (Figure 2). The MCS is a methylcitrate cycle specific enzyme and promotes the condensation of propionyl-CoA with oxaloacetate^{34,46}. Additionally, the enzyme 2-methylcitrate dehydratase (PADG_04718) was up regulated in *Pb18* under hypoxia (Table S1). These enzymes catalyze the second step of the methylcitrate cycle of propionate catabolism⁴⁶. One of the products from methylcitrate pathway is pyruvate, reinforcing all the carbon flux suggested (Figure 1). To complete, the enzyme aspartate aminotransferase (PADG_01621) was up regulated and is involved in oxaloacetate and glutamate production from aspartate⁴⁹.

Concerning to alcoholic fermentation, in cytoplasm, ethanol can also be produced from pyruvate (Figure 1). The enzyme alcohol dehydrogenase 1 (PADG_11405) and aldehyde dehydrogenase (PADG_05081) are related to ethanol and acetate production, respectively, from pyruvate⁵⁰. Ethanol measurement was performed, and the results showed that there is a significantly higher level of ethanol under hypoxia stress compared to normoxia (Figure 3). Possibly, these molecules can be used as energy source since gluconeogenesis is important to supply structural molecules such those involved in cell wall. In fact, there is an attempt to overcome the negative effect of the oxygen-limitation in the electrons transport chain. Microscopy analysis using specific dyes showed that the amount of mitochondria in hypoxia and normoxia cells was similar (Figure 4A). On the other hand, the mitochondrial electric potential was affected by hypoxia (Figure 4B). Rhodamine is a permeable lipophilic cationic fluorescent probe that accumulates in mitochondria and is distributed electrophoretically into the mitochondrial matrix in response to mitochondrial electric potential^{51,52}. Interestingly, several proteins from oxidative phosphorylation were up regulated but some of them, especially from cytochrome c complex, were down regulated in our analysis (Table S2). The proteins detected were: cytochrome c oxidase assembly factor 6, PADG_08152; cytochrome c oxidase subunit, PADG_06995; cytochrome c oxidase subunit 4 mitochondrial, PADG_04397 and cytochrome c oxidase-assembly factor COX23 mitochondrial, PADG_04072; ATP synthase subunit delta, PADG_07789; F-type H⁺-transporting ATPase subunit h, PADG_00688; NADH-ubiquinone oxidoreductase, PADG_11513; and ubiquinol-cytochrome c reductase subunit 7, PADG_04501. In this sense, we measured the activity of cytochrome c oxidase as shown in Figure 5. The oxidized Ferrocyanochrome C was maintained when tested with the hypoxic protein extract, contrary

to normoxia samples, that similar to the positive control, reduced the Ferrocyanochrome C to Ferricytchrome C. Cytochrome c oxidase reduces molecular oxygen in a reaction coupled with a proton pumping process ⁵³. For this reason, we believe that the mitochondrial reactions are being affected by hypoxia.

Hypoxia induces membrane and cell wall remodeling

The response to oxygen-limitation affects the cell wall and membrane of fungi leading to overall changes in those structures ⁵⁴⁻⁵⁶ and can enhances innate immune activation ⁵⁴. For adequate evaluation of cell wall remodeling in hypoxia, Aniline Blue and Calcofluor White dyes were used to label glucans and chitin, respectively. As shown in Figure 6, upon hypoxia, *P. brasiliensis* increases its glucan content in the cell wall (Figure 6A). On the other hand, there was no change in the levels of chitin, which remains in basal amounts (Figure 6B). These findings indicate that glucose production by gluconeogenesis is directed to the glucans synthesis. An accumulation of glucan was also found when yeast cells of *P. lutzii* were subjected to osmotic stress, ensuring osmo-cell homeostasis ³⁷. It is known that the external layer of α-glucan prevents the recognition of *Histoplasma capsulatum* ^{57,58} and *Paracoccidioides* sp. ⁵⁹ by host's immune system . In opposing, *Aspergillus fumigatus* increased the exposure of β-glucan during hypoxia, enhances the dectin-1 recognition ⁵⁴.

Acetyl-CoA had a buildup from the beta-oxidation pathway and oxidation of pyruvate from pyruvate dehydrogenase complex. The evidence is that the acetyl-CoA molecule is feeding the mevalonate pathway because the enzyme acetyl-CoA C-acetyltransferase (PADG_06382 and PADG_02751) was up regulated (Table S1). This enzyme is also named as Erg10 and catalyzes the formation of acetoacetyl-CoA in the biosynthesis of mevalonate, an intermediate required for the biosynthesis of sterols and nonsterol isoprenoids ⁶⁰. Acetoacetyl-CoA probably is produced by the butanoate metabolism since we found the 3-hydroxybutyryl-CoA dehydrogenase (PADG_01228) with high expression level (Table S1). It catalyzes the NAD-dependent oxidation of beta-hydroxybutyryl-CoA to acetoacetyl-CoA from butanoate metabolism ⁶¹, also supporting the ergosterol biosynthesis (Figure 1). In fungi such as *Candida albicans*, *Cryptococcus neoformans*, *A. fumigatus* and *Aspergillus nidulans*, it is described that the fatty acids and

ergosterol metabolism are increased in response to hypoxia and is clear that the ergosterol molecule is important to stability, fluidity and structure of the fungi plasma membrane^{11,12,62-65}. In *P. lutzii*, submitted to hypoxia, proteins involved with ergosterol metabolism were also detected⁹.

Neutralization of stress generated by H₂O₂

The peroxisomal beta-oxidation could generate reactive oxygen species such as hydrogen peroxide⁴⁵. Interesting, we found the peroxiredoxin enzyme (PADG_04912) as up regulated under hypoxia. This enzyme is a peroxidase that can reduce hydroperoxides and it has been viewed mainly as a cytoprotective antioxidant enzyme acting against endogenous or exogenous peroxide attacks⁶⁶. Other peroxiredoxin are thiol specific antioxidant (TSA) and thioredoxin peroxidase (TPx)⁶⁷. These enzymes share the same basic catalytic mechanism in which a redox active site is oxidized to a sulfenic acid by the peroxide substrate⁶⁸. In this sense, we performed a dosage of reduced thiol from normoxia and hypoxia protein samples and the result show that this organosulfur compound is more reduced in hypoxia than normoxia (Figure 7). Additionally, mitochondrial response to oxidative stress is prevented by the action of cytochrome c peroxidase - PADG_03163 (Figure 7), while superoxide dismutase [Cu-Zn] (PADG_07418) and glutathione peroxidase (PADG_04587) are down regulated (Figure 7). Notably, disulfide-isomerase (PADG_03841) also up regulated. (Figure 7). The activity of such proteins enables the process of cellular detoxification generated by the metabolic processes during hypoxia.

Phosphoproteome and phosphopeptide analysis

We hypothesize that hypoxia response could be regulated, in part, by the phosphorylation events. That way, we aimed at verifying the *P. brasiliensis* phosphoproteome during hypoxic stress. For this, was obtained the protein extract in phospho-protective extraction buffer and were carried out the immunoassay and phospho-enrichment following by MS analyzes.

For proper qualitatively assess the profile of phosphorylation during O₂-limitation, immunoassays were performed using anti-phosphoSer/Thr and anti-phosphoTyr antibodies. As shown in Figure 8, thereis a distinct band pattern in the phosphorylation to serine/threonine (panel A) and tyrosine (panel B) phosphorylation makers. Bands distribution clearly indicates that the hypoxia conditions modulate distinct phosphorylation events, and this suggest that different patterns could be directly linked to *P. brasiliensis* response to hypoxia. In pioneering studies, proteomic analysis clearly showed the important role of phosphorylation in the dimorphic transition of *P. brasiliensis* (in submission), as well as when subjected to oxidative stress ²⁷, reinforcing our hypothesis that phosphorylation may also be involved in adaptation to hypoxia.

In order to access the profile of phosphorylated proteins during hypoxia, we applied the TiO₂ enrichment technique. This technical step allows concentrating phosphopeptides that are less abundant when in the complex sample mixture by the affinity between the phosphate group and the covalent oxides metals ⁶⁹. According to the inclusion criteria, it was possible to identify 206 phosphorylation sites in 160 peptides comprising 73 proteins (Supplementary Figure 3, panel A; Table 1). Most of the peptides (119 out of 160 - 74.4%) presented only one phosphorylated site, while 22.5% (36 out 160) and 3.1% (5 out 160) flaunted two or three phosphorylated sites, respectively (Supplementary Figure 3, panel B). The most numerous phosphorylated amino acid residue was that of serine, followed by that of threonine (Supplementary Figure 3, panel C). It is known that histidine is also a target for phosphorylation, but the binding of the phosphate in this amino acid residue is intensely labile ²¹, impairing the identification by the current proteomic methods.

The phosphorylation event depends on the recognition of a consensus amino acid sequence. Using the SGD Yeast Proteome as reference, we searched for the consensus sequences using the Motif-X algorithm as depicted in Figure 9. Remarkably, the result shows a large repeat of the alanine residue in all of the best hits motifs analyzed.

Analysis of biological processes of phosphoproteins revealed that the transcription process has the largest cluster of phosphorylated proteins (18%), followed by the proteins involved in the cell cycle (15%) and protein fate and degradation (10%) as shown in Figure 10, panel A, and Table 1. Interestingly, more than 30% of the phosphorylated proteins have unknown functions (Figure 10, panel A, Table 1). To determine the expression levels of the

phosphorylated proteins, we used the Student's *t*-test at p-value ≤ 0.05 (Table 1). With this statistical filter, 27 proteins were regulated; unexpectedly, all down regulated (Table 1). The main processes in which down-phosphoproteins participate are transcription (22%) and cell cycle (19%), with 37% of them having an unknown function (Figure 10, panel B). By the way, 17 out 27 down-phosphoproteins were down regulated also in the global proteome (Table 1 and S2). As mentioned above, the main group of down regulated proteins in the global proteome during hypoxia were cell cycle and transcription (Figure supplementary 1B, Table S2). Similarly, these clusters were the most phosphorylated, and down regulated when enriched with TiO₂ (Figure 10, Table 1).

Regarding the cell cycle, several proteins had their expression decreased in the global proteome during hypoxia (Table S2). This finding suggests that the cellular command center is operating slowly, probably for energy savings. In addition, phosphoproteome revealed a part of proteins involved with cell segregation had their phosphorylation down regulated during hypoxia. Nuclear segregation protein Bfr1 (PADG_00849) is involved in the secretory pathway, in the spindle pole body and bud formation ^{70,71}. Further, it is directly linked to nuclear segregation, nuclear spindle formation ⁷¹ and acts on the entry and exit of mRNAs in processing bodies, affecting the gene regulation ⁷². Likewise, the Spindle poison sensitivity Scp3 (PADG_05935) is associated with the formation of microtubules related to cytokinesis and chromosomal segregation ⁷³, acting on the microtubule orientation during the mitotic spindle ⁷⁴. It is also correlated with reproduction asexual in fungi ⁷³. Septum formation protein Maf (PADG_06763), drebrin-like protein (PADG_00011) and GYF domain-containing protein (PADG_06945) were phospho-down regulated Table 1.

Concerning phospho-down regulated proteins reported to transcription, RNA polymerase-associated protein LEO1 (PADG_02315), mRNA stability protein (PADG_02346), NTF2 and RRM domain-containing (PADG_07714), Pre-mRNA-splicing factor srp1 (PADG_05340), THO complex subunit 4 (PADG_07285) and PAB1 binding protein (PADG_02996) are involved in RNA synthesis and processing (Table 1). Also, proteins responsible for the initiation of the transcription process were also phospho-down regulated (Table 1). The LEO 1 protein composes the PAF1 complex that directly implicates in the histone modifications, transcript site selection ⁷⁵ and transcriptional elongation by RNA polymerase II ⁷⁶. THO protein is a component of the TREX complex involved in nuclear export of spliced and unspliced mRNA ⁷⁷. Similarly, the NTF2 and PAB1 protein

binds to RNA, through poly (A) tail; NTF2 is responsible by transport the mature mRNA target⁷⁸, while PAB1 participates in the control of poly (A) length⁷⁹.

Interestingly, 19 and 32% of down-regulated proteins in the global proteome and phosphoproteome, respectively, were not eligible for functional classification. These proteins should be better studied because they can have a key secret in the regulation of *P. brasiliensis* during hypoxic stress.

Conclusion

In this research, we have studied the hypoxic adaptation of *P. brasiliensis* by iTRAQ-labelling proteomic, biochemical and molecular analyses. Results revealed that *P. brasiliensis* supports low oxygen tensions, reprogramming its metabolism, living transiently anaerobically. For this, *P. brasiliensis* uses β-oxidation and TCA to support the methylcitrate cycle in the formation of pyruvate, which is then directed towards alcoholic fermentation, contrary of *P. lutzii*. The membrane and cell wall are remodeling increased the content of ergosterol and glucan, respectively. The defense against metabolic residual ROS is active by peroxiredoxin and cytochrome c peroxidase. We also investigated the phosphoproteome. Notably, the global proteome and phosphoproteome revealed that during hypoxia, the yeast cells of *P. brasiliensis* prevents the cell division and has decreased transcription-related functions.

References

1. Teixeira, M. D. M. et al. *Paracoccidioides lutzii* sp. nov.: biological and clinical implications. *Med. Mycol.* **52**, 1–10 (2013).
2. Martinez, R. New Trends in Paracoccidioidomycosis Epidemiology. *J. Fungi* **3**, 1–13 (2017).
3. Coutinho, Z. F. et al. Hospital morbidity due to paracoccidioidomycosis in Brazil (1998-2006). *Trop. Med. Int. Heal.* **20**, 673–680 (2015).
4. Prado, M., da Silva, M. B., Laurenti, R., Travassos, L. R. & Taborda, C. P. Mortality due to systemic mycoses as a primary cause of death or in association with AIDS in Brazil: A review from 1996 to 2006. *Mem. Inst. Oswaldo Cruz* **104**, 513–521 (2009).
5. Mendes-Giannini, M. J. S., Soares, C. P., Da Silva, J. L. M. & Andreotti, P. F. Interaction of pathogenic fungi with host cells: Molecular and cellular approaches.

- FEMS Immunol. Med. Microbiol.* **45**, 383–394 (2005).
- 6. Mendes, R. P. *et al.* Paracoccidioidomycosis: Current Perspectives from Brazil. *Open Microbiol. J.* **11**, 224–282 (2017).
 - 7. Shikanai-Yasuda, M. A. *et al.* Brazilian guidelines for the clinical management of paracoccidioidomycosis. *Rev. Soc. Bras. Med. Trop.* **50**, 715–740 (2017).
 - 8. Grahl, N. *et al.* In vivo hypoxia and a fungal alcohol dehydrogenase influence the pathogenesis of invasive pulmonary aspergillosis. *PLoS Pathog.* **7**, (2011).
 - 9. Lima, P. de S., Chung, D., Bailão, A. M., Cramer, R. A. & Soares, C. M. de A. Characterization of the *Paracoccidioides* Hypoxia Response Reveals New Insights into Pathogenesis Mechanisms of This Important Human Pathogenic Fungus. *PLoS Negl. Trop. Dis.* **9**, 1–25 (2015).
 - 10. Chang, Y. C., Bien, C. M., Lee, H., Espenshade, P. J. & Kwon-Chung, K. J. Sre1p, a regulator of oxygen sensing and sterol homeostasis, is required for virulence in *Cryptococcus neoformans*. *Mol. Microbiol.* **64**, 614–629 (2007).
 - 11. Chun, C. D., Liu, O. W. & Madhani, H. D. A link between virulence and homeostatic responses to hypoxia during infection by the human fungal pathogen *Cryptococcus neoformans*. *PLoS Pathog.* **3**, 0225–0238 (2007).
 - 12. Shimizu, M., Fujii, T., Masuo, S., Fujita, K. & Takaya, N. Proteomic analysis of *Aspergillus nidulans* cultured under hypoxic conditions. *Proteomics* **9**, 7–19 (2009).
 - 13. Vödisch, M. *et al.* Analysis of the *Aspergillus fumigatus* proteome reveals metabolic changes and the activation of the pseurotin A biosynthesis gene cluster in response to hypoxia. *J. Proteome Res.* **10**, 2508–2524 (2011).
 - 14. Dubois, J. C., Pasula, R., Dade, J. E. & Smulian, A. G. Yeast Transcriptome and In Vivo Hypoxia Detection Reveals *Histoplasma capsulatum* Response to Low Oxygen Tension. 40–58 (2016). doi:10.1093/mmy/myv073
 - 15. de Groot, M. J. L. *et al.* Quantitative proteomics and transcriptomics of anaerobic and aerobic yeast cultures reveals post-transcriptional regulation of key cellular processes. *Microbiology* **153**, 3864–3878 (2007).
 - 16. Silverman-Gavrila, L. B. *et al.* Neural phosphoproteomics of a chronic hypoxia model-*Lymnaea stagnalis*. *Neuroscience* **161**, 621–634 (2009).
 - 17. Albataineh, M. T. & Kadosh, D. Regulatory roles of phosphorylation in model and pathogenic fungi. *Med. Mycol.* **54**, 333–52 (2016).
 - 18. Humphrey, S. J., James, D. E. & Mann, M. Protein Phosphorylation : A Major Switch Mechanism for Metabolic Regulation. *Trends Endocrinol. Metab.* **xx**, 1–12 (2015).
 - 19. Jünger, M. A. & Aebersold, R. Mass spectrometry-driven phosphoproteomics: patterning the systems biology mosaic. *Wiley Interdiscip. Rev. Dev. Biol.* **3**, 83–112 (2014).
 - 20. Ubersax, J. A. & Jr, J. E. F. Mechanisms of specificity in protein phosphorylation. *Nat. Rev. Mol. Cell Biol.* **8**, 530–542 (2007).
 - 21. Puttick, J., Baker, E. N. & Delbaere, L. T. J. Histidine phosphorylation in biological systems. *Biochim. Biophys. Acta - Proteins Proteomics* **1784**, 100–105 (2008).
 - 22. Thingholm, T. E., Jensen, O. N. & Larsen, M. R. Analytical strategies for phosphoproteomics. *Proteomics* **9**, 1451–1468 (2009).

23. Fernandes, L. *et al.* Cell signaling pathways in *Paracoccidioides brasiliensis*--inferred from comparisons with other fungi. *Genet. Mol. Res.* **4**, 216–231 (2005).
24. Berg, J. M., Tymoczko, J. L. & Stryer, L. *Biochemistry*. (2002).
25. Sestari, S. J., Brito, W. A., Neves, B. J., Soares, C. M. A. & Salem-Izacc, S. M. Inhibition of protein kinase A affects *Paracoccidioides lutzii* dimorphism. *Int. J. Biol. Macromol.* **113**, 1214–1220 (2018).
26. Da Silva Cruz, A. H. *et al.* Phosphorylation is the major mechanism regulating isocitrate lyase activity in *Paracoccidioides brasiliensis* yeast cells. *FEBS J.* **278**, 2318–2332 (2011).
27. Chaves, A. F. A. A. *et al.* Phosphosite-specific regulation of the oxidative-stress response of *Paracoccidioides brasiliensis*: a shotgun phosphoproteomic analysis. *Microbes Infect.* **19**, 34–46 (2017).
28. Grahl, N., Shepardson, K. M., Chung, D. & Cramer, R. A. Hypoxia and fungal pathogenesis: To air or not to air? *Eukaryot. Cell* **11**, 560–570 (2012).
29. Chung, D., Haas, H. & Cramer, R. Coordination of hypoxia adaptation and iron homeostasis in human pathogenic fungi. *Front. Microbiol.* **3**, 1–13 (2012).
30. Villén, J. & Gygi, S. P. The SCX/IMAC enrichment approach for global phosphorylation analysis by mass spectrometry. *Nat. Protoc.* **3**, 1630–1638 (2008).
31. Queiroz, R. M. L. *et al.* Quantitative Proteomic and Phosphoproteomic Analysis of *Trypanosoma cruzi* Amastigogenesis. *Mol. Cell. Proteomics* **13**, 3457–3472 (2014).
32. Yao, L. *et al.* Global Proteomics Deciphered Novel-Function of Osthole Against Pulmonary Arterial Hypertension. *Sci. Rep.* **8**, 5556 (2018).
33. Chou, M. F. & Schwartz, D. Using the scan-x web site to predict protein post-translational modifications. *Curr. Protoc. Bioinforma.* 1–19 (2011). doi:10.1002/0471250953.bi1316s36
34. Brock, M. & Buckel, W. On the mechanism of action of the antifungal agent propionate. Propionyl-CoA inhibits glucose metabolism in *Aspergillus nidulans*. *Eur. J. Biochem.* **271**, 3227–3241 (2004).
35. Grossklaus, D. A. *et al.* Response to oxidative stress in *Paracoccidioides* yeast cells as determined by proteomic analysis. *Microbes Infect.* **15**, 347–364 (2013).
36. Parente, A. F. A. *et al.* The response of *Paracoccidioides* spp. to nitrosative stress. *Microbes Infect.* **17**, 575–585 (2015).
37. Rodrigues, L. N. da S. *et al.* Osmotic stress adaptation of *Paracoccidioides lutzii*, Pb01, monitored by proteomics. *Fungal Genet. Biol.* **95**, 13–23 (2016).
38. Parente, A. F. A. *et al.* Proteomic analysis reveals that iron availability alters the metabolic status of the pathogenic fungus *paracoccidioides brasiliensis*. *PLoS One* **6**, (2011).
39. Parente, A. F. A. *et al.* A proteomic view of the response of *Paracoccidioides* yeast cells to zinc deprivation. *Fungal Biol.* **117**, 399–410 (2013).
40. Lima, P. de S. *et al.* Transcriptional and Proteomic Responses to Carbon Starvation in *Paracoccidioides*. *PLoS Negl. Trop. Dis.* **8**, (2014).
41. de Curcio, J. S. *et al.* Identification of membrane proteome of *Paracoccidioides lutzii* and its regulation by zinc. *Futur. Sci. OA* **3**, FSO232 (2017).

42. Oliveira, H. C. *et al.* Alterations of protein expression in conditions of copper-deprivation for *Paracoccidioides lutzii* in the presence of extracellular matrix components. *BMC Microbiol.* **14**, e302 (2014).
43. Parente-Rocha, J. A. *et al.* Macrophage interaction with *paracoccidioides brasiliensis* yeast cells modulates fungal metabolism and generates a response to oxidative stress. *PLoS One* **10**, 1–18 (2015).
44. Pigosso, L. L. *et al.* *Paracoccidioides brasiliensis* presents metabolic reprogramming and secretes a serine proteinase during murine infection. *Virulence* **0**, 1–18 (2017).
45. Nelson, D. L. & Cox, M. *Princípios de Bioquímica de Lehninger*. (Artmed, 2014).
46. Brock, M., Fischer, R., Linder, D. & Buckel, W. Methylcitrate synthase from *Aspergillus nidulans*: implications for propionate as an antifungal agent. *Mol. Microbiol.* **35**, 961–973 (2000).
47. Tielens, A. G. & Van Hellemond, J. J. The electron transport chain in anaerobically functioning eukaryotes. *Biochim. Biophys. Acta* **1365**, 71–8 (1998).
48. Camarasa, C., Faucet, V. & Dequin, S. Role in anaerobiosis of the isoenzymes for *Saccharomyces cerevisiae* fumarate reductase encoded by OSM1 and FRDS1. *Yeast* **24**, 391–401 (2007).
49. Verleur, N., Elgersma, Y., Van Roermund, C. W., Tabak, H. F. & Wanders, R. J. Cytosolic aspartate aminotransferase encoded by the AAT2 gene is targeted to the peroxisomes in oleate-grown *Saccharomyces cerevisiae*. *Eur. J. Biochem.* **247**, 972–80 (1997).
50. Baeza, L. C. *et al.* Differential metabolism of a two-carbon substrate by members of the *Paracoccidioides* genus. *Front. Microbiol.* **8**, 1–17 (2017).
51. Baracca, A., Sgarbi, G., Solaini, G. & Lenaz, G. Rhodamine 123 as a probe of mitochondrial membrane potential: evaluation of proton flux through F(0) during ATP synthesis. *Biochim. Biophys. Acta* **1606**, 137–46 (2003).
52. Tupe, S. G. *et al.* Possible mechanism of antifungal phenazine-1-carboxamide from *Pseudomonas* sp. against dimorphic fungi *Benjaminiella poitrasii* and human pathogen *Candida albicans*. *J. Appl. Microbiol.* **118**, 39–48 (2015).
53. Tsukihara, T. *et al.* Structures of metal sites of oxidized bovine heart cytochrome c oxidase at 2.8 Å. *Science* **269**, 1069–74 (1995).
54. Shepardson, K. M. *et al.* Hypoxia enhances innate immune activation to *Aspergillus fumigatus* through cell wall modulation. *Microbes Infect.* **15**, 259–269 (2013).
55. Synnott, J. M., Guida, A., Mulhern-Haughey, S., Higgins, D. G. & Butler, G. Regulation of the Hypoxic Response in *Candida albicans*. *Eukaryot. Cell* **9**, 1734–1746 (2010).
56. Blatzer, M. *et al.* SREBP Coordinates Iron and Ergosterol Homeostasis to Mediate Triazole Drug and Hypoxia Responses in the Human Fungal Pathogen *Aspergillus fumigatus*. *PLoS Genet.* **7**, e1002374 (2011).
57. Rappleye, C. A., Engle, J. T. & Goldman, W. E. RNA interference in *Histoplasma capsulatum* demonstrates a role for α -(1,3)-glucan in virulence. *Mol. Microbiol.* **53**, 153–165 (2004).
58. Rappleye, C. A., Eissenberg, L. G. & Goldman, W. E. *Histoplasma capsulatum* alpha-

- (1,3)-glucan blocks innate immune recognition by the beta-glucan receptor. *Proc. Natl. Acad. Sci. U. S. A.* **104**, 1366–70 (2007).
59. San-Blas, G., San-Blas, F. & Serrano, L. E. Host-parasite relationships in the yeastlike form of *Paracoccidioides brasiliensis* strain IVIC Pb9. *Infect. Immun.* **15**, 343–6 (1977).
60. Karst, F. & Lacroute, F. Ergosterol biosynthesis in *Saccharomyces cerevisiae*: mutants deficient in the early steps of the pathway. *Mol. Gen. Genet.* **154**, 269–77 (1977).
61. Taylor, R. C., Brown, A. K., Singh, A., Bhatt, A. & Besra, G. S. Characterization of a -hydroxybutyryl-CoA dehydrogenase from *Mycobacterium tuberculosis*. *Microbiology* **156**, 1975–1982 (2010).
62. Askew, C. *et al.* Transcriptional Regulation of Carbohydrate Metabolism in the Human Pathogen *Candida albicans*. *PLoS Pathog.* **5**, e1000612 (2009).
63. Setiadi, E. R., Doedt, T., Cottier, F., Noffz, C. & Ernst, J. F. Transcriptional Response of *Candida albicans* to Hypoxia: Linkage of Oxygen Sensing and Efg1p-regulatory Networks. *J. Mol. Biol.* **361**, 399–411 (2006).
64. Lee, H. *et al.* Cobalt chloride, a hypoxia-mimicking agent, targets sterol synthesis in the pathogenic fungus *Cryptococcus neoformans*. *Mol. Microbiol.* **65**, 1018–1033 (2007).
65. Barker, B. M. *et al.* Transcriptomic and proteomic analyses of the *Aspergillus fumigatus* hypoxia response using an oxygen-controlled fermenter. *BMC Genomics* **13**, 62 (2012).
66. Knoops, B., Goemaere, J., Van der Eecken, V. & Declercq, J.-P. Peroxiredoxin 5: Structure, Mechanism, and Function of the Mammalian Atypical 2-Cys Peroxiredoxin. *Antioxid. Redox Signal.* **15**, 817–829 (2011).
67. Chae, H. Z. & Rhee, S. G. A thiol-specific antioxidant and sequence homology to various proteins of unknown function. *Biofactors* **4**, 177–80 (1994).
68. Claiborne, A. *et al.* Protein-sulfenic acids: diverse roles for an unlikely player in enzyme catalysis and redox regulation. *Biochemistry* **38**, 15407–16 (1999).
69. von Stechow, L. *Phospho-Proteomics Methods and Protocols*. (Springer, 2016). doi:<https://doi.org/10.1007/978-1-4939-3049-4>
70. Lang, B. D., Li Am, A., Black-Brewster, H. D. & Fridovich-Keil, J. L. The brefeldin A resistance protein Bfr1p is a component of polyribosome-associated mRNP complexes in yeast. *Nucleic Acids Res.* **29**, 2567–74 (2001).
71. Xue, Z., Shan, X., Sinelnikov, A. & Mélèse, T. Yeast mutants that produce a novel type of ascus containing asci instead of spores. *Genetics* **144**, 979–89 (1996).
72. Simpson, C. E., Lui, J., Kershaw, C. J., Sims, P. F. G. & Ashe, M. P. mRNA localization to P-bodies in yeast is bi-phasic with many mRNAs captured in a late Bfr1p-dependent wave. *J. Cell Sci.* **127**, 1254–62 (2014).
73. Goulin, E. H. *et al.* Identification of genes associated with asexual reproduction in *Phyllosticta citricarpa* mutants obtained through *Agrobacterium tumefaciens* transformation. *Microbiol. Res.* **192**, 142–147 (2016).
74. Ozaki, K., Chikashige, Y., Hiraoka, Y. & Matsumoto, T. Fission Yeast Scp3 Potentially Maintains Microtubule Orientation through Bundling. *PLoS One* **10**,

- e0120109 (2015).
- 75. Kim, J., Guermah, M. & Roeder, R. G. The human PAF1 complex acts in chromatin transcription elongation both independently and cooperatively with SII/TFIIS. *Cell* **140**, 491–503 (2010).
 - 76. Chen, Y. *et al.* DSIF, the Paf1 complex, and Tat-SF1 have nonredundant, cooperative roles in RNA polymerase II elongation. *Genes Dev.* **23**, 2765–2777 (2009).
 - 77. Viphakone, N. *et al.* Luzp4 defines a new mRNA export pathway in cancer cells. *Nucleic Acids Res.* **43**, 2353–2366 (2015).
 - 78. Katahira, J., Dimitrova, L., Imai, Y. & Hurt, E. NTF2-like domain of Tap plays a critical role in cargo mRNA recognition and export. *Nucleic Acids Res.* **43**, 1894–1904 (2015).
 - 79. Amrani, N., Minet, M., Le Gouar, M., Lacroute, F. & Wyers, F. Yeast Pab1 interacts with Rna15 and participates in the control of the poly(A) tail length in vitro. *Mol. Cell. Biol.* **17**, 3694–701 (1997).

Figures

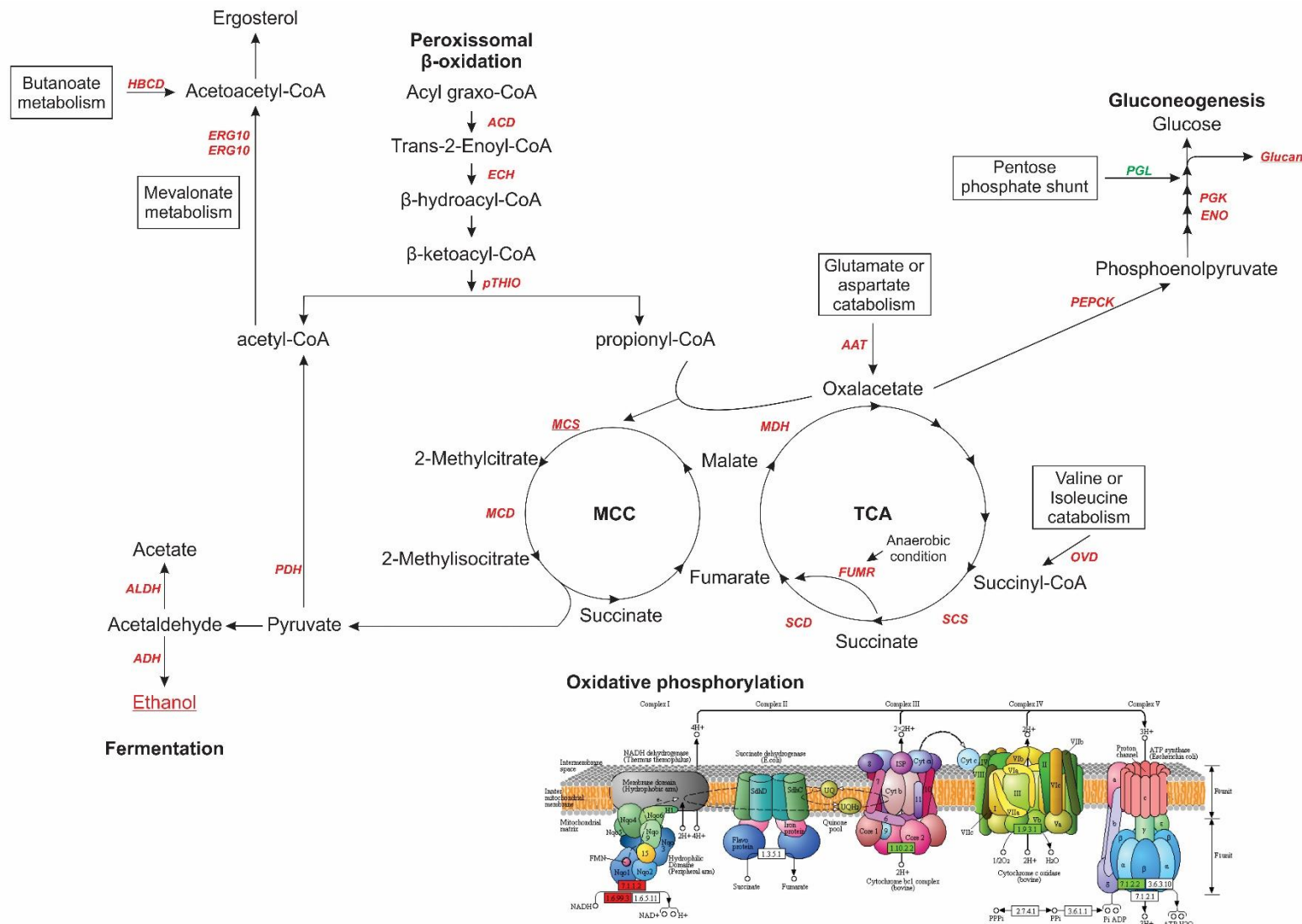


Figure 1. Overview of metabolic responses of *P. brasiliensis* submitted to hypoxia. (A)
The figure summarizes the data from proteomic analyses and suggests the mechanism used by the *P. brasiliensis* generated by hypoxia. Red or green indicate up or down regulated proteins, respectively. Underline indicate the up regulated confirmed by biochemical assays. HBCD: 3-hydroxybutyryl-CoA dehydrogenase - PADG_01228; ERG10: Acetyl-CoA C-acetyltransferase (ERG 10) - PADG_06382, PADG_02751; ALDH: Aldehyde dehydrogenase - PADG_05081; ADH: Alcohol dehydrogenase 1 - PADG_11405; PDH: complex of Pyruvate dehydrogenase: Pyruvate dehydrogenase kinase 2/3/4 - PADG_12250, Dihydrolipoamide acetyltransferase - PADG_07213 and Dihydrolipoyl dehydrogenase - PADG_06494; ACD: Acyl-CoA dehydrogenase - PADG_06805; ECH: Enoyl-CoA hydratase - PADG_01209; pTHIO: Peroxisomal 3-ketoacyl-CoA thiolase - PADG_03194; MCS: Methylcitrate synthase; MCD: 2-methylcitrate dehydratase - PADG_04718; SCS: Succinyl-CoA synthetase alpha subunit - PADG_02260; SCD: Succinate dehydrogenase [ubiquinone] iron-sulfur subunit - PADG_08013; FUMR: Fumarate reductase (NADH) - PADG_02592; MDH: Malate dehydrogenase, NAD-dependent - PADG_07210, AAT: Aspartate aminotransferase - PADG_01621; OVD: 2-oxoisovalerate dehydrogenase subunit alpha - PADG_03514; PEPCK: Phosphoenolpyruvate carboxykinase - PADG_08503 , ENO: Enolase - PADG_04059, PGK: Phosphoglycerate kinase - PADG_01896 , PGL: 6-phosphogluconolactonase - PADG_07771.

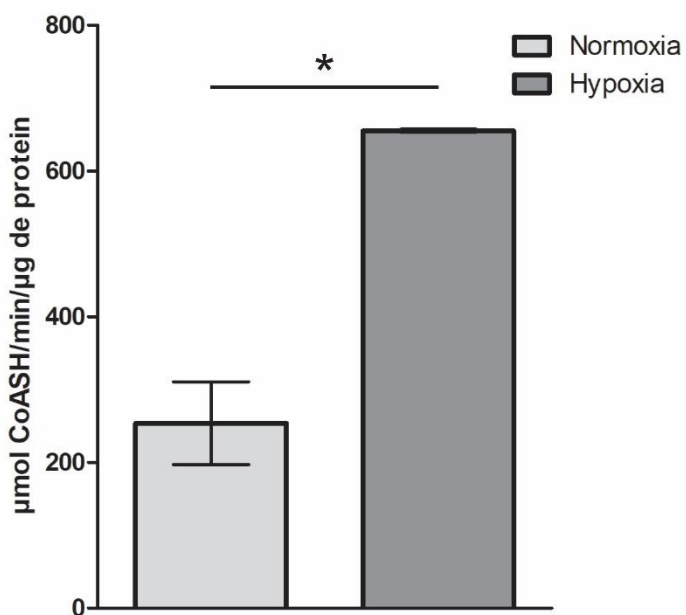


Figure 2. Enzymatic activity of methylcitrate synthase in *P. brasiliensis* protein extracts after 12 h of hypoxia. The condensation of propionyl-CoA with oxaloacetate was measured by the production of CoASH read at 412 nm. The mean \pm standard deviation (error bars) of biological triplicates samples as used. “*” indicates p -values ≤ 0.01 by Student’s *t*-test.

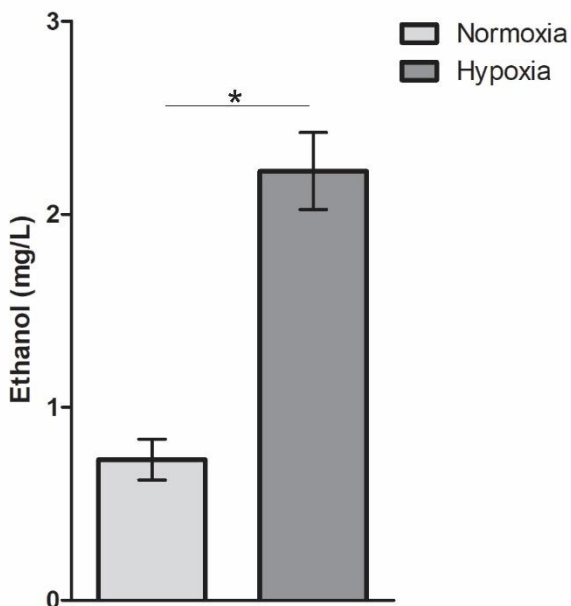


Figure 3. Ethanol measurement in *P. brasiliensis* protein extracts after 12 h of hypoxia. Intracellular ethanol production was measured in yeast cells submitted to normoxia and hypoxia. The mean \pm standard deviation (error bars) of biological triplicates samples as used. “*” indicates p -values ≤ 0.01 by Student’s *t*-test.

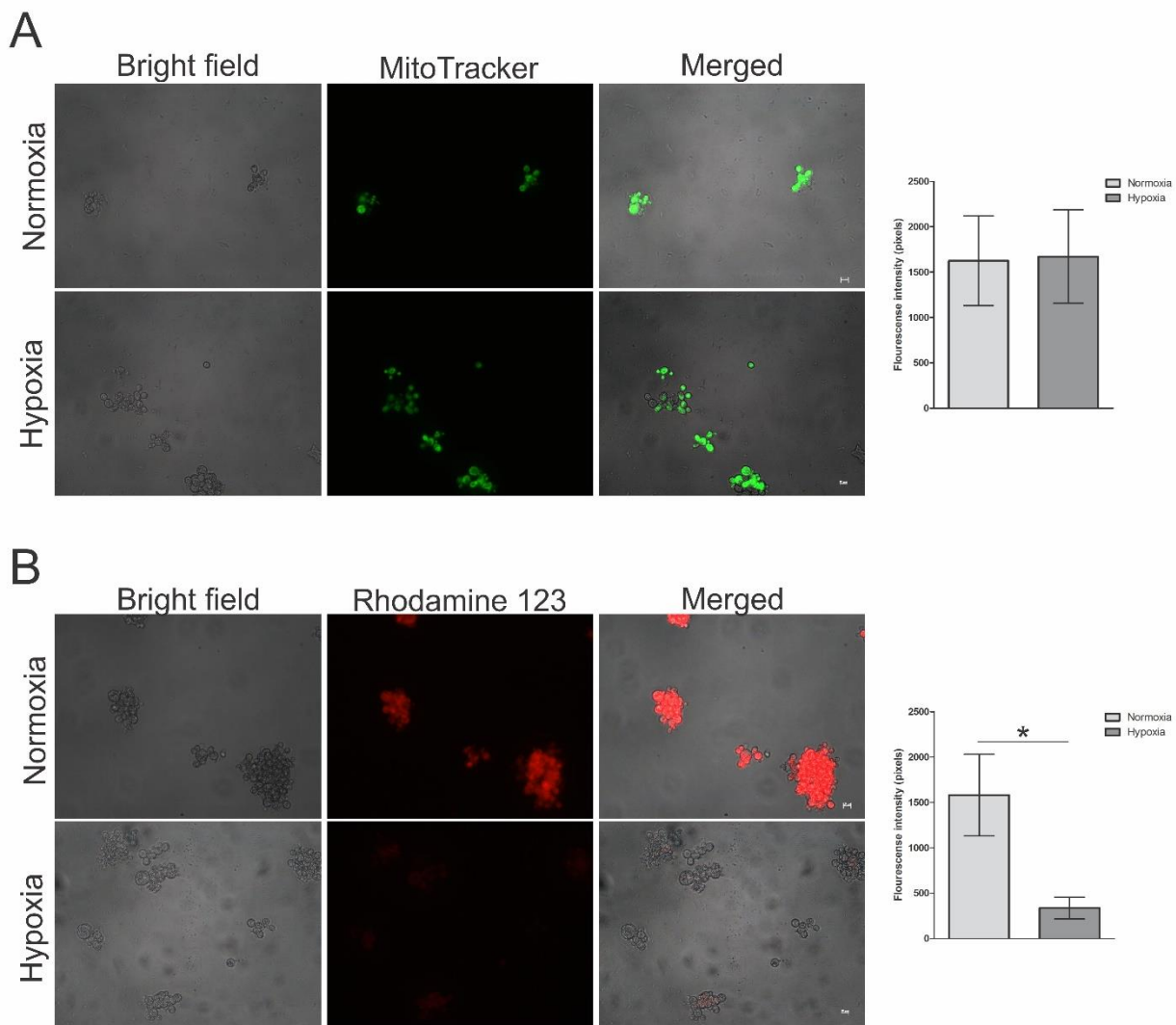


Figure 4. Mitochondrial integrity and activity of *P. brasiliensis* submitted to normoxic and hypoxic stress. (A) The mitochondrial integrity was evaluate by using MitoTracker Green FM as a dye for mitochondrial structural integrity. **(B)** The mitochondrial activity was evaluate by using Rhodamine 123 as a dye for mitochondrial membrane potential. The mean values of fluorescence intensity (in pixels) and the standard deviation of each analysis were used to plot graph (right). “**” indicates p-values ≤ 0.01 by Student’s t-test. All images were obtained in magnification of 400X.

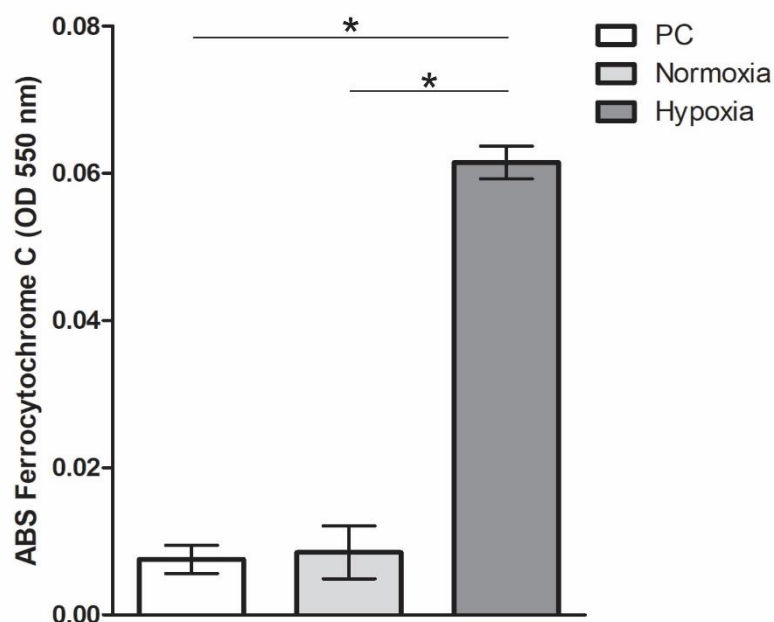


Figure 5. Enzymatic activity of cytochrome c oxidase in *P. brasiliensis* protein extracts after 12 h of hypoxia. The reduced ferrocytochrome C as measured at 550 nm. The positive control (PC) and normoxia reveals a decrease of reduced ferrocytochrome C absorbance due to oxidation by cytochrome c oxidase. The mean \pm standard deviation (error bars) of biological triplicates samples as used. “*” indicates p -values ≤ 0.01 by Student’s t -test.

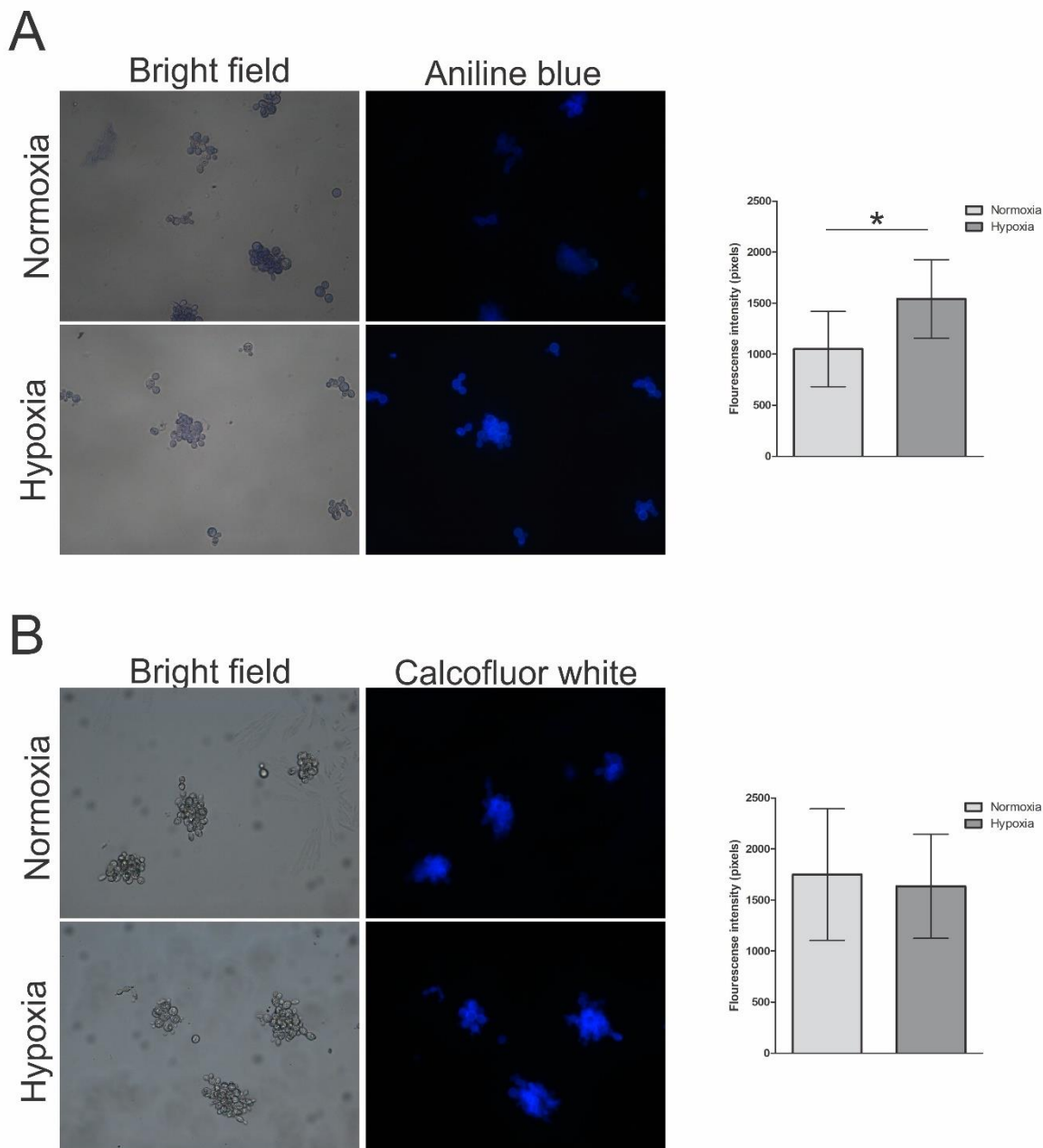


Figure 6. Content of cell wall polymers of *P. brasiliensis* submitted to normoxic and hypoxic stress. (A) The glucan content was evaluate by using Aniline blue as a dye. **(B)** The chitin content was evaluate by using Calcofluor white as a dye. The mean values of fluorescence intensity (in pixels) and the standard deviation of each analysis were used to plot graph (right). “*” indicates p-values ≤ 0.05 by Student’s *t*-test. All images were obtained in magnification of 400X.

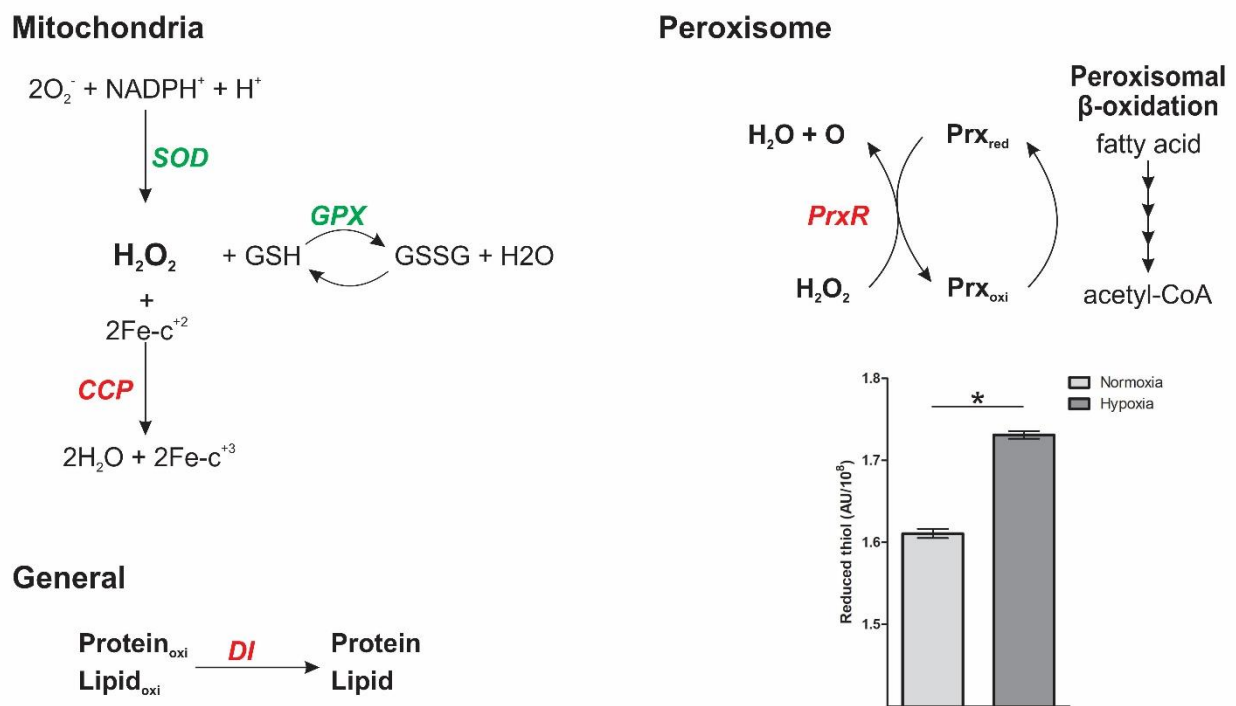


Figure 7 Overview of detoxification mechanisms against oxidative stress in *P. brasiliensis* submitted to normoxic and hypoxic stress. (A) The figure summarizes data from proteomic analyses and suggests the mechanisms used by the fungus to counteract oxidative stress generated by hypoxia. Red or green indicate up or down regulated proteins, respectively. SOD: superoxide dismutase - PADG_07418, GPX: glutathione peroxidase - PADG_04587, CCP: cytochrome c peroxidase - PADG_03163, DI: disulfide isomerase - PADG_03841, PrxR: peroxiredoxin - PADG_04912. The reduced thiol levels was measured in yeast cells submitted to normoxia and hypoxia. The mean values (in pixels) and the standard deviation of each analysis were used to plot graph (right). “*” indicates p-values ≤ 0.05 by Student’s t-test.

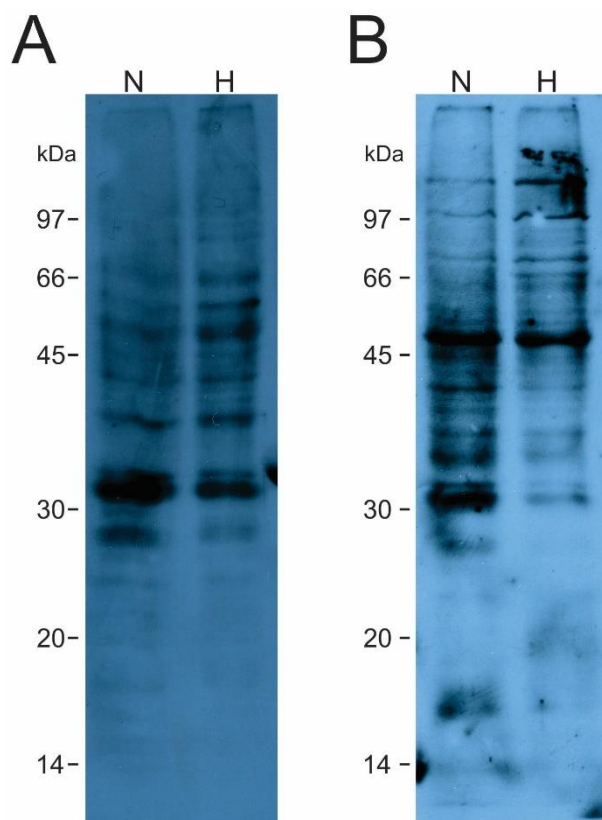


Figure 8. Phosphoprotein profile highlighted by immunoblotting assays of *P. brasiliensis* under hypoxia. Western blotting analysis with 40 µg of normoxia and hypoxia protein extracts revealed by anti-phosphoSer/Thr (A) and anti- phosphoTyr (B) polyclonal antibody. Molecular mass protein standards (kDa) are indicated on the left of the images. **kDa:** molecular weight marker; **H:** hypoxia extract; **N:** normoxia extract.

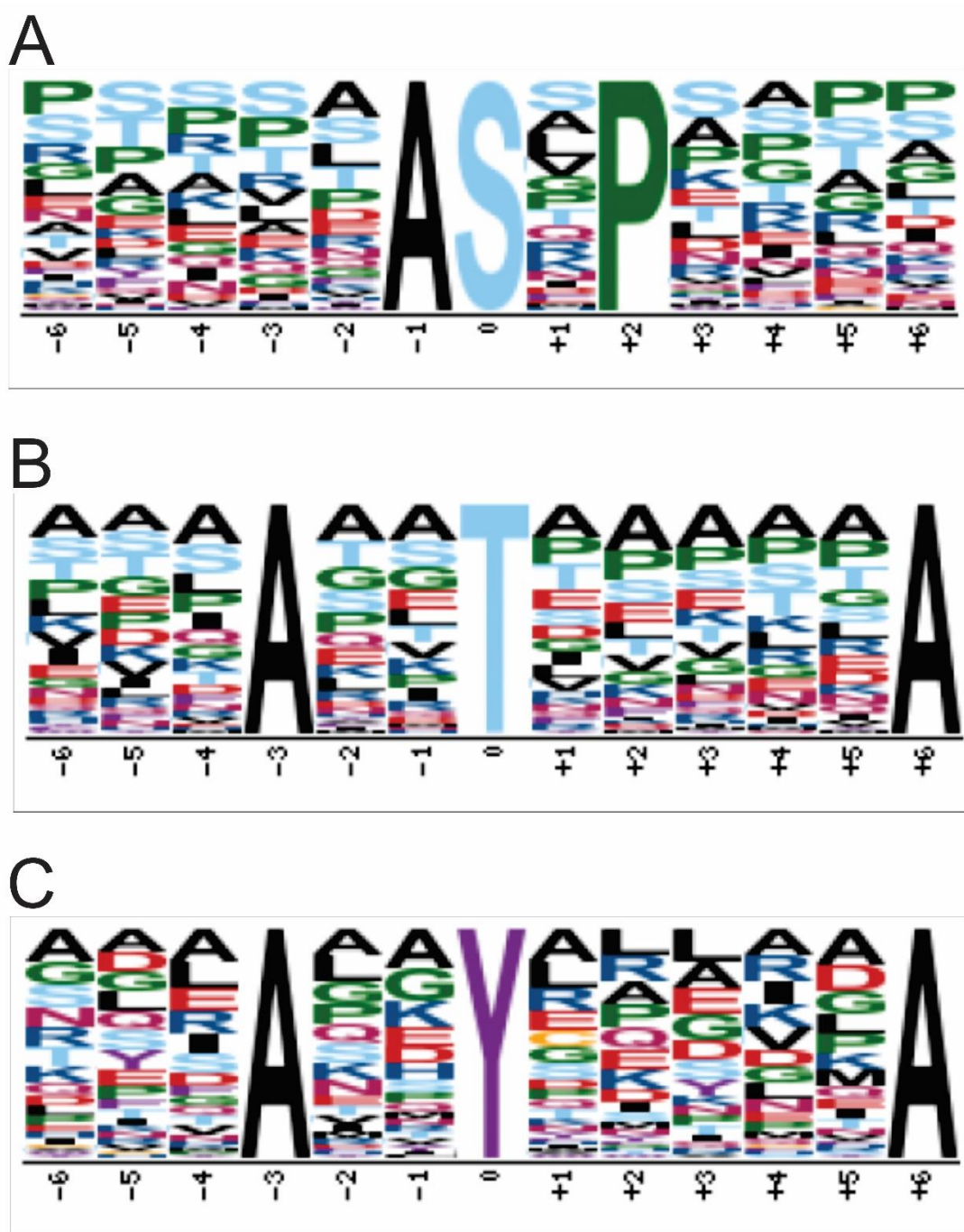
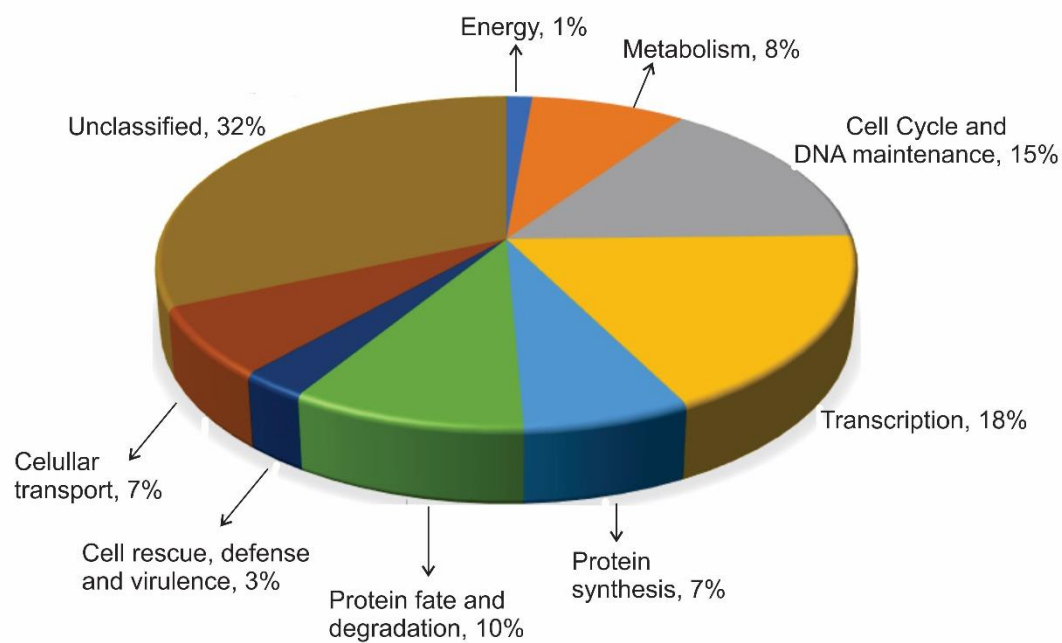


Figure 9. Consensus motifs of phosphoproteins of *P. brasiliensis* under hypoxia.
Consensus sequences were determined using the online algorithm Motif-X with build of 13 amino acids centered on phosphorylation site. **A)** Motifs of serine phosphorylation. **B)** Motifs of threonine phosphorylation. **C)** Motifs of tyrosine phosphorylation.

A



B

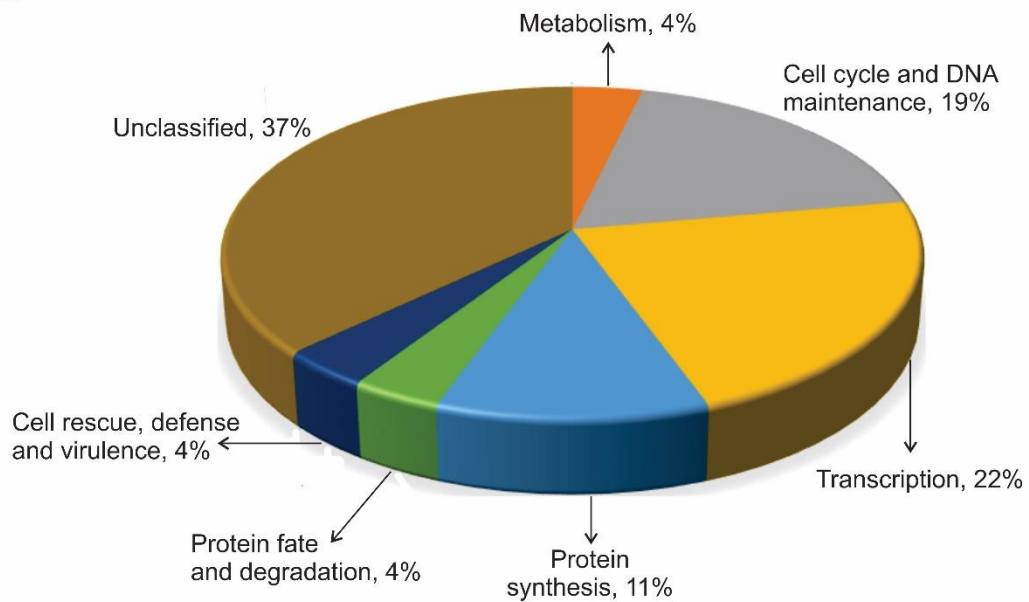
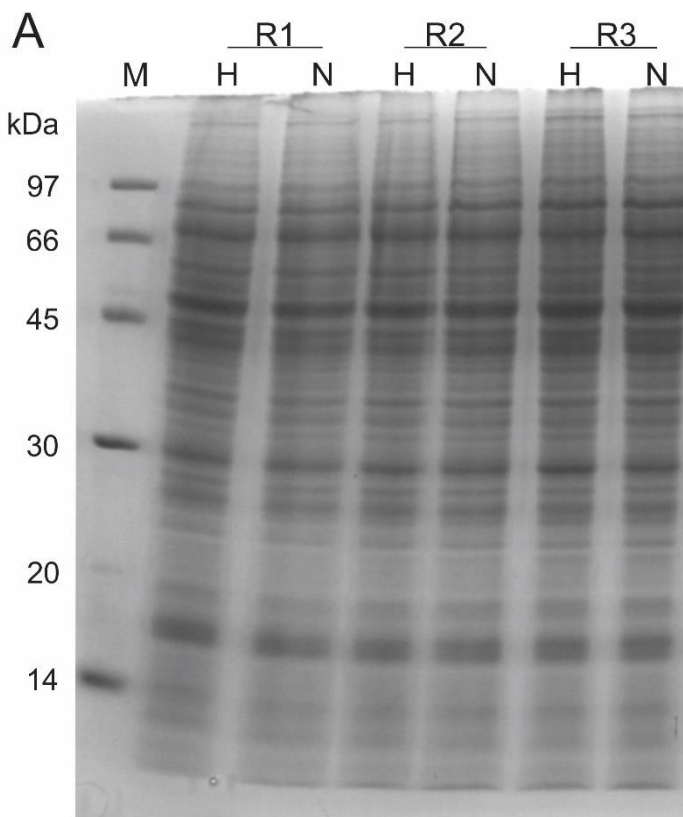
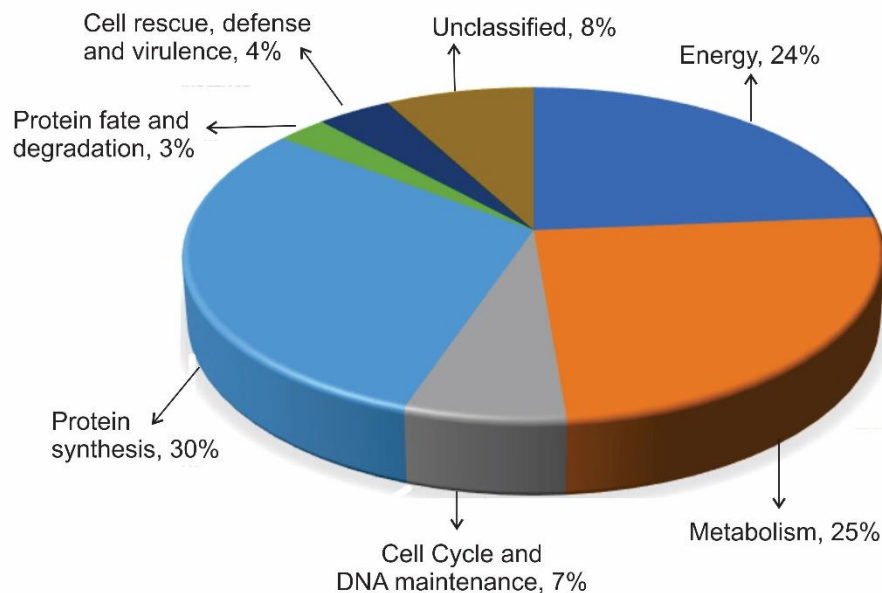


Figure 10. Functional distribution of phosphoproteins of *P. brasiliensis* (*Pb18*) under hypoxia. Prediction of the biological function for all phosphorylated proteins (A) and down-phosphorylated proteins (B) during hypoxia.

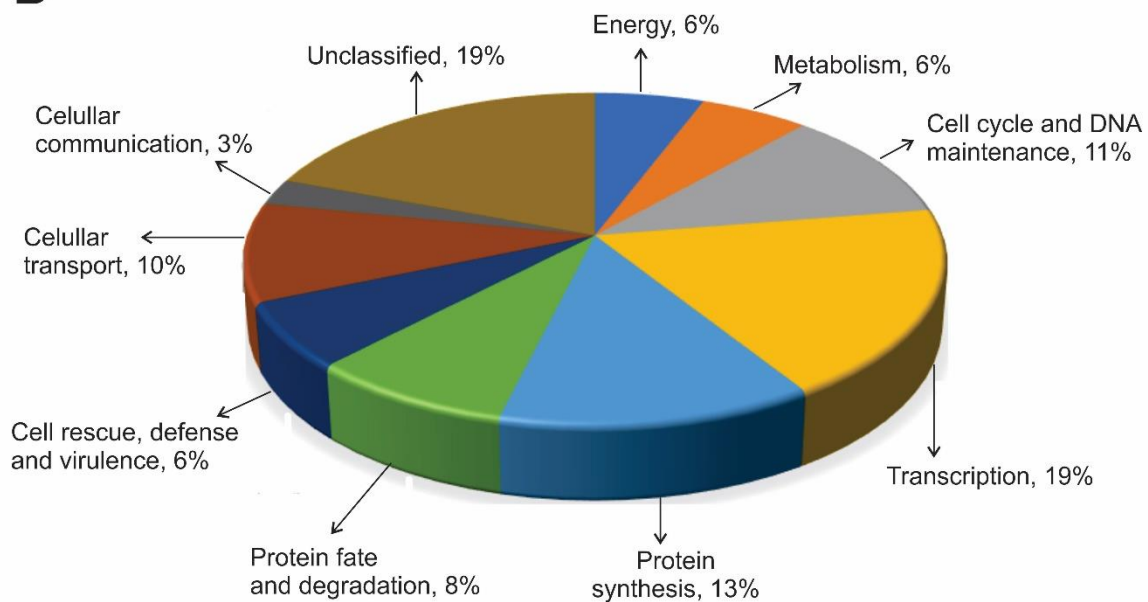


Supplementary Figure 1. Total extract quality analysis. Protein extract of the normoxia and hypoxia conditions of *Pb18* using 12% gel electrophoresis (SDS-PAGE). Molecular mass protein standards (kDa) are indicated on the left of the gels. **MW:** molecular weight marker; **R:** indicates as biological replicates; **H:** hypoxia extract; **N:** normoxia extract.

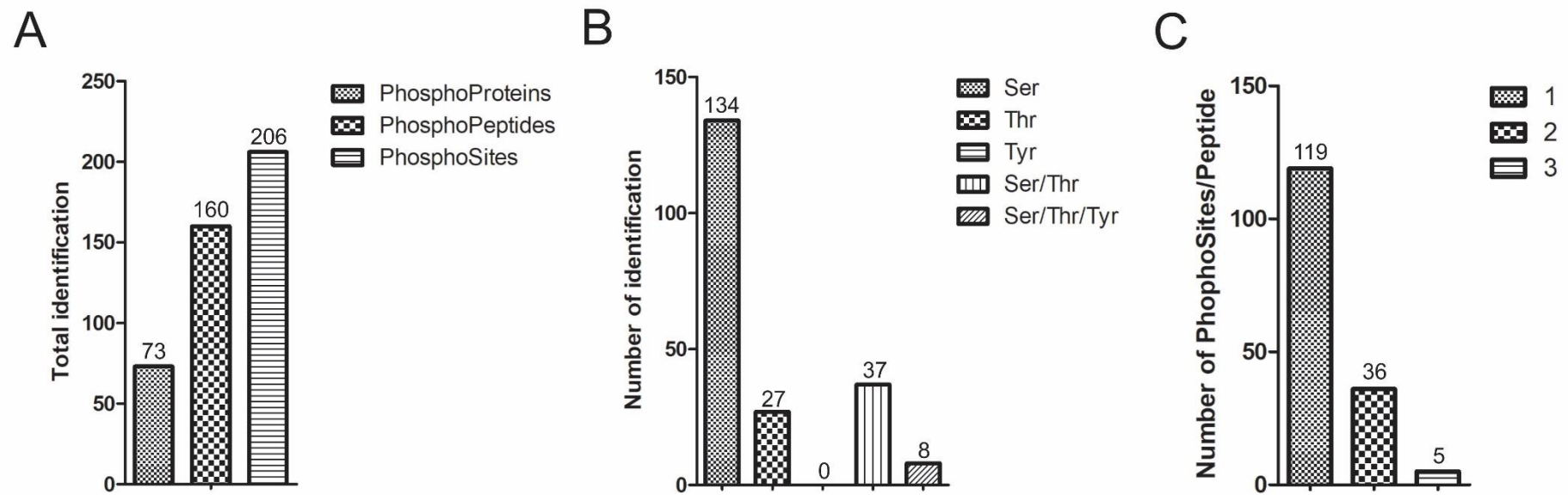
A



B



Supplementary Figure 2. Functional distribution of global proteome of *P. brasiliensis* (*Pb18*) under hypoxia. Prediction of the biological function of up regulated (A) and down regulated proteins (B) during hypoxia.



Supplementary Figure 3. Data analysis of phosphoproteome of *P. brasiliensis* under hypoxia. A bar graph shows **A)** absolute number of identified phosphorylated proteins, peptides and sites. **B)** Number of Ser, Thr, Tyr, Ser/Thr and Ser/Thr/Tyr phosphosites identified. **C)** Number of phosphosites per peptide.

Table 1: Functional categorization of *P. brasiliensis* phosphoproteins identified under hypoxic conditions.

Acession Numbe	Gene Description	EC number	Phosphorylation position	p-value	Global expression	TiO2 expression	Subclassification
Functional categories							
1. ENERGY							
Pentose-phosphate pathway							
PADG_00780	ribose-phosphate pyrophosphokinase	EC:2.7.6.1	Phospho [T125(87.8); S167(98.7)]	0,64099			carbohydrate metabolism
2. METABOLISM							
Carbon Metabolism							
PADG_02063	pyruvate dehydrogenase (acetyl-transferring) E1 component, alpha subunit	EC:1.2.4.1	Phospho [S307(100)]/Phospho [S307]	0,51664			glycolysis
Amino Acid Metabolism							
PADG_03514	2-oxoisovalerate dehydrogenase subunit alpha	EC:1.2.4.4	Phospho [S338(98.9); S340(98.9)]	0,48729	Up		amino acid metabolism
Metabolism of vitamins, cofactors, and prosthetic groups							
PADG_05433	pyridoxamine 5'-phosphate oxidase	EC:1.4.3.5	Phospho [T129(99)]	0,25732			metabolism of cofactors and vitamins
Lipid, fatty acid and isoprenoid metabolism							
PADG_02299	choline-phosphate cytidylyltransferase	EC:2.7.7.15	Phospho [S18(100); S397(99.2)]	0,1404	Down		lipid metabolism
PADG_06645	choline kinase	EC:2.7.1.32	Phospho [S34(98.7)]	0,2775			lipid metabolism
Nucleotide/nucleoside/nucleobase metabolism							

PADG_07782	Deoxyuridine 5'-triphosphate nucleotidohydrolase	EC:3.6.1.23	Phospho [S29(100); S30(100)]	0,00088	Down	Down	pyrimidine metabolism
------------	--	-------------	------------------------------	---------	------	------	-----------------------

3. CELL CYCLE AND DNA MAINTENANCE

Cell cycle

PADG_00849	Nuclear segregation protein Bfr1	Phospho [S60(100)]	0,00109	Down	Down	mitotic cell cycle and cell cycle control
PADG_05935	spindle poison sensitivity Scp3*	Phospho [S438(97.8); S468(98.3)]/Phospho [T369; S370]	0,00449	Down	Down	cell growth
PADG_06763	septum formation protein Maf	Phospho [T43(78.1)]	0,02907		Down	cell growth

Cytoskeleton

PADG_00945	actin related protein 2/3 complex, subunit 5	Phospho [S141(98.8)]/Phospho [S139; S141]	0,11256			actin binding
PADG_00011	drebrin-like protein	Phospho [T496(98.9); S540(100)]/Phospho [S540]	0,03826	Down		actin binding
PADG_06945	GYF domain-containing protein*	Phospho [S564(98.8)]	0,05167	Down		cytoskeleton-dependent transport
PADG_00951	microtubule-associated protein, RP/EB family	Phospho [T172(100)]	-			microtubule binding

DNA maintenance

PADG_00177	actin-related protein 5	Phospho [S561(100)]	0,52846			chromatin remodeling factors
PADG_07812	DNA topoisomerase I	EC:5.99.1.2	Phospho [S144(100); S146(100)]	0,13577		DNA binding
PADG_03869	HMG box domain-containing*		Phospho [S117(100)]	0,66513		DNA binding
PADG_04730	nascent polypeptide-associated complex subunit alpha		Phospho [S26(100); S27(100); S29(100)]	0,06415		DNA binding

4. TRANSCRIPTION

RNA synthesis and processing

PADG_02315	RNA polymerase-associated protein LEO1	Phospho [S517(100)]	0,01599	Down	Down	mRNA synthesis
PADG_00814	splicing factor 1	Phospho [S51(100); S127(99.9); S129(96.8)]	0,19517			mRNA splicing
PADG_02346	mRNA stability protein	Phospho [S47(100); S172(100)]	0,01262	Down	Down	mRNA binding
PADG_06486	CCR4-NOT transcription complex subunit 3	Phospho [S364(97.3)]	0,16656			RNA binding
PADG_07714	NTF2 and RRM domain-containing*	Phospho [S409(99)]	0,02541		Down	RNA binding
PADG_05340	Pre-mRNA-splicing factor srp1	Phospho [S182]	-	Down	Down	RNA binding
PADG_04934	RNP domain protein	Phospho [S48(98.9)]	0,10597	Down		RNA binding
PADG_04369	Splicing factor U2AF	Phospho [T205(98.4)]	0,15603	Down		RNA binding
PADG_07285	THO complex subunit 4	Phospho [S174(100)]	0,03828		Down	RNA binding
PADG_07689	Transformer-SR ribonucleoprotein	Phospho [S36(100); S38(100); T152(99.2)]	0,16979	Down		RNA binding
PADG_07880	U3 small nucleolar RNA-associated protein 14	Phospho [T839(96.4); T841(98.1)]	-			rRNA binding
PADG_02996	PAB1 binding protein	Phospho [S724(96.6); S739(98.4)]	0,03708	Down	Down	3'-end RNA-processing complex

Transcription control

PADG_00256	transcription initiation factor TFIIF subunit alpha	Phospho [S523(100)]	0,5995		DNA binding
------------	---	---------------------	--------	--	-------------

5. PROTEIN SYNTHESIS

Translation factors

PADG_01079	translation initiation factor 4B	Phospho [S200(100); S258(100); T345(97.1)]	0,00291	Down	Down	RNA binding
PADG_00457	translation initiation factor 4G	Phospho [S500(92.7)]	0,02861		Down	RNA binding
PADG_02896	elongation factor 1-beta	Phospho [S93(100)]/Phospho [S93]	0,40257			elongation factors
PADG_04057	eukaryotic translation initiation factor 3 subunit J	Phospho [S101(100)]/Phospho [S101]	0,00495		Down	protein modification

Ribosome

PADG_03778	60S ribosomal protein L10-A	Phospho [S221(100)]	0,25876		Translation
------------	-----------------------------	---------------------	---------	--	-------------

6. PROTEIN FATE and DEGRADATION

Protein degradation

PADG_02887	26S proteasome regulatory subunit N13	Phospho [S183(100)]	0,10497		folding, sorting and degradation	
PADG_07515	UBX domain-containing protein	Phospho [S110(100); S114(100)]	0,00294	Down	Down	folding, sorting and degradation
PADG_03715	FK506-binding nuclear protein	EC:5.2.1.8 Phospho [T270(100); S295(100)]	0,23834			peptidylprolyl isomerase

Protein modification

PADG_03544	Ser/Thr protein phosphatase*	Phospho [S674(99.2)]	0,26192	Down	transferring phosphorus-containing groups
PADG_11474	protein-serine/threonine kinase	EC:2.7.11 Phospho [S51(100)]	0,11956		transferring phosphorus-containing groups
PADG_02300	protein phosphatase PTC2/3	EC:3.1.3.16 Phospho [S458(100)]	0,27305		transferring phosphorus-containing groups
PADG_08239	CBS and PB1 domain-containing*	Phospho [S47(95.9); S462(99.4)]	0,62363		protein binding

7. CELL RESCUE, DEFENSE AND VIRULENCE

Stress response

PADG_00207	HSP40	Phospho [S82(100)]/Phospho [S82]	0,12144		stress response	
PADG_06699	HSP20 family protein	Phospho [S62(95.9)]	0,00099	Down	Down	stress response

8. CELLULAR TRANSPORT, TRANSPORT FACILITIES AND TRANSPORT ROUTES

General transport

PADG_00442	ADP-ribosylation factor GTPase-activating protein 2/3	Phospho [S174(98.2); S193(85.7)]	0,06629	Down	membrane trafficking/Endocytosis
PADG_01114	importin subunit alpha-1	Phospho [S84(92.4)]	-		nuclear import signal receptor activity
PADG_03728	nucleoporin NUP159	Phospho [S1064(100); S1070(100)]	0,10775		nuclear pore complex
PADG_07856	SRP40_C domain	Phospho [S20(100)]	0,10353		chaperone involved in nucleocytoplasmic transport
PADG_07659	transport protein SEC9	Phospho [S370(99.9)]	-	Down	vesicle fusion

9. UNCLASSIFIED

PADG_12447	Uncharacterized protein	Phospho [S383(100)]	0,33105		translation
PADG_03526	Uncharacterized protein	Phospho [T1257(96.7)]	0,06264		transcription factors
PADG_02652	Uncharacterized protein	Phospho [S316(100); S323(97)]/Phospho [S130; S136]	0,00054	Down	RNA binding
PADG_11302	Uncharacterized protein	Phospho [S397(97)]	0,22662		regulation of transcription
PADG_00676	Uncharacterized protein	Phospho [S215; T216; S439(100)]	0,00289	Down	protein binding
PADG_00085	Uncharacterized protein	Phospho [S56(100); S58(100)]	0,4532		nucleic acid binding
PADG_12437	Uncharacterized protein	Phospho [S1119(98.1)]	0,00195	Down	ion binding
PADG_00140	Uncharacterized protein	Phospho [T266]	-		cell redox homeostasis
PADG_02967	Uncharacterized protein	Phospho [T484(98.5)]	0,01253	Down	-
PADG_00680	Uncharacterized protein	Phospho [S495(100)]	0,6393		-
PADG_02709	Uncharacterized protein	Phospho [S271(99.3); S298(98.5)]	-		-
PADG_03827	Uncharacterized protein	Phospho [S22(98.9)]/Phospho [S22]	0,02077	Down	-
PADG_05584	Uncharacterized protein	Phospho [S38(97.7); S70(100); S74(100)]/Phospho [S63; S68; S70; S74]	0,03957	Down	-
PADG_06262	Uncharacterized protein	Phospho [S561(100)]	0,00443	Down	-
PADG_06966	Uncharacterized protein	Phospho [S536(98)]	0,3521		-

PADG_07250	Uncharacterized protein	Phospho [T112(97.5); S571(99.3)]	-	-
PADG_12012	Uncharacterized protein	Phospho [S559(100); S562(100)]	-	-
PADG_01141	Uncharacterized protein	Phospho [S19(95.6)]	0,01191	Down
PADG_05959	Uncharacterized protein	Phospho [S104(100)]	0,04915	Down
PADG_07022	Uncharacterized protein	Phospho [S79(100); T113(98); S137(100)]	0,02343	Down
PADG_12301	Uncharacterized protein	Phospho [S440(100)]	0,06772	-
PADG_00899	Uncharacterized protein	Phospho [T153(100); S155(99.8)]	0,09638	-
PADG_08288	Uncharacterized protein	Phospho [S149(98.2)]	0,2036	-

Supplementary Table 1: Functional categorization of proteins up-regulated 12 hours after hypoxia with *Paracoccidioides brasiliensis*.

Acession number	Gene Description	EC number	MS Score	Unique Peptide	Peptide Score	p-value	Subclassification
Functional categories							
1. ENERGY							
Glycolysis and Gluconeogenesis							
PADG_05109	2,3-bisphosphoglycerate-independent phosphoglycerate mutase	EC:5.4.2.12	466,79	7	17,997	0,001425	glycolysis/Gluconeogenesis
PADG_01896	Phosphoglycerate kinase	EC:2.7.2.3	3975,95	18	89,528	0,0169332	glycolysis/Gluconeogenesis
PADG_04059	Enolase	EC:4.2.1.11	16350,3	23	190,61	0,0116724	glycolysis/Gluconeogenesis
PADG_08503	Phosphoenolpyruvate carboxykinase	EC:4.1.1.49	3139,13	17	69,623	0,016514	glycolysis/Gluconeogenesis
Tricarboxylic-acid pathway							
PADG_02260	Succinyl-CoA synthetase alpha subunit	EC:6.2.1.4 6.2.1.5	4851,11	11	74,824	0,0031772	citrate cycle
PADG_08013	Succinate dehydrogenase [ubiquinone] iron-sulfur subunit, mitochondrial	EC:1.3.5.1	2143,56	14	48,398	0,0010905	citrate cycle
PADG_02592	Fumarate reductase (NADH)	EC:1.3.5.1 1.3.5.4	7757,57	27	144,865	0,0013953	citrate cycle
PADG_07210	Malate dehydrogenase, NAD-dependent	EC:1.1.1.37	10423,23	22	147,931	0,0001309	citrate cycle
Methylcitrate cycle							
PADG_04718	2-methylcitrate dehydratase	EC:4.2.1.79	3918,52	22	108,864	0,0042934	propanoate metabolism
Fermentation							
PADG_11405	Alcohol dehydrogenase 1	EC:1.1.1.1	1311,9	6	26,013	0,0183022	ethanol production from pyruvate
PADG_05081	Aldehyde dehydrogenase	EC:1.2.1.3	1746,42	12	55,462	0,000671	acetate production from pyruvate

Electron Transport and Membrane-associated Energy Conservation

PADG_07813	ATP synthase F1, gamma subunit	-	1026,21	7	25,949	1,425E-06	oxidative phosphorylation
PADG_02578	ATP synthase subunit 4, mitochondrial	-	3001,73	11	54,821	0,0125706	oxidative phosphorylation
PADG_07749	NAD(P)H:quinone oxidoreductase, type IV	EC:1.6.5.2	1576,29	6	40,603	0,0002357	oxidative phosphorylation
PADG_03516	NADH dehydrogenase (ubiquinone) Fe-S protein 3	EC:1.6.5.3 1.6.99.3	1300,11	3	18,86	0,0162627	oxidative phosphorylation
PADG_12148	NADH-ubiquinone oxidoreductase 78 kDa subunit, mitochondrial	EC:1.6.5.3 1.6.99.3	1849,96	8	36,656	0,0016957	oxidative phosphorylation
PADG_08394	Ubiquinol-cytochrome c reductase subunit 2	-	3778,36	14	82,611	0,0175585	oxidative phosphorylation
PADG_03872	NADH-cytochrome b5 reductase 2	EC:1.6.2.2	653,28	6	32,451	0,0101996	oxidative phosphorylation

2. METABOLISM

Amino Acid Metabolism

PADG_04939	3-oxoacid CoA-transferase	EC:2.8.3.5	941,82	10	39,372	0,0001771	amino acid metabolism
PADG_01621	Aspartate aminotransferase	EC:2.6.1.1	625,15	2	11,977	5,301E-05	aspartate (Oxo) and glutamate (alfa-ceto) metabolism
PADG_04570	Branched-chain amino acid aminotransferase	EC:2.6.1.42	2923,02	10	47,586	0,0007255	leucine, isoleucine and valine metabolism
PADG_08406	O-acetylhomoserine (Thiol)-lyase	EC:2.5.1.49 2.5.1.47	1544,91	8	40,982	0,0034454	cysteine and methionine metabolism
PADG_05277	Serine hydroxymethyltransferase	EC:2.1.2.1	2112,18	6	38,677	0,0083538	glycine, serine and threonine metabolism
PADG_06429	Ketol-acid reductoisomerase, mitochondrial	EC:1.1.1.86	2720,03	13	49,866	0,0043014	valine, leucine and isoleucine biosynthesis
PADG_03514	2-oxoisovalerate dehydrogenase subunit alpha	EC:1.2.4.4	1061,09	8	31,657	0,0010002	valine, leucine and isoleucine degradation

Carbon Metabolism

PADG_12250	Pyruvate dehydrogenase kinase 2/3/4	EC:2.7.11.2		1	2,427	0,0087592	pyruvate/acetyl-CoA metabolism
PADG_07213	Pyruvate dehydrogenase complex dihydrolipoamide acetyltransferase	EC:2.3.1.12	2441,53	13	54,614	0,001576	pyruvate/acetyl-CoA metabolism

PADG_06494	Dihydrolipoyl dehydrogenase	EC:1.8.1.4	5644,67	27	116,746	2,16E-05	pyruvate/acetyl-CoA metabolism
Nitrogen, sulfur and selenium metabolism							
PADG_06490	Formamidase	EC:3.5.1.49	1220	5	26,918	0,0083895	nitrogen metabolism
PADG_00446	Oxidoreductase 2-nitropropane dioxygenase	-	142,59	4	12,837	0,0077629	nitrogen, sulfur and selenium metabolism
Nucleotide/nucleoside/nucleobase metabolism							
PADG_08098	Adenylate kinase 1	EC:2.7.4.3	286,2	3	9,974	0,0148644	purine metabolism
Lipid, fatty acid and isoprenoid metabolism							
PADG_06805	Acyl-CoA dehydrogenase	EC:1.3.8.7	738,41	1	9,028	0,0051585	beta-oxidation
PADG_01209	Enoyl-CoA hydratase	EC:4.2.1.17	2165,18	10	57,017	5,704E-05	beta-oxidation
PADG_01228	3-hydroxybutyryl-CoA dehydrogenase	EC:1.1.1.157	2202,66	5	34,657	0,0019274	butanoate metabolism
PADG_06382	Acetyl-CoA C-acetyltransferase (ERG 10)	EC:2.3.1.9	2146,96	6	39,903	0,0161383	ergosterol pathway
PADG_02751	Acetyl-CoA C-acetyltransferase (ERG 10)	EC:2.3.1.9		2	5,38	3,682E-05	ergosterol pathway
PADG_03194	Peroxisomal 3-ketoacyl-CoA thiolase	EC:2.3.1.16	1547,36	9	38,719	0,0041943	beta-oxidation
3. CELL CYCLE AND DNA MAINTENANCE							
Cell cycle							
PADG_04318	Protein PET117	-		3	4,874	0,0084097	mitochondrial biogenesis
DNA maintenance							
PADG_01867	HMG box domain containing protein	-	6599,15	18	106,001	7,262E-05	DNA binding
PADG_00466	Mitochondrial genome maintenance protein MGM101	-	1029,02	5	17,972	0,0081786	DNA synthesis and replication
PADG_05907	Histone H2B	-	1399,98	8	32,947	0,0096171	nucleosome assembly

PADG_00873	Histone H3	-	1141,69	5	25,396	0,0016124	nucleosome assembly
------------	------------	---	---------	---	--------	-----------	---------------------

4. PROTEIN SYNTHESIS

Translation factors

PADG_01949	Translation elongation factor Tu	-	5965,26	17	93,135	0,0005212	translation initiation
PADG_07895	Translation initiation factor eIF-2	-	202,53	3	10,128	0,000155	translation initiation

Ribosome

PADG_01267	40S ribosomal protein S11	-	1872,35	8	34,168	0,0076532	translation
PADG_06313	40S ribosomal protein S18	-	1962,9	12	45,687	4,922E-05	translation
PADG_04315	40S ribosomal protein S24	-	4224,87	12	66,23	0,0024871	translation
PADG_03315	40S ribosomal protein S4	-	3170,46	15	66,29	0,0054929	translation
PADG_01654	40S ribosomal protein S6-A	-	4309,01	14	62,41	0,0096091	translation
PADG_12365	40S ribosomal protein S8	-	2607,33	9	50,06	0,0001122	translation
PADG_11227	60S ribosomal protein L13	-	2528,58	4	39,431	0,0078643	translation
PADG_04731	60S ribosomal protein L14e	-	1178,78	4	23,286	0,0116074	translation
PADG_00514	60S ribosomal protein L16	-	197,82	1	2,818	0,0121517	translation
PADG_06726	60S ribosomal protein L17	-	899,8	6	48,04	0,0003696	translation
PADG_03325	60S ribosomal protein L21e	-	789,48	4	13,702	0,0058956	translation
PADG_07924	60S ribosomal protein L24e	-	1917,53	7	36,902	0,0049484	translation
PADG_05025	60S ribosomal protein L26e	-	1992,25	4	46,956	0,0106979	translation
PADG_00612	60S ribosomal protein L27e	-	514,83	4	14,162	0,0025505	translation
PADG_12253	60S ribosomal protein L3	-	3037,55	13	49,01	0,0052869	translation
PADG_11832	60S ribosomal protein L31e	-	955,72	7	24,104	0,0028706	translation
PADG_01083	60S ribosomal protein L32	-	1151,21	8	39,292	0,0004539	translation
PADG_01914	60S ribosomal protein L35	-	1361,27	4	21,145	9,588E-05	translation
PADG_05721	60S ribosomal protein L4e	-	4922,8	13	96,5	3,585E-06	translation

PADG_02888	60S ribosomal protein L6	-	2148,71	7	28,846	0,0023564	translation
PADG_04848	60S ribosomal protein L8-B	-	949,53	7	20,751	0,0027703	translation

5. PROTEIN FATE and DEGRADATION

PADG_04167	Aspartyl aminopeptidase	EC:3.4.11.21	98,21	1	3,407	0,0139421	protein/peptide degradation
PADG_02895	ATP-dependent Clp protease ATP-binding subunit ClpB	-	1233,52	9	35,47	0,0026096	protein/peptide degradation

6. CELL RESCUE, DEFENSE AND VIRULENCE

Stress response

PADG_00430	Hsp7-like protein	-	22327,9	47	362,858	5,125E-05	stress response
PADG_03238	Hsp40	-	1317,1	4	26,641	0,0006215	stress response
PADG_08369	Hsp60-like protein	-	44444,47	58	561,378	0,0001515	stress response

Detoxification

PADG_03163	Cytochrome c peroxidase	EC:1.11.1.5	4147,08	16	86,359	0,0005427	acting on a peroxide as acceptor
PADG_03841	Disulfide-isomerase	EC:5.3.4.1	10234,01	22	162,778	0,0041623	oxidoreductase
PADG_04912	Peroxiredoxin	EC:1.11.1.15	1277,64	8	24,334	2,305E-07	acting on a peroxide as acceptor

7. UNCLASSIFIED

PADG_05342	Uncharacterized protein	-	396,02	1	3,898	0,005088	-
PADG_05798	Uncharacterized protein	-	551,88	2	11,601	4,959E-06	-
PADG_07414	Uncharacterized protein	-	1380,2	5	23,928	0,006516	-
PADG_02338	Uncharacterized protein	-	352,34	4	12,045	0,0198828	-
PADG_06996	Uncharacterized protein	-	298,28	1	2,877	0,0038121	-
PADG_03210	Uncharacterized protein	-	501,82	2	7,817	0,0014091	-

Supplementary Table 2: Functional categorization of proteins down-regulated 12 hours after hypoxia with *Paracoccidioides brasiliensis*.

Accession number	Gene Description	EC number	MS Score	Unique Peptide	Peptide Score	p-value	Subclassification
Functional categories							
1. ENERGY							
Pentose-phosphate pathway							
PADG_07771	6-phosphogluconolactonase	EC:3.1.1.31	1390,7	5	19,662	0,0099017	pentose phosphate pathway
Electron Transport and Membrane-associated Energy Conservation							
PADG_07789	ATP synthase subunit delta, mitochondrial	-	883,86	2	16,12	0,0043477	oxidative phosphorylation
PADG_08152	Cytochrome c oxidase assembly factor 6	-	1063,5	5	26,563	0,0001662	complex IV assembly
PADG_06995	Cytochrome c oxidase subunit	-	567,1	3	8,179	0,0188571	complex IV assembly
PADG_04397	Cytochrome c oxidase subunit 4, mitochondrial	-		1	15,244	0,00401	complex IV assembly
PADG_04072	Cytochrome c oxidase-assembly factor COX23, mitochondrial	-	128,19	1	1,223	0,0015287	complex IV assembly
PADG_00688	F-type H+-transporting ATPase subunit h	-	1807,96	1	20,513	0,0007879	oxidative phosphorylation
PADG_11513	NADH-ubiquinone oxidoreductase	-	525,27	5	15,962	0,0025695	oxidative phosphorylation
PADG_04501	Ubiquinol-cytochrome c reductase subunit 7	-	1241,71	3	24,307	6,002E-05	oxidative phosphorylation
2. METABOLISM							
Amino Acid Metabolism							
PADG_08468	4-hydroxyphenylpyruvate dioxygenase	EC:1.13.11.27	2674,53	11	54,685	0,0002398	tyrosine metabolism
PADG_01286	Homoisocitrate dehydrogenase	EC:1.1.1.87		2	3,9	0,0012552	lysine biosynthesis
Nucleotide/nucleoside/nucleobase metabolism							

PADG_07782	Deoxyuridine 5'-triphosphate nucleotidohydrolase	EC:3.6.1.23	973,27	2	28,653	0,0008786	pyrimidine metabolism
PADG_01615	Homocitrate synthase, mitochondrial	EC:2.3.3.14	2022,65	10	41,898	0,0120782	pyruvate metabolism
PADG_04099	Phosphoribosylaminoimidazolecarboxamide formyltransferase/IMP cyclohydrolase	EC:2.1.2.3 3.5.4.10	3084,16	16	76,149	4,809E-05	purine metabolism

Metabolism of vitamins, cofactors, and prosthetic groups

PADG_05490	Molybdopterin binding domain-containing protein	-	309,66	1	4,115	0,0085831	metabolism of vitamins, cofactors, and prosthetic groups
------------	---	---	--------	---	-------	-----------	--

Secondary metabolism

PADG_02981	ThiJ/PfpI family protein	-	861,59	3	15,778	0,0092613	metabolism of polyketides
PADG_03785	UPF0135 protein yqfO*	-	104,7	1	3,13	0,0094729	hydrolase activity

Lipid, fatty acid and isoprenoid metabolism

PADG_02299	Choline-phosphate cytidylyltransferase	EC:2.7.7.15	283,32	2	8,55	0,0007666	glycerophospholipid metabolism
------------	--	-------------	--------	---	------	-----------	--------------------------------

3. CELL CYCLE AND DNA MAINTENANCE

Cell cycle

PADG_02388	Cell-cycle control medial ring component*	-	146,23	1	5,311	0,005173	cell cycle control
PADG_11950	Ran-binding protein 1	-	1653,41	4	33,457	0,0006064	cell cycle control
PADG_00011	Actin binding protein	-	2290,96	12	55,559	0,0098232	cell growth
PADG_02763	Cyclin-dependent kinase regulatory subunit CKS1	-	131,28	3	9,603	0,0150178	cell growth and death
PADG_07948	Altered inheritance of mitochondria protein 13*	-	652,13	2	9,399	0,0060823	mitochondrial biogenesis
PADG_03669	Mitochondrial protein import protein ZIM17*	-	557,78	4	13,888	0,0031893	mitochondrial biogenesis
PADG_05239	Tubulin-specific chaperone A	-	369,77	2	5,017	0,0151725	mitotic cell cycle and cell cycle
PADG_05714	Cell division control protein	-	663,8	4	16,882	0,0110585	mitotic cell cycle and cell cycle control

PADG_00849	Nuclear segregation protein Bfr1	-	3818,42	18	77,467	0,0081675	mitotic cell cycle and cell cycle control
PADG_08676	RNA binding effector protein Scp160*	-	154	3	9,455	0,0004591	mitotic cell cycle and cell cycle control
PADG_02243	Spo12 family protein	-	437,49	1	5,015	0,0002594	mitotic cell cycle and cell cycle control
PADG_03073	Nuclear movement protein nudC	-		2	8,734	0,0011568	nuclear migration
PADG_05935	Spindle poison sensitivity protein Scp3	-	697,7	5	27,035	0,0044944	cell cycle

Cytoskeleton

PADG_07249	Coronin	-	388,16	3	17,734	0,0190911	cytoskeleton proteins
PADG_01562	Dynactin 2	-	210,58	1	2,262	0,0181762	cytoskeleton proteins/Microtubules
PADG_08724	RPEL repeat protein	-	309,8	3	11,627	0,0025366	action binding

DNA maintenance

PADG_05893	Nucleosome assembly protein	-	840,5	4	30,87	0,0093703	organization of chromosome structure
------------	-----------------------------	---	-------	---	-------	-----------	--------------------------------------

4. TRANSCRIPTION

RNA synthesis and processing

PADG_05405	DNA-directed RNA polymerase I subunit RPA12	-	364,77	1	6,884	0,0126615	general transcription activities
PADG_04222	Multiprotein-bridging factor 1	-	293,56	5	13,896	0,0126957	positive regulation of transcription by RNA polymerase II
PADG_02315	RNA polymerase-associated protein LEO1	-		1	4,01	5,118E-05	mRNA synthesis
PADG_05340	Pre-mRNA-splicing factor srp1	-	2656,03	8	36,091	0,0142336	mRNA synthesis
PADG_06666	RNA-binding protein 39	-	348,99	1	3,596	0,006721	mRNA synthesis
PADG_06528	Splicing factor 3B subunit 2	-	327,94	3	12,963	0,0020335	mRNA synthesis
PADG_03836	Heterogeneous nuclear ribonucleoprotein A1	-	630,36	3	13,039	0,015579	mRNA biogenesis

PADG_08124	CCCH zinc finger and RRM domain-containing protein	-	71,83	1	2,108	0,0017689	mRNA processing
PADG_02996	PAB1 binding protein	-	495,53	3	11,555	0,0091439	mRNA processing (3'-end processing)
PADG_03788	Polyadenylation factor subunit CstF64	-	154,46	2	7,468	0,0197143	mRNA processing (splicing, 5'-, 3'-end processing)
PADG_05587	Small nuclear ribonucleoprotein U	-	1528,19	8	29,547	0,0015727	mRNA processing (splicing, 5'-, 3'-end processing)
PADG_04369	Splicing factor U2AF	-	328,44	1	8,045	0,0015786	mRNA processing (splicing, 5'-, 3'-end processing)
PADG_07689	Transformer-SR ribonucleoprotein	-	4514,76	11	73,206	0,0175019	mRNA processing (splicing, 5'-, 3'-end processing)
PADG_07884	Polyadenylate-binding protein	-	5746,76	24	118,69	0,0046711	mRNA surveillance
PADG_02346	mRNA stability protein	-	247,64	4	12,207	0,0027604	mRNA binding
PADG_03844	HAT1-interacting factor 1	-	340,4	2	7,839	0,0075617	genetic information processing
PADG_08423	RuvB-like helicase 2	EC:3.6.4.12	2610,2	10	44,737	0,0016002	genetic information processing
PADG_08424	U5 snRNP 52K protein	-	139,25	2	5,723	0,0099347	spliceosome
PADG_11958	U6 snRNA-associated Sm-like protein LSm3	-		1	2,178	1,375E-05	spliceosome
PADG_12196	Nucleolar protein 58		132,63	2	12,741	0,0062349	rRNA biogenesis
PADG_00044	28 kDa ribonucleoprotein	-	2180,63	11	59,911	0,0009185	rRNA processing
PADG_07495	rRNA processing protein RRP15	-	296,55	1	3,193	0,0008548	rRNA processing
PADG_11254	ATP-dependent RNA helicase DBP2	EC:3.6.4.13	1001,46	5	23,242	0,0020289	rRNA processing
PADG_07582	Phenylalanyl-tRNA synthetase alpha chain	EC:6.1.1.20	602,02	2	9,658	0,0198253	tRNA biosynthesis
PADG_02783	RNA-binding La domain-containing protein	-	1042,64	3	18,546	0,0098753	RNA processing
PADG_04934	RNP domain protein	-	4266,49	12	74,411	0,0134612	RNA transport

Transcription control

PADG_11936	APSES transcription factor	-	312,84	5	19,67	0,003556	transcription factor
PADG_01241	General negative regulator of transcription subunit 2	-	107,04	2	6,33	0,005563	transcriptional control
PADG_04311	Zinc knuckle protein	-	574,48	6	22,18	0,0015986	transcriptional control

5. PROTEIN SYNTHESIS

Translation factors

PADG_07229	Elongation factor 3	-	619,84	4	10,326	0,0001873	translation initiation
PADG_02296	Eukaryotic translation initiation factor 3 subunit F	-	915,46	3	15,138	0,0052836	translation initiation
PADG_04251	Eukaryotic translation initiation factor 3 subunit I	-	121,43	3	10,504	0,0001439	translation initiation
PADG_04057	Eukaryotic translation initiation factor 3 subunit J	-	1535,27	8	52,346	0,0028741	translation initiation
PADG_07888	Eukaryotic translation initiation factor 5A	-	1633,15	6	35,055	0,0015247	translation initiation
PADG_01079	Translation initiation factor 4B	-	6655,95	22	129,406	0,0020401	translation initiation

Ribosome

PADG_00784	40S ribosomal protein S0	-	1157,45	6	24,898	0,0171089	translation
PADG_01427	40S ribosomal protein S12	-	2475,51	7	42,757	0,0001853	translation
PADG_07583	40S ribosomal protein S21	-	1016,5	7	22,679	0,0129357	translation
PADG_00995	40S ribosomal protein S27a	-	3178,01	3	44,111	0,0044422	translation
PADG_08605	40S ribosomal protein S28	-	905,6	3	16,839	0,0008453	translation
PADG_01503	40S ribosomal protein S35*	-	155,61	2	4,515	0,0064232	translation
PADG_07870	40S ribosomal protein S7	-	314,72	2	8,558	0,0046531	translation
PADG_08244	60S acidic ribosomal protein P1	-	2423,75	1	18,954	0,0008252	translation
PADG_07803	60S ribosomal protein L12	-	2444,68	7	42,244	0,0011324	translation
PADG_03873	60S ribosomal protein L20	-		4	10,601	0,0068539	translation
PADG_05939	60S ribosomal protein L27a	-	1445,72	5	24,585	0,0045467	translation
PADG_08715	60S ribosomal protein L28e*	-	2734,54	10	58,997	0,0184882	translation
PADG_03781	60S ribosomal protein L30	-	1338,34	2	16,827	1,745E-05	translation
PADG_00046	60S ribosomal protein L54	-	1122,52	2	25,372	0,0010263	translation

6. PROTEIN FATE and DEGRADATION

Protein degradation

PADG_12029	26S proteasome regulatory subunit N3	-		1	2,05	0,017107	protein/peptide degradation
PADG_08095	26S proteasome regulatory subunit rpn-8	-	750,76	6	27,306	0,0010486	protein/peptide degradation
PADG_03221	Metallopeptidase MepB	EC:3.4.24.-	1258,99	4	18,006	0,0162953	protein/peptide degradation
PADG_03982	Proteasome endopeptidase complex	EC:3.4.25.1	1687,12	8	36,679	0,0033778	protein/peptide degradation
PADG_03967	Proteasome subunit beta 6	EC:3.4.25.1	1553,25	5	31,077	0,0012299	protein/peptide degradation
PADG_03424	Ubiquitin-activating enzyme E1	EC:6.2.1.45	155,35	2	10,884	0,0152041	protein/peptide degradation
PADG_07925	Ubiquitin-conjugating enzyme E2 N	EC:2.3.2.23	1043,89	3	20,186	0,012275	protein/peptide degradation
PADG_07515	UBX domain-containing protein	-	1016,39	5	24,908	0,0014923	protein/peptide degradation

Protein modification

PADG_04795	Deubiquitination-protection protein dph1	-	1612,9	6	33,196	0,0024714	protein binding
PADG_03544	Ser/Thr protein phosphatase*	-	2296,44	9	38,237	0,0003595	transferring phosphorus-containing groups
PADG_00809	Ubiquitin-conjugating enzyme	-	677,94	2	9,671	0,0170763	protein modification
PADG_02908	Ubiquitin-like modifier SUMO	-	764,46	3	10,747	0,0034056	protein sumoylation
PADG_05245	Ubiquitin-NEDD8-like protein RUB2	-	351,52	1	4,103	9,946E-05	ubiquitin system

7. CELL RESCUE, DEFENSE AND VIRULENCE

Stress response

PADG_03963	30 kDa heat shock protein	-	6159,41	15	106,464	3,696E-05	stress response
PADG_08599	DnaJ domain protein	-		1	9,035	0,015092	stress response
PADG_02785	Heat shock protein Hsp88	-	5772,18	29	138,128	0,0003157	stress response
PADG_06699	Hsp20 family protein	-	801,22	5	26,006	0,0006575	stress response
PADG_05139	Hsp70-like protein	-	519,79	4	14,682	0,0081819	stress response
PADG_02761	Hsp75-like protein	-	5807,83	25	151,607	0,0013069	stress response
PADG_05032	Hsp90 binding co-chaperone (Sba1)	-	1141,54	5	17,522	0,0049918	stress response
PADG_01711	Hsp90 co-chaperone AHA1	-	369,35	1	19,582	0,0006684	stress response

Detoxification

PADG_04587	Glutathione peroxidase	EC:1.11.1.9		1	2,663	0,0102724	acting on a peroxide as acceptor
PADG_07418	Superoxide dismutase [Cu-Zn]	EC:1.15.1.1	1390,12	4	18,208	0,0103609	acting on superoxide as acceptor

8. CELLULAR TRANSPORT, TRANSPORT FACILITIES AND TRANSPORT ROUTES

General transport

PADG_00442	ADP-ribosylation factor GTPase-activating protein 2/3	-	1618,2	9	39,014	7,85E-06	membrane trafficking/Endocytosis
PADG_04439	ATPase inhibitor, mitochondrial		270,37	3	6,7	0,0001063	membrane trafficking/Autophagy
PADG_08646	Class E vacuolar protein-sorting machinery protein HSE1	-	113,49	5	10,445	0,0010261	membrane trafficking/Endocytosis
PADG_04100	Clathrin heavy chain	-	537,59	2	11,94	0,0004596	membrane trafficking/Endocytosis
PADG_02022	Clathrin light chain	-	1803,32	6	34,253	0,0012536	membrane trafficking/Endocytosis
PADG_06655	Coatomer subunit delta	-	238,01	3	7,827	0,0166407	membrane trafficking
PADG_03005	Dynein light chain	-		1	3,959	0,0011776	motor for the intracellular transport/vesicular
PADG_07590	Epsin	-	459,63	3	8,026	0,0101317	transport/Membrane
PADG_04048	Small COPII coat GTPase sar1	EC:3.6.5.-	232,88	1	4,736	0,019791	trafficking/Endocytosis protein/peptide degradation
PADG_03509	Stromal membrane-associated protein	-	196,69	1	2,743	0,000374	ER to Golgi transport
PADG_07659	Transport protein SEC9	-	858,15	4	13,936	0,0049569	mesicle fusion
PADG_08615	Tropomyosin	-	1472,23	5	33,828	0,0111149	vacuolar/lysosomal transport/actin lateral binding

Organelle membrane transport

PADG_01994	Mitochondrial import receptor subunit TOM22	-	300,91	1	4,412	0,0088448	mitochondrial transport
------------	---	---	--------	---	-------	-----------	-------------------------

PADG_04441	Nuclear pore complex protein Nup62	-	481,18	2	8,48	0,0140546	structural constituent of nuclear pore
PADG_04319	V-type ATPase, G subunit	EC:3.1.1.3	1044,65	2	16,247	0,0038164	-

9. CELLULAR COMMUNICATION/SIGNAL TRANSDUCTION MECHANISM

Signal Transduction

PADG_06568	TCTP family protein	-	689,6	3	19,577	0,0036104	Ca(2+)- and microtubule-binding/anti-apoptosis
PADG_03219	Myosin regulatory light chain cdc4	-	1498,33	8	37,732	0,0024009	Ca2+ mediated signal transduction
PADG_08191	cAMP-dependent protein kinase regulatory	-	362,66	1	10,224	0,004818	cAMP/cGMP mediated signal transduction
PADG_02385	Fe-S cluster assembly protein DRE2	-	443,42	3	10,059	0,0016678	signaling proteins

10. UNCLASSIFIED

PADG_00421	Uncharacterized protein	-	411,76	1	3,957	0,0115199	-
PADG_00674	Uncharacterized protein	-	120,95	3	10,255	0,0006776	-
PADG_00676	Uncharacterized protein	-	4662,38	16	115,19	0,0002213	-
PADG_00690	Uncharacterized protein	-		2	2,883	0,0145467	-
PADG_00824	Uncharacterized protein	-	5196,05	14	95,355	0,0015143	-
PADG_01010	Uncharacterized protein	-	149,82	4	11,244	0,0040897	-
PADG_01141	Uncharacterized protein	-		2	3,683	0,0119089	-
PADG_01285	Uncharacterized protein	-	1101,29	5	17,644	0,005802	-
PADG_01857	Uncharacterized protein	-	886,28	6	28,505	0,0008753	-
PADG_02118	Uncharacterized protein	-	296,6	2	8,255	0,0150718	-
PADG_02307	Uncharacterized protein	-	1020,98	4	14,475	0,0094666	-
PADG_02501	Uncharacterized protein	-	1237,17	7	25,952	0,0077317	-
PADG_02652	Uncharacterized protein	-	7384,19	18	121,516	1,155E-06	-
PADG_02909	Uncharacterized protein	-	308,92	1	10,079	0,0123272	-

PADG_02967	Uncharacterized protein	-	4706,8	18	96,143	0,003786	-
PADG_04086	Uncharacterized protein	-		1	2,243	0,0049157	-
PADG_04549	Uncharacterized protein	-	299,65	1	4,941	0,0022838	-
PADG_05408	Uncharacterized protein	-	750,65	3	11,432	0,0073624	-
PADG_05959	Uncharacterized protein	-	442,6	3	14,678	0,0114935	-
PADG_06262	Uncharacterized protein	-		2	3,132	0,0044253	-
PADG_06690	Uncharacterized protein	-	566,51	4	11,315	0,0020324	-
PADG_06945	Uncharacterized protein	-	181,75	5	13,349	0,0046252	-
PADG_07034	Uncharacterized protein	-		1	2,983	0,0170546	-
PADG_07896	Uncharacterized protein	-		2	3,001	1,866E-05	-
PADG_08270	Uncharacterized protein	-	655,26	2	8,763	0,0025914	-
PADG_08467	Uncharacterized protein	-	857,05	4	19,772	0,0010757	-
PADG_08702	Uncharacterized protein	-	732,23	1	8,736	0,0183461	-
PADG_11101	Uncharacterized protein	-	324,35	3	10,144	0,0006553	-
PADG_11214	Uncharacterized protein	-	1426,21	1	24,778	0,0167616	-
PADG_12437	Uncharacterized protein	-	535,89	4	16,207	0,0002072	-

Capítulo IV

6. CONCLUSÃO

A diminuição do oxigênio é um estresse que os fungos do gênero *Paracoccidioides* enfrentam. Eles só conseguem sobreviver, pois possuem mecanismos adaptativos para perceber a ausência do oxigênio e de modo consequente, remodelar todo seu metabolismo celular. Neste trabalho identificamos uma proteína globular responsiva à hipóxia, bem como evidenciamos as mudanças metabólicas através de análise proteômica quantitativa.

A respeito da fungoglobina, FglA, verificamos que todas as espécies de *Paracoccidioides* possuem essa proteína. Em seguida, demonstramos que suas características estruturais permitem a entrada e saída do oxigênio ligado ao grupo protético heme. Quando células leveduriformes de *P. brasiliensis* são submetidas a condições que mimetizam um ambiente hipóxico, os níveis transcripcionais e proteicos da FglA são aumentados. Sua expressão retorna à níveis basais quando o suporte de oxigênio retorna à tensões atmosféricas normais. Essa habilidade nos indica que a FglA pode atuar como um sensor dos níveis de oxigênio. Esses dados são corroborados durante a infecção *in vivo* em modelo murino, no qual a FglA também é super-expressa, sugerindo um papel na biologia fúngica durante a infecção.

As análises em larga escala do perfil proteico de leveduras de *P. brasiliensis* submetidas a hipóxia revelaram que o metabolismo energético é direcionado para a fermentação alcoólica. O aumento do ergosterol e da glucana reflete na reorganização da membrana e parede celular, respectivamente. A glucana pode exercer um papel protetor para a célula fúngica. Além disso, é nítido que durante a hipóxia os mecanismos do ciclo celular e transcrição são minimizados, garantindo a economia de energia. Esses dados são suportados pela análises das amostras fosfoenriquecidas. As proteínas fosforiladas relacionadas com o ciclo celular e transcrição são a maioria e estão com a expressão diminuída durante a hipóxia. Portanto, acreditamos que a fosforilação tem papel importante na regulação desses processos.

Apesar de aplicarmos, em conjunto, métodos de análises *in silico*, moleculares bioquímicos, proteômicos e funcionais, sabemos que durante a infecção vários estresses ocorrem simultaneamente. Para melhor entender os dados prévios aqui mostrados, isolados com supressão ou deleção de genes-chave devem ser construídos, bem como experimentos em modelos de infecção *in vivo* mais robustos devem ser realizados.

Finalmente, em nosso conhecimento, esse é o primeiro trabalho que estuda o fungoglobina e o fosfoproteoma no gênero *Paracoccidioides* durante o estresse hipóxico. Espera-se que o trabalho possa contribuir servindo de referência para escolha de alvos para novas pesquisas.

7. PERSPECTIVAS

A partir da compreensão obtida neste trabalho, podemos traçar novas metas seguindo essa linha de pesquisa. As perspectivas são:

- Construir um isolado silenciado/deletado para o gene da FglA e outras proteínas importantes na resposta à hipóxia e realizar ensaios de virulência em modelos *in vivo*, a fim de verificarmos a importância desses genes para a biologia de *Paracoccidioides*;
- Analisar detalhadamente as vias de ativação pela fosforilação/defosforilação relacionadas ao ciclo celular e a adaptação à infecção;
- Buscar compostos e/ou peptídeos bioativos ligantes a essas proteínas-chave, com o propósito de melhorar a terapêutica e controlar a doença.

8. REFERÊNCIAS

- Alberts, B., Johnson, A., Morgan, D., Raff, M., and Roberts, K. (2017). *Biologia Molecular da Célula*. 6º edição. Porto Alegre: Artmed.
- Almeida, F. P. (1930a). Comparative study of coccidioidal granuloma in the United States and Brazil, establishing a new genus for the Brazilian parasite. *An. Fac. Med. S. Paulo* 5, 125.
- Almeida, F. P. (1930b). Differential features of the etiologic agents of coccidioidal granuloma of the United States and Brazil. *C. R. Soc. Biol.* 105, 315–316.
- Arantes, T. D., Theodoro, R. C., Da Graça Macoris, S. A., and Bagagli, E. (2013). Detection of *Paracoccidioides* spp. in environmental aerosol samples. *Med. Mycol.* 51, 83–92. doi:10.3109/13693786.2012.698444.
- Araújo, F. S., Coelho, L. M., Silva, L. do C., da Silva Neto, B. R., Parente-Rocha, J. A., Bailão, A. M., et al. (2016). Effects of Argentilactone on the Transcriptional Profile, Cell Wall and Oxidative Stress of *Paracoccidioides* spp. *PLoS Negl. Trop. Dis.* 10, e0004309. doi:10.1371/journal.pntd.0004309.
- Aristizabal, B. H., Clemons, K. V., Stevens, D. A., and Restrepo, A. (1998). Morphological transition of *Paracoccidioides brasiliensis* conidia to yeast cells: in vivo inhibition in females. *Infect. Immun.* 66, 5587–91. Available at: <http://www.ncbi.nlm.nih.gov/pubmed/9784579> [Accessed December 9, 2018].
- Arnold, F., West, D., and Kumar, S. (1987). Wound healing: the effect of macrophage and tumour derived angiogenesis factors on skin graft vascularization. *Br. J. Exp. Pathol.* 68, 569–74. Available at: <http://www.ncbi.nlm.nih.gov/pubmed/2443156> [Accessed March 7, 2018].
- Askew, C., Sellam, A., Epp, E., Hogues, H., Mullick, A., Nantel, A., et al. (2009). Transcriptional Regulation of Carbohydrate Metabolism in the Human Pathogen *Candida albicans*. *PLoS Pathog.* 5, e1000612. doi:10.1371/journal.ppat.1000612.
- Bagagli, E., Bosco, S. M. G., Theodoro, R. C., and Franco, M. (2006). Phylogenetic and evolutionary aspects of *Paracoccidioides brasiliensis* reveal a long coexistence with animal hosts that explain several biological features of the pathogen. *Infect. Genet. Evol.* 6, 344–351. doi:10.1016/j.meegid.2005.12.002.
- Bagagli, E., Franco, M., Bosco, S. D. M. G., Hebeler-barbosa, F., Trinca, L. A., and Montenegro, M. R. (2003). High frequency of *Paracoccidioides brasiliensis* infection

- in armadillos (*Dasyprocta novemcinctus*): an ecological study. *Med. Mycol.* 41, 217–223. doi:10.1080/13693780310001597368.
- Bagagli, E., Theodoro, R. C., Bosco, S. M. G., and McEwen, J. G. (2008). *Paracoccidioides brasiliensis*: Phylogenetic and ecological aspects. *Mycopathologia* 165, 197–207. doi:10.1007/s11046-007-9050-7.
- Bantscheff, M., Boesche, M., Eberhard, D., Matthieson, T., Sweetman, G., and Kuster, B. (2008). Robust and Sensitive iTRAQ Quantification on an LTQ Orbitrap Mass Spectrometer. *Mol. Cell. Proteomics* 7, 1702–1713. doi:10.1074/mcp.M800029-MCP200.
- Barker, B. M., Kroll, K., Vödisch, M., Mazurie, A., Kniemeyer, O., and Cramer, R. A. (2012). Transcriptomic and proteomic analyses of the *Aspergillus fumigatus* hypoxia response using an oxygen-controlled fermenter. *BMC Genomics* 13, 62. doi:10.1186/1471-2164-13-62.
- Bellissimo-Rodrigues, F., Machado, A. A., and Martinez, R. (2011). Paracoccidioidomycosis Epidemiological Features of a 1,000-Cases Series from a Hyperendemic Area on the Southeast of Brazil. *Am. J. Trop. Med. Hyg.* 85, 546–550. doi:10.4269/ajtmh.2011.11-0084.
- Benard, G. (2008). An overview of the immunopathology of human paracoccidioidomycosis. *Mycopathologia* 165, 209–221. doi:10.1007/s11046-007-9065-0.
- Benchimol, J., and Sá, M. (2004). *Adolpho Lutz: Dermatologia e Micologia*. V. 1, Book. , eds. J. Benchimol and M. Sá Rio de Janeiro: Editora Fiocruz.
- Blatzer, M., Barker, B. M., Willger, S. D., Beckmann, N., Blosser, S. J., Cornish, E. J., et al. (2011). SREBP Coordinates Iron and Ergosterol Homeostasis to Mediate Triazole Drug and Hypoxia Responses in the Human Fungal Pathogen *Aspergillus fumigatus*. *PLoS Genet.* 7, e1002374. doi:10.1371/journal.pgen.1002374.
- Block, H., Maertens, B., Spriestersbach, A., Brinker, N., Kubicek, J., Fabis, R., et al. (2009). Chapter 27 Immobilized-Metal Affinity Chromatography (IMAC). A Review. *Methods Enzymol.* 463, 439–473. doi:10.1016/S0076-6879(09)63027-5.
- Borba, J. V. V. B., Tauhata, S. B. F., Oliveira, C. M. A. de, Ferreira Marques, M., Bailão, A. M., Soares, C. M. de A., et al. (2018). Chemoproteomic identification of molecular targets of antifungal prototypes, thiosemicarbazide and a camphene derivative of thiosemicarbazide, in *Paracoccidioides brasiliensis*. *PLoS One* 13, e0201948.

- doi:10.1371/journal.pone.0201948.
- Brasil (2009). *Guia de Vigilância Epidemiológica*. 7º edição. , ed. Ministério da Saúde
Brasília: Editora MS.
- Brasil (2010). *Doenças infecciosas e parasitárias: guia de bolso*. 8º edição. , ed. Ministério
da Saúde Brasília: Editora MS.
- Brasil (2013). “Módulo 8: Detecção e identificação de fungos de importância médica,” in
Microbiologia Clínica para o Controle de Infecção Relacionada à Assistência à Saúde,
ed. Agência Nacional de Vigilância Sanitária (Brasília: ANVISA), 46.
- Brasil (2016). Portaria N° 204, de 17 de Fevereiro de 2016. Brasil: Ministério da Saúde.
- Brasil (2018). DATASUS: Departamento de Informática do SUS. Available at:
<http://datasus.saude.gov.br/>.
- Brummer, E., Castaneda, E., and Restrepo, A. (1993). Paracoccidioidomycosis: An update.
Clin. Microbiol. Rev. 6, 89–117. doi:10.1128/CMR.6.2.89.Updated.
- Bustamante-Simon, B., McEwen, J. G., Tabares, A. M., Arango, M., and Restrepo-Moreno,
A. (1985). Characteristics of the conidia produced by the mycelial form of
Paracoccidioides brasiliensis. *Sabouraudia* 23, 407–14. Available at:
<http://www.ncbi.nlm.nih.gov/pubmed/4095647> [Accessed June 1, 2017].
- Butler, G. (2013). Hypoxia and gene expression in eukaryotic microbes. *Annu. Rev. Microbiol.* 67, 291–312. doi:10.1146/annurev-micro-092412-155658.
- Carreau, A., Hafny-Rahbi, B. El, Matejuk, A., Grillon, C., and Kieda, C. (2011). Why is the
partial oxygen pressure of human tissues a crucial parameter? Small molecules and
hypoxia. *J. Cell. Mol. Med.* 15, 1239–1253. doi:10.1111/j.1582-4934.2011.01258.x.
- Carrero, L. L., Niño-Vega, G., Teixeira, M. M., Carvalho, M. J. A., Soares, C. M. A., Pereira,
M., et al. (2008). New *Paracoccidioides brasiliensis* isolate reveals unexpected
genomic variability in this human pathogen. *Fungal Genet. Biol.* 45, 605–612.
doi:10.1016/j.fgb.2008.02.002.
- Chang, Y. C., Bien, C. M., Lee, H., Espenshade, P. J., and Kwon-Chung, K. J. (2007). Sre1p,
a regulator of oxygen sensing and sterol homeostasis, is required for virulence in
Cryptococcus neoformans. *Mol. Microbiol.* 64, 614–629. doi:10.1111/j.1365-
2958.2007.05676.x.
- Chaves, A. F. A. A., Castilho, D. G., Navarro, M. V., Oliveira, A. K., Serrano, S. M. T. T.,
Tashima, A. K., et al. (2017). Phosphosite-specific regulation of the oxidative-stress
response of *Paracoccidioides brasiliensis*: a shotgun phosphoproteomic analysis.

- Microbes Infect.* 19, 34–46. doi:10.1016/j.micinf.2016.08.004.
- Chun, C. D., Liu, O. W., and Madhani, H. D. (2007a). A link between virulence and homeostatic responses to hypoxia during infection by the human fungal pathogen *Cryptococcus neoformans*. *PLoS Pathog.* 3, e22. doi:10.1371/journal.ppat.0030022.
- Chun, C. D., Liu, O. W., and Madhani, H. D. (2007b). A link between virulence and homeostatic responses to hypoxia during infection by the human fungal pathogen *Cryptococcus neoformans*. *PLoS Pathog.* 3, 0225–0238. doi:10.1371/journal.ppat.0030022.
- Chun, C. D., Liu, O. W., and Madhani, H. D. (2007c). A Link between Virulence and Homeostatic Responses to Hypoxia during Infection by the Human Fungal Pathogen *Cryptococcus neoformans*. *PLoS Pathog.* 3, e22. doi:10.1371/journal.ppat.0030022.
- Chung, D., Haas, H., and Cramer, R. (2012). Coordination of hypoxia adaptation and iron homeostasis in human pathogenic fungi. *Front. Microbiol.* 3, 1–13. doi:10.3389/fmicb.2012.00381.
- Cohen, P. (2002). The origins of protein phosphorylation. 4.
- Corredor, G. G., Peralta, L. A., Castaño, J. H., Zuluaga, J. S., Henao, B., Arango, M., et al. (2005). The naked-tailed armadillo *Cabassous centralis* (Miller 1899): a new host to *Paracoccidioides brasiliensis*. Molecular identification of the isolate. *Med. Mycol.* 43, 275–80. Available at: <http://www.ncbi.nlm.nih.gov/pubmed/16010854> [Accessed December 9, 2018].
- Coutinho, Z. F.; Da Silva, D.; Lazera, M.; Petri, V.; Oliveira, R. M.; Sabroza, P. C.; Wanke, B. (2002). Paracoccidioidomycosis mortality in Brazil (1980-1995). *Cad. saude publica / Minist. da Saude, Fund. Oswaldo Cruz, Esc. Nac. Saude Publica* 18, 1441–1454. doi:10.1590/S0102-311X2002000500037.
- De Albornoz, M. B. (1971). Isolation of *Paracoccidioides brasiliensis* from rural soil in Venezuela. *Sabouraudia* 9, 248–53. Available at: <http://www.ncbi.nlm.nih.gov/pubmed/4944202> [Accessed December 9, 2018].
- Delom, F., and Chevet, E. (2006). Phosphoprotein analysis: from proteins to proteomes. *Proteome Sci.* 4, 15. doi:10.1186/1477-5956-4-15.
- Dewhirst, M. W. (1998). Concepts of oxygen transport at the microcirculatory level. *Semin. Radiat. Oncol.* 8, 143–50. Available at: <http://www.ncbi.nlm.nih.gov/pubmed/9634491> [Accessed March 7, 2018].
- Dubois, J. C., and Smulian, A. G. (2016). Sterol Regulatory Element Binding Protein (Srb1)

- Is Required for Hypoxic Adaptation and Virulence in the Dimorphic Fungus *Histoplasma capsulatum*. 1–19. doi:10.1371/journal.pone.0163849.
- Silva, K. S., da S Neto, B. R., Zambuzzi-Carvalho, P. F., de Oliveira, C. M., Pires, L. B., Kato, L., et al. (2018). Response of *Paracoccidioides lutzii* to the antifungal camphene thiosemicarbazide determined by proteomic analysis. *Future Microbiol.* 13, 1473–1496. doi:10.2217/fmb-2018-0176.
- Ernst, J. F., and Tielker, D. (2009). Microreview Responses to hypoxia in fungal pathogens. *Cell. Microbiol.* 11, 183–190. doi:10.1111/j.1462-5822.2008.01259.x.
- Fernandes, L., Araújo, M. A. M., Amaral, A., Reis, V. C. B., Martins, N. F., and Felipe, M. S. (2005). Cell signaling pathways in *Paracoccidioides brasiliensis*--inferred from comparisons with other fungi. *Genet. Mol. Res.* 4, 216–231. doi:Pb02 [pii].
- Ferreira, K. S., Maranhão, A. Q., Garcia, M. C. C., Brígido, M. M., Santos, S. S., Lopes, J. D., et al. (2011). Dendritic Cells Transfected with scFv from Mab 7.B12 Mimicking Original Antigen gp43 Induces Protection against Experimental Paracoccidioidomycosis. *PLoS One* 6, e15935. doi:10.1371/journal.pone.0015935.
- Ferreira, M. S., Freitas, L. H., Lacaz, C. da S., del Negro, G. M., de Melo, N. T., Garcia, N. M., et al. (1990). Isolation and characterization of a *Paracoccidioides brasiliensis* strain from a dogfood probably contaminated with soil in Uberlândia, Brazil. *J. Med. Vet. Mycol.* 28, 253–6. Available at: <http://www.ncbi.nlm.nih.gov/pubmed/2213439> [Accessed December 9, 2018].
- Fortes, M. R. P., Miot, H. A., Kurokawa, C. S., Marques, M. E. A., and Marques, S. A. (2010). Immunology of paracoccidioidomycosis. *An. Bras. Dermatol.* 86, 516–24. Available at: <http://www.ncbi.nlm.nih.gov/pubmed/21738969> [Accessed March 7, 2018].
- Gafken, P. R., and Lampe, P. D. (2006). Methodologies for Characterizing Phosphoproteins by Mass Spectrometry. *Cell Commun. Adhes.* 13, 249–262. doi:10.1080/15419060601077917.
- Garcia, N. M., Del Negro, G. M., Heins-Vaccari, E. M., de Melo, N. T., de Assis, C. M., and Lacaz, C. da S. (1993). *Paracoccidioides brasiliensis*, a new sample isolated from feces of a penguin (*Pygoscelis adeliae*). *Rev. Inst. Med. Trop. Sao Paulo* 35, 227–35. Available at: <http://www.ncbi.nlm.nih.gov/pubmed/8278752> [Accessed December 9, 2018].
- Grahl, N., Puttikamonkul, S., Macdonald, J. M., Gamcsik, M. P., Ngo, L. Y., Hohl, T. M.,

- et al. (2011). In vivo hypoxia and a fungal alcohol dehydrogenase influence the pathogenesis of invasive pulmonary aspergillosis. *PLoS Pathog.* 7. doi:10.1371/journal.ppat.1002145.
- Grahl, N., Shepardson, K. M., Chung, D., and Cramer, R. A. (2012). Hypoxia and fungal pathogenesis: To air or not to air? *Eukaryot. Cell* 11, 560–570. doi:10.1128/EC.00031-12.
- Greer, S. N., Metcalf, J. L., Wang, Y., and Ohh, M. (2012). The updated biology of hypoxia-inducible factor. *EMBO J.* 31, 2448–2460. doi:10.1038/emboj.2012.125.
- Guida, A., Lindstädt, C., Maguire, S. L., Ding, C., Higgins, D. G., Corton, N. J., et al. (2011). Using RNA-seq to determine the transcriptional landscape and the hypoxic response of the pathogenic yeast *Candida parapsilosis*. *BMC Genomics* 12, 628. doi:10.1186/1471-2164-12-628.
- Guillemin, K., and Krasnow, M. A. (1997). The hypoxic response: huffing and HIFing. *Cell* 89, 9–12. Available at: <http://www.ncbi.nlm.nih.gov/pubmed/9094708> [Accessed December 10, 2018].
- Hanslin, H. M., Sæbø, A., and Bergersen, O. (2005). Estimation of oxygen concentration in the soil gas phase beneath compost mulch by means of a simple method. *Urban For. Urban Green.* 4, 37–40. doi:10.1016/j.ufug.2005.05.001.
- Hedges, S., Blair, J. E., Venturi, M. L., and Shoe, J. L. (2004). A molecular timescale of eukaryote evolution and the rise of complex multicellular life. *BMC Evol. Biol.* 4, 2. doi:10.1186/1471-2148-4-2.
- Hillmann, F., Linde, J., Beckmann, N., Cyrulies, M., Strassburger, M., Heinekamp, T., et al. (2014). The novel globin protein fungoglobin is involved in low oxygen adaptation of *Aspergillus fumigatus*. *Mol. Microbiol.* 93, 539–553. doi:10.1111/mmi.12679.
- Hoogewijs, D., Dewilde, S., Vierstraete, A., Moens, L., and Vinogradov, S. N. (2012). A phylogenetic analysis of the globins in Fungi. *PLoS One* 7, 1–15. doi:10.1371/journal.pone.0031856.
- Ingavale, S. S., Chang, Y. C., Lee, H., McClelland, C. M., Leong, M. L., and Kwon-Chung, K. J. (2008). Importance of Mitochondria in Survival of *Cryptococcus neoformans* Under Low Oxygen Conditions and Tolerance to Cobalt Chloride. *PLoS Pathog.* 4, e1000155. doi:10.1371/journal.ppat.1000155.
- Jensen, S. S., and Larsen, M. R. (2007). Evaluation of the impact of some experimental procedures on different phosphopeptide enrichment techniques. *Rapid Commun. Mass*

- Spectrom.* 21, 3635–3645. doi:10.1002/rcm.3254.
- Lacaz, C., Porto, E., Martins, J., Heins-Vaccari, E., and Melo, N. (2002). *Tratado de Micologia Médica Lacaz*. 9th ed. São Paulo: Sarvier.
- Lee, H., Bien, C. M., Hughes, A. L., Espenshade, P. J., Kwon-Chung, K. J., and Chang, Y. C. (2007). Cobalt chloride, a hypoxia-mimicking agent, targets sterol synthesis in the pathogenic fungus *Cryptococcus neoformans*. *Mol. Microbiol.* 65, 1018–1033. doi:10.1111/j.1365-2958.2007.05844.x.
- Lima, P. de S., Chung, D., Bailão, A. M., Cramer, R. A., and Soares, C. M. de A. (2015). Characterization of the *Paracoccidioides* Hypoxia Response Reveals New Insights into Pathogenesis Mechanisms of This Important Human Pathogenic Fungus. *PLoS Negl. Trop. Dis.* 9, 1–25. doi:10.1371/journal.pntd.0004282.
- Lutz, A. (1908). Uma mycose pseudococcídica localizada na boca e observada no Brazil. Contribuição ao conhecimento das hyphoblastomycoses americanas. *Bras-Med* 22, 121–4.
- Lutz, A. (1945). Uma micose pseudococcídica localizada na boca e observada no Brasil . Contribuição ao conhecimento das. *Adolpho Lutz - Obra Completa*, 483–494.
- MacPherson, S., Akache, B., Weber, S., De Deken, X., Raymond, M., and Turcotte, B. (2005). *Candida albicans* Zinc Cluster Protein Upc2p Confers Resistance to Antifungal Drugs and Is an Activator of Ergosterol Biosynthetic Genes. *Antimicrob. Agents Chemother.* 49, 1745–1752. doi:10.1128/AAC.49.5.1745-1752.2005.
- Margraf Bittencourt, J. I., Magalhaes de Oliveira, R., and Coutinho, Z. F. (2005). Paracoccidioidomycosis mortality in the State of Paraná , Brazil , 1980 / 1998 *Cad Saude Publica* 21, 1856–1864.
- Marques, S. A. (2008). Paracoccidioidomycose: centenário do primeiro relato de caso. Available at: <http://www.bvslutz.coc.fiocruz.br/php/index.php> [Accessed December 5, 2018].
- Marques, S. A. (2012). Paracoccidioidomycosis. *Clin. Dermatol.* 30, 610–615. doi:10.1016/j.clindermatol.2012.01.006.
- Martinez, R. (2017). New Trends in Paracoccidioidomycosis Epidemiology. *J. Fungi* 3, 1–13. doi:10.3390/jof3010001.
- Masuo, S., Terabayashi, Y., Shimizu, M., Fujii, T., Kitazume, T., and Takaya, N. (2010). Global gene expression analysis of *Aspergillus nidulans* reveals metabolic shift and transcription suppression under hypoxia. *Mol. Genet. Genomics* 284, 415–424.

doi:10.1007/s00438-010-0576-x.

- Matthews, H. R. (1995). Protein kinases and phosphatases that act on histidine, lysine, or arginine residues in eukaryotic proteins: a possible regulator of the mitogen-activated protein kinase cascade. *Pharmacol. Ther.* 67, 323–50. Available at: <http://www.ncbi.nlm.nih.gov/pubmed/8577821> [Accessed December 6, 2018].
- Matute, D. R., McEwen, J. G., Puccia, R., Montes, B. A., San-Blas, G., Bagagli, E., et al. (2006a). Cryptic Speciation and Recombination in the Fungus *Paracoccidioides brasiliensis* as Revealed by Gene Genealogies. *Mol. Biol. Evol.* 23, 65–73. doi:10.1093/molbev/msj008.
- Matute, D. R., Sepulveda, V. E., Quesada, L. M., Goldman, G. H., Taylor, J. W., Restrepo, A., et al. (2006b). Microsatellite analysis of three phylogenetic species of *Paracoccidioides brasiliensis*. *J. Clin. Microbiol.* 44, 2153–2157. doi:10.1128/JCM.02540-05.
- McEwen, J. G., Bedoya, V., Patiño, M. M., Salazar, M. E., and Restrepo, A. (1987). Experimental murine paracoccidiomycosis induced by the inhalation of conidia. *J. Med. Vet. Mycol.* 25, 165–75. Available at: <http://www.ncbi.nlm.nih.gov/pubmed/3612432> [Accessed December 9, 2018].
- Mendes, R. P., Cavalcante, R. de S., Marques, S. A., Marques, M. E. A., Venturini, J., Sylvestre, T. F., et al. (2017). Paracoccidiomycosis: Current Perspectives from Brazil. *Open Microbiol. J.* 11, 224–282. doi:10.2174/1874285801711010224.
- Mertins, P., Udeshi, N. D., Clauser, K. R., Mani, D., Patel, J., Ong, S., et al. (2012). iTRAQ Labeling is Superior to mTRAQ for Quantitative Global Proteomics and Phosphoproteomics. *Mol. Cell. Proteomics* 11, M111.014423. doi:10.1074/mcp.M111.014423.
- Montenegro, M. R., and Franco, M. (1994). “Pathology,” in *Paracoccidioidomycosis*, eds. M. Franco, C. S. Lacaz, A. Restrepo-Moreno, and G. Del Negro (Boca Raton: CRC Press), 131–150.
- Mukherji, M. (2005). Phosphoproteomics in analyzing signaling pathways. *Expert Rev. Proteomics* 2, 117–128. doi:10.1586/14789450.2.1.117.
- Muñoz, J. F., Farrer, R. A., Desjardins, C. A., Gallo, J. E., Sykes, S., Sakthikumar, S., et al. (2016). Genome Diversity, Recombination, and Virulence across the Major Lineages of *Paracoccidioides*. *mSphere* 1, e00213-16. doi:10.1128/MSPHERE.00213-16.
- Nardini, M., Pesce, A., Thijs, L., Saito, J. a, Dewilde, S., Alam, M., et al. (2008). Archaeal

- protoglobin structure indicates new ligand diffusion paths and modulation of haem-reactivity. *EMBO Rep.* 9, 157–63. doi:10.1038/sj.embor.7401153.
- Nelson, D. L., and Cox, M. (2014). *Princípios de Bioquímica de Lehninger*. 6th ed. Porto Alegre: Artmed.
- Pesce, A., Thijs, L., Nardini, M., Desmet, F., Sisinni, L., Gourlay, L., et al. (2009). HisE11 and HisF8 Provide Bis-histidyl Heme Hexa-coordination in the Globin Domain of *Geobacter sulfurreducens* Globin-coupled Sensor. *J. Mol. Biol.* 386, 246–260. doi:10.1016/j.jmb.2008.12.023.
- Poulos, T. L. (2014). Heme Enzyme Structure and Function. *Chem. Rev.* doi:dx.doi.org/10.1021/cr400415k.
- Prado, M., da Silva, M. B., Laurenti, R., Travassos, L. R., and Taborda, C. P. (2009). Mortality due to systemic mycoses as a primary cause of death or in association with AIDS in Brazil: A review from 1996 to 2006. *Mem. Inst. Oswaldo Cruz* 104, 513–521. doi:10.1590/S0074-02762009000300019.
- Puttick, J., Baker, E. N., and Delbaere, L. T. J. (2008). Histidine phosphorylation in biological systems. *Biochim. Biophys. Acta - Proteins Proteomics* 1784, 100–105. doi:10.1016/j.bbapap.2007.07.008.
- Ramsubramaniam, N., Harris, S. D., and Marten, M. R. (2014). The phosphoproteome of *Aspergillus nidulans* reveals functional association with cellular processes involved in morphology and secretion. *Proteomics* 14, 2454–2459. doi:10.1002/pmic.201400063.
- Raymond, J., and Segrè, D. (2006). The Effect of Oxygen on Biochemical Networks and the Evolution of Complex Life. *Science* (80-.). 311, 1764–1767. doi:10.1126/science.1118439.
- Restrepo, A., McEwen, J. G., and Castañeda, E. (2001). The habitat of *Paracoccidioides brasiliensis*: how far from solving the riddle? *Med. Mycol.* 39, 233–41. Available at: <http://www.ncbi.nlm.nih.gov/pubmed/11446526> [Accessed June 1, 2017].
- Rodrigues de Farias, M., Anuska Zeni Condas, L., Garcia Ribeiro, M., de Moraes Gimenes Bosco, S., Dominguez Muro, M., Werner, J., et al. (2011). Paracoccidioidomycosis in a Dog: Case Report of Generalized Lymphadenomegaly. *Mycopathologia* 172, 147–152. doi:10.1007/s11046-011-9412-z.
- Salazar, M. E., Restrepo, A., and Stevens, D. A. (1988). Inhibition by estrogens of conidium-to-yeast conversion in the fungus *Paracoccidioides brasiliensis*. *Infect. Immun.* 56, 711–3. Available at: <http://www.ncbi.nlm.nih.gov/pubmed/3343055> [Accessed

December 9, 2018].

- Salgado-Salazar, C., Jones, L. R., Restrepo, Á., and McEwen, J. G. (2010). The human fungal pathogen *Paracoccidioides brasiliensis* (Onygenales: Ajellomycetaceae) is a complex of two species: phylogenetic evidence from five mitochondrial markers. *Cladistics* 26, 613–624. doi:10.1111/j.1096-0031.2010.00307.x.
- San-Blas, G., Niño-Vega, G., and Iturriaga, T. (2002). *Paracoccidioides brasiliensis* and paracoccidioidomycosis: molecular approaches to morphogenesis, diagnosis, epidemiology, taxonomy and genetics. *Med. Mycol.* 40, 225–42. Available at: <http://www.ncbi.nlm.nih.gov/pubmed/12146752> [Accessed June 1, 2017].
- Sano, A., Defaveri, J., Tanaka, R., Yokoyama, K., Kurita, N., Franco, M., et al. (1998). Pathogenicities and GP43kDa gene of three *Paracoccidioides brasiliensis* isolates originated from a nine-banded armadillo *Dasypus novemcinctus*). *Mycopathologia* 144, 61–66. doi:10.1023/A:1007024923042.
- Santos, W. A. dos, Silva, B. M. da, Passos, E. D., Zandonade, E., and Falqueto, A. (2003). Associação entre tabagismo e paracoccidioidomicose: um estudo de caso-controle no Estado do Espírito Santo, Brasil. *Cad. Saude Publica* 19, 245–253. doi:10.1590/S0102-311X2003000100027.
- Selvan, L. D. N., Renuse, S., Kaviyil, J. E., Sharma, J., Pinto, S. M., Yelamanchi, S. D., et al. (2014). Phosphoproteome of *Cryptococcus neoformans*. *J. Proteomics* 97, 287–295. doi:10.1016/j.jprot.2013.06.029.
- Semenza, G. L. (2007). Life with oxygen. *Science* 318, 62–4. doi:10.1126/science.1147949.
- Setiadi, E. R., Doedt, T., Cottier, F., Noffz, C., and Ernst, J. F. (2006). Transcriptional Response of *Candida albicans* to Hypoxia: Linkage of Oxygen Sensing and Efg1p-regulatory Networks. *J. Mol. Biol.* 361, 399–411. doi:10.1016/j.jmb.2006.06.040.
- Severo, L. C., Geyer, G. R., Londero, A. T., Porto, N. S., and Rizzon, C. F. (1979). The primary pulmonary lymph node complex in paracoccidioidomycosis. *Mycopathologia* 67, 115–8. Available at: <http://www.ncbi.nlm.nih.gov/pubmed/481558> [Accessed December 9, 2018].
- Shankar, J., Restrepo, A., Clemons, K. V., and Stevens, D. A. (2011). Hormones and the Resistance of Women to Paracoccidioidomycosis. *Clin. Microbiol. Rev.* 24, 296–313. doi:10.1128/CMR.00062-10.
- Shikanai-Yasuda, M. A., Mendes, R. P., Colombo, A. L., de Queiroz-Telles, F., Kono, A. S. G., Paniago, A. M. M., et al. (2017). Brazilian guidelines for the clinical management

- of paracoccidioidomycosis. *Rev. Soc. Bras. Med. Trop.* 50, 715–740. doi:10.1590/0037-8682-0230-2017.
- Shikanai-Yasuda, M. A., Telles Filho, F. D. Q., Mendes, R. P., Colombo, A. L., Moretti, M. L., Kono, A., et al. (2006). Consenso em paracoccidioidomicose. *Rev. Soc. Bras. Med. Trop.* 39, 297–310. doi:10.1590/S0037-86822006000300017.
- Shimizu, M., Fujii, T., Masuo, S., Fujita, K., and Takaya, N. (2009). Proteomic analysis of *Aspergillus nidulans* cultured under hypoxic conditions. *Proteomics* 9, 7–19. doi:10.1002/pmic.200701163.
- Silva, L. C., Neves, B. J., Gomes, M. N., Melo-Filho, C. C., Soares, C. M., Andrade, C. H., et al. (2018a). Computer-aided identification of novel anti-paracoccidioidomycosis compounds. *Future Microbiol.* 13, 1523–1535. doi:10.2217/fmb-2018-0175.
- Silva, L. do C., Tauhata, S. B. F., Baeza, L. C., Oliveira, C. M. A. de, Kato, L., Borges, C. L., et al. (2018b). Argentilactone Molecular Targets in *Paracoccidioides brasiliensis* Identified by Chemoproteomics. *Antimicrob. Agents Chemother.* 62, e00737-18. doi:10.1128/AAC.00737-18.
- Silvana dos Santos, S., Ferreira, K. S., and Almeida, S. R. (2011). *Paracoccidioides brasiliensis*-Induced Migration of Dendritic Cells and Subsequent T-Cell Activation in the Lung-Draining Lymph Nodes. *PLoS One* 6, e19690. doi:10.1371/journal.pone.0019690.
- Simmen, H. P., Battaglia, H., Giovanoli, P., and Blaser, J. (1994). Analysis of pH, pO₂ and pCO₂ in drainage fluid allows for rapid detection of infectious complications during the follow-up period after abdominal surgery. *Infection* 22, 386–9. Available at: <http://www.ncbi.nlm.nih.gov/pubmed/7698834> [Accessed March 7, 2018].
- Soares, C. M. A., Madlun, E. E. W. I. M., da Silva, S. P., Pereira, M., and Felipe, M. S. S. (1995). Characterization of *Paracoccidioides brasiliensis* isolates by random amplified polymorphic DNA analysis. *J. Clin. Microbiol.* 33, 505–507.
- Soares, C. M. D. A., Mendes-Giannini, M. J. S., Felipe, M. S. S., and Chaturvedi, V. (2008). A centennial: Discovery of *Paracoccidioides brasiliensis*. *Mycopathologia* 165, 179–181. doi:10.1007/s11046-008-9114-3.
- Splendore, A. (1912). *Zymonematosi* con localizzazione nella cavità della bocca, osservata in Brasile. *Bull. la Société Pathol. Exot.* 5, 313–319.
- Summons, R. E., Bradley, A. S., Jahnke, L. L., and Waldbauer, J. R. (2006). Steroids, triterpenoids and molecular oxygen. *Philos. Trans. R. Soc. Lond. B. Biol. Sci.* 361, 951–

68. doi:10.1098/rstb.2006.1837.
- Sylvestre, T. F., Cavalcante, R. de S., da Silva, J. de F., Paniago, A. M. M., Weber, S. S., Pauletti, B. A., et al. (2018a). Ceruloplasmin, transferrin and apolipoprotein A-II play important role in treatment's follow-up of paracoccidioidomycosis patients. *PLoS One* 13, e0206051. doi:10.1371/journal.pone.0206051.
- Sylvestre, T. F., Cavalcante, R. de S., da Silva, J. de F., Paniago, A. M. M., Weber, S. S., Pauletti, B. A., et al. (2018b). Serological proteomic biomarkers to identify *Paracoccidioides* species and risk of relapse. *PLoS One* 13, e0202804. doi:10.1371/journal.pone.0202804.
- Synnott, J. M., Guida, A., Mulhern-Haughey, S., Higgins, D. G., and Butler, G. (2010). Regulation of the Hypoxic Response in *Candida albicans*. *Eukaryot. Cell* 9, 1734–1746. doi:10.1128/EC.00159-10.
- Taborda, C. P., Nakaie, C. R., Cilli, E. M., Rodrigues, E. G., Silva, L. S., Franco, M. F., et al. (2004). Synthesis and Immunological Activity of a Branched Peptide Carrying the T-cell Epitope of gp43, the Major Exocellular Antigen of *Paracoccidioides brasiliensis*. *Scand. J. Immunol.* 59, 58–65. doi:10.1111/j.0300-9475.2004.01359.x.
- Tarrant, M. K., and Cole, P. A. (2009). The Chemical Biology of Protein Phosphorylation. *Annu. Rev. Biochem.* 78, 797–825. doi:10.1146/annurev.biochem.78.070907.103047.
- Taylor, C. T. (2008). Mitochondria and cellular oxygen sensing in the HIF pathway. *Biochem. J.* 409, 19–26. doi:10.1042/BJ20071249.
- Taylor, C. T., and McElwain, J. C. (2010). Ancient Atmospheres and the Evolution of Oxygen Sensing Via the Hypoxia-Inducible Factor in Metazoans. *Physiology* 25, 272–279. doi:10.1152/physiol.00029.2010.
- Teixeira, M. D. M., Theodoro, R. C., Oliveira, F. F. M. De, Machado, G. C., Hahn, R. C., Bagagli, E., et al. (2013). *Paracoccidioides lutzii* sp. nov.: biological and clinical implications. *Med. Mycol.* 52, 1–10. doi:10.3109/13693786.2013.794311.
- Teixeira, M. M., Theodoro, R. C., de Carvalho, M. J. A., Fernandes, L., Paes, H. C., Hahn, R. C., et al. (2009). Phylogenetic analysis reveals a high level of speciation in the *Paracoccidioides* genus. *Mol. Phylogenet. Evol.* 52, 273–283. doi:10.1016/j.ympev.2009.04.005.
- Teixeira, M. M., Theodoro, R. C., Nino-Vega, G., Bagagli, E., and Felipe, M. S. S. (2014). *Paracoccidioides* Species Complex: Ecology, Phylogeny, Sexual Reproduction, and Virulence. *PLoS Pathog.* 10. doi:10.1371/journal.ppat.1004397.

- Terçarioli, G. R., Bagagli, E., Reis, G. M., Theodoro, R. C., Bosco, S. D. M. G., Macoris, S. A. da G., et al. (2007). Ecological study of *Paracoccidioides brasiliensis* in soil: growth ability, conidia production and molecular detection. *BMC Microbiol.* 7, 92. doi:10.1186/1471-2180-7-92.
- Theodoro, R. C., Candeias, J. M. G., Araújo, J. P., Bosco, S. D. M. G., Macoris, S. A. D. G., Junior, L. O. P., et al. (2005). Molecular detection of *Paracoccidioides brasiliensis* in soil. *Med. Mycol.* 43, 725–729. doi:10.1080/13693780500129418.
- Theodoro, R. C., Teixeira, M. de M., Felipe, M. S. S., Paduan, K. dos S., Ribolla, P. M., San-Blas, G., et al. (2012). Genus *Paracoccidioides*: Species recognition and biogeographic aspects. *PLoS One* 7, e37694. doi:10.1371/journal.pone.0037694.
- Thingholm, T. E., Jensen, O. N., and Larsen, M. R. (2009). Analytical strategies for phosphoproteomics. *Proteomics* 9, 1451–1468. doi:10.1002/pmic.200800454.
- Todd, B. L., Stewart, E. V., Burg, J. S., Hughes, A. L., and Espenshade, P. J. (2006). Sterol Regulatory Element Binding Protein Is a Principal Regulator of Anaerobic Gene Expression in Fission Yeast. *Mol. Cell. Biol.* 26, 2817–2831. doi:10.1128/MCB.26.7.2817-2831.2006.
- Travassos, L. R., and Taborda, C. P. (2012). Paracoccidioidomycosis vaccine. *Hum. Vaccines Immunother.* 8, 1450–1453. doi:10.4161/hv.21283.
- Trejo-Chávez, A., Ramírez-Romero, R., Ancer-Rodríguez, J., Nevárez-Garza, A. M., and Rodríguez-Tovar, L. E. (2011). Disseminated Paracoccidioidomycosis in a Southern Two-Toed Sloth (*Choloepus didactylus*). *J. Comp. Pathol.* 144, 231–234. doi:10.1016/j.jcpa.2010.08.012.
- Turissini, D. A., Gomez, O. M., Teixeira, M. M., McEwen, J. G., and Matute, D. R. (2017). Species boundaries in the human pathogen *Paracoccidioides*. *Fungal Genet. Biol.* 106, 9–25. doi:10.1016/j.fgb.2017.05.007.
- Untereiner, W. A., Scott, J. A., Naveau, F. A., Sigler, L., Bachewich, J., and Angus, A. (2004). The *Ajellomycetaceae*, a new family of vertebrate-associated *Onygenales*. *Mycologia* 96, 812–821. doi:10.2307/3762114.
- Valle, A. C. F. de, Macedo, P. M. de, Almeida-Paes, R., Romão, A. R., Lazéra, M. dos S., and Wanke, B. (2017). Paracoccidioidomycosis after Highway Construction, Rio de Janeiro, Brazil. *Emerg. Infect. Dis.* 23, 1917–1919. doi:doi.org/10.3201/eid2311.170934.
- Vieira, G. de D., Alves, T. da C., Lima, S. M. D. de, Camargo, L. M. A., Sousa, C. M. de,

- Vieira, G. de D., et al. (2014). Paracoccidioidomycosis in a western Brazilian Amazon State: Clinical-epidemiologic profile and spatial distribution of the disease. *Rev. Soc. Bras. Med. Trop.* 47, 63–68. doi:10.1590/0037-8682-0225-2013.
- Vik A, and Rine, J. (2001). Upc2p and Ecm22p, dual regulators of sterol biosynthesis in *Saccharomyces cerevisiae*. *Mol. Cell. Biol.* 21, 6395–405. Available at: <http://www.ncbi.nlm.nih.gov/pubmed/11533229> [Accessed March 7, 2018].
- Vinogradov, S. N., Hoogewijs, D., Bailly, X., Mizuguchi, K., Dewilde, S., Moens, L., et al. (2007). A model of globin evolution. *Gene* 398, 132–142. doi:10.1016/j.gene.2007.02.041.
- Vödisch, M., Scherlach, K., Winkler, R., Hertweck, C., Braun, H.-P. P., Roth, M., et al. (2011). Analysis of the *Aspergillus fumigatus* proteome reveals metabolic changes and the activation of the pseurotin A biosynthesis gene cluster in response to hypoxia. *J. Proteome Res.* 10, 2508–2524. doi:10.1021/pr1012812.
- von Stechow, L. (2016). *Phospho-Proteomics Methods and Protocols*. Second. , ed. L. von Stechow New York: Springer doi:<https://doi.org/10.1007/978-1-4939-3049-4>.
- Wang, W., Wang, X., Liu, J., Ishii, M., Igarashi, Y., and Cui, Z. (2007). Effect of Oxygen Concentration on the Composting Process and Maturity. *Compost Sci. Util.* 15, 184–190. doi:10.1080/1065657X.2007.10702331.
- Willger, S. D., Cornish, E. J., Chung, D., Fleming, B. A., Lehmann, M. M., Puttikamonkul, S., et al. (2012). Dsc Orthologs Are Required for Hypoxia Adaptation, Triazole Drug Responses, and Fungal Virulence in *Aspergillus fumigatus*. *Eukaryot. Cell* 11, 1557–1567. doi:10.1128/EC.00252-12.
- Willger, S. D., Liu, Z., Olarte, R. A., Adamo, M. E., Stajich, J. E., Myers, L. C., et al. (2015). Analysis of the *Candida albicans* phosphoproteome. *Eukaryot. Cell* 14, 474–485. doi:10.1128/EC.00011-15.
- Willger, S. D., Puttikamonkul, S., Kim, K.-H., Burritt, J. B., Grahl, N., Metzler, L. J., et al. (2008). A sterol-regulatory element binding protein is required for cell polarity, hypoxia adaptation, azole drug resistance, and virulence in *Aspergillus fumigatus*. *PLoS Pathog.* 4, e1000200. doi:10.1371/journal.ppat.1000200.
- Wilson-Grady, J. T., Villén, J., and Gygi, S. P. (2008). Phosphoproteome Analysis of Fission Yeast. *J. Proteome Res.* 7, 1088–1097. doi:10.1021/pr7006335.
- Zarembor, K. A., and Malech, H. L. (2005). HIF-1 : a master regulator of innate host defenses? *J. Clin. Invest.* 115, 1702–1704. doi:10.1172/JCI25740.

Zhang, W., and Phillips, G. N. (2003). Structure of the oxygen sensor in *Bacillus subtilis*: Signal transduction of chemotaxis by control of symmetry. *Structure* 11, 1097–1110. doi:10.1016/S0969-2126(03)00169-2.

Capítulo V

9. PRODUÇÕES

Oliveira, L. N., Casaletti, L., Bão, S. N., Borges, C. L., de Sousa Lima, P., and de Almeida Soares, C. M. (2016). Characterizing the nuclear proteome of *Paracoccidioides* spp. *Fungal Biol.* 120, 1209–1224. doi:10.1016/j.funbio.2016.07.003.



Characterizing the nuclear proteome of *Paracoccidioides* spp.



Lucas Nojosa OLIVEIRA^a, Luciana CASALETTI^{a,b}, Sônia Nair BÃO^c, Clayton Luiz BORGES^a, Patrícia DE SOUSA LIMA^a, Célia Maria DE ALMEIDA SOARES^{a,*}

^aLaboratório de Biologia Molecular, Instituto de Ciências Biológicas, ICB II, Campus II, Universidade Federal de Goiás, Goiânia, Goiás, 74690-900, Brazil

^bEscola de Engenharia, Pontifícia Universidade Católica de Goiás, Goiânia, Goiás, 74605-010, Brazil

^cLaboratório de Microscopia, Departamento de Biologia Celular, Instituto de Ciências Biológicas, Universidade de Brasília, Brasília, Distrito Federal, 70910-900, Brazil

ARTICLE INFO

Article history:

Received 29 February 2016

Received in revised form

5 July 2016

Accepted 7 July 2016

Available online 17 July 2016

Corresponding Editor:

Steven Bates

Keywords:

Bioinformatic analysis

Cell biology

MS^a proteomics

Nuclear proteins and

paracoccidioidomycosis

ABSTRACT

Paracoccidioidomycosis is an endemic disease in Latin America, caused by thermo dimorphic fungi of the genus *Paracoccidioides*. Although previous proteome analyses of *Paracoccidioides* spp. have been carried out, the nuclear subproteome of this pathogen has not been described. In this way, we aimed to characterize the nuclear proteome of *Paracoccidioides* species, in the yeast form. For that, yeast cells were disrupted and submitted to cell fractionation. The purity of the nuclear fraction was confirmed by fluorescence and electron microscopy. Liquid chromatography coupled to tandem mass spectrometry (LC-MS/MS) allowed the identification of 867 proteins. In order to support our enrichment method for nuclear proteins, bioinformatics analysis were applied that allowed the identification of 281 proteins with nuclear localization. This analysis revealed proteins related to DNA maintenance, gene expression, synthesis and processing of messenger and ribosomal RNAs, likewise proteins of nuclear-cytoplasmic traffic. It was also possible to detect some proteins that are poorly expressed, like transcription factors involved in important roles such as resistance to abiotic stress, sporulation, cellular growth and DNA and chromatin maintenance. This is the first descriptive nuclear proteome of *Paracoccidioides* spp. that can be useful as an important platform base for fungi-specific nuclear processes.

© 2016 British Mycological Society. Published by Elsevier Ltd. All rights reserved.

* Corresponding author. Laboratório de Biologia Molecular, Instituto de Ciências Biológicas II, Campus Samambaia, Universidade Federal de Goiás, 74690-900, Goiânia, Goiás, Brazil. Tel./fax: +55 62 3521 1110.

E-mail address: cmsoares@gmail.com (C. M. de Almeida Soares).

<http://dx.doi.org/10.1016/j.funbio.2016.07.003>

1878-6146/© 2016 British Mycological Society. Published by Elsevier Ltd. All rights reserved.

Casaletti, L., Lima, P. de S., Oliveira, L. N., Borges, C. L., Bá, S. N., Bailão, A. M., et al. (2017). Analysis of *Paracoccidioides lutzii* mitochondria: a proteomic approach. *Yeast* 34, 179–188. doi:10.1002/yea.3225



Yeast

Yeast 2017; 34: 179–188.

Published online 26 January 2017 in Wiley Online Library
(wileyonlinelibrary.com) DOI: 10.1002/yea.3225

Research Article

Analysis of *Paracoccidioides lutzii* mitochondria: a proteomic approach

L. Casaletti^{1,2}, P. S. Lima¹, L. N. Oliveira^{1,3}, C. L. Borges¹, S. N. Bá⁴, A. M. Bailão¹ and C. M. A. Soares^{1,*}

¹Laboratório de Biologia Molecular, Instituto de Ciências Biológicas, ICB, Campus II, Universidade Federal de Goiás, 74001-970, Goiânia, Goiás, Brazil

²Escola de Engenharia, Pontifícia Universidade Católica de Goiás, 74605-010, Goiânia, Goiás, Brazil

³Programa de Pós-graduação em Patologia Molecular, Faculdade de Medicina, Universidade de Brasília, 70910-900, Brasília, Distrito Federal, Brazil

⁴Laboratório de Microscopia, Departamento de Biologia Celular, Instituto de Ciências Biológicas, Universidade de Brasília, 70910-900, Brasília, Distrito Federal, Brazil

*Correspondence to: C. M. A. Soares, Laboratório de Biologia Molecular, Instituto de Ciências Biológicas, ICB, Campus II, Universidade Federal de Goiás, 74001-970 Goiânia, Goiás, Brazil.
E-mail: cmasoares@gmail.com

Abstract

The genus *Paracoccidioides* is composed of thermal dimorphic fungi, causative agents of paracoccidioidomycosis, one of the most frequent systemic mycoses in Latin America. Mitochondria have sophisticated machinery for ATP production, which involves metabolic pathways such as citric acid and glyoxylate cycles, electron transport chain and oxidative phosphorylation. In addition, this organelle performs a variety of functions in the cell, working as an exceptional metabolic signalling centre that contributes to cellular stress responses, as autophagy and apoptosis in eukaryotic organisms. The aim of this work was to perform a descriptive proteomic analysis of mitochondria in *Paracoccidioides lutzii* yeast cells. After mitochondria fractionation, samples enriched in mitochondrial proteins were digested with trypsin and analysed using a NanoUPLC-MS^E system (Waters Corporation, Manchester, UK). Our results revealed that the established protocol for purification of mitochondria was very effective for *P. lutzii*, and 298 proteins were identified as primarily mitochondrial, in our analysis. To our knowledge, this is the first compilation of mitochondrial proteins from *P. lutzii*, to date. Copyright © 2016 John Wiley & Sons, Ltd.

Keywords: mitochondrial proteome; MS^E proteomics; metabolism and energy production; *Paracoccidioides lutzii*

Received: 27 June 2016
Accepted: 20 November 2016

Introduction

Mitochondria perform a variety of functions, not only the unquestionable production of ATP, which involves metabolic pathways such as citric acid and glyoxylate cycles, electron transport chain and oxidative phosphorylation, but they are also exceptional metabolic signalling centres that contribute to cellular stress responses, as autophagy and apoptosis in eukaryotic organisms (Nunnari and Suomalainen, 2012). Mitochondria also play important roles in various cellular processes including amino acid, lipid and iron metabolism (Lill and Kispal, 2000).

Morphologically, mitochondria are highly dynamic organelles that form interconnected membrane networks, whose biogenesis and structure are highly influenced by the needs of the cell (Lackner, 2014). For example, in the best-characterized fungus, *Saccharomyces cerevisiae*, mitochondria form long filaments creating a branched tubular network within the cell, although this network dismantles as the culture progresses (Chimi *et al.*, 2013; Volejnikova *et al.*, 2013). These morphological changes positively indicate that series of proteins must be expressed in a much-regulated fashion. As predicted, this was confirmed by proteomic analysis of yeast

Oliveira, A. R. de, Oliveira, L. N., Chaves, E. G. A., Weber, S. S., Bailão, A. M., Parente-Rocha, J. A., et al. (2018). Characterization of extracellular proteins in members of the *Paracoccidioides* complex. *Fungal Biol.* 122, 738–751. doi:10.1016/j.funbio.2018.04.001.

Fungal Biology 122 (2018) 738–751



Contents lists available at ScienceDirect

Fungal Biology

journal homepage: www.elsevier.com/locate/funbio



Characterization of extracellular proteins in members of the *Paracoccidioides* complex



Amanda Rodrigues de Oliveira ^{a,1}, Lucas Nojosa Oliveira ^{a,b,1},
Edilânia Gomes Araújo Chaves ^a, Simone Schneider Weber ^{c,d}, Alexandre Melo Bailão ^a,
Juliana Alves Parente-Rocha ^a, Lilian Cristiane Baeza ^a, Célia Maria de Almeida Soares ^a,
Clayton Luiz Borges ^{a,*}

^a Laboratório de Biologia Molecular, Instituto de Ciências Biológicas, Universidade Federal de Goiás, Goiânia, Goiás, Brazil

^b Programa de Pós-graduação em Patobiologia Molecular, Faculdade de Medicina, Universidade de Brasília, Brasília, Distrito Federal, Brazil

^c Instituto de Ciências Exatas e Tecnologia, Universidade Federal do Amazonas, Itacoatiara, Amazonas, Brazil

^d Faculdade de Ciências Farmacêuticas, Alimentos e Nutrição, Universidade Federal do Mato Grosso do Sul, Campo Grande, Mato Grosso do Sul, Brazil

ARTICLE INFO

Article history:
Received 24 November 2017
Received in revised form
11 March 2018
Accepted 3 April 2018
Available online 11 April 2018

Corresponding Editor: Steven Bates

Keywords:
Label-free proteomics
Macrophage infection
Paracoccidioides species
Secretome
Virulence factors

ABSTRACT

Paracoccidioides is a thermodimorphic fungus that causes Paracoccidioidomycosis (PCM) – an endemic systemic mycosis in Latin America. The genus comprises several phylogenetic species which present some genetic and serological differences. The diversity presented among isolates of the same genus has been explored in several microorganisms. There have also been attempts to clarify differences that might be related to virulence existing in isolates that cause the same disease. In this work, we analyzed the secretome of two isolates in the *Paracoccidioides* genus, isolates Pb01 and PbEpm83, and performed infection assays in macrophages to evaluate the influence of the secretomes of those isolates upon an *in vitro* model of infection. The use of a label-free proteomics approach (LC-MS²) allowed us to identify 92 proteins that are secreted by those strains. Of those proteins, 35 were differentially secreted in Pb01, and 36 in PbEpm83. According to the functional annotation, most of the identified proteins are related to adhesion and virulence processes. These results provide evidence that different members of the *Paracoccidioides* complex can quantitatively secrete different proteins, which may influence the characteristics of virulence, as well as host-related processes.

© 2018 British Mycological Society. Published by Elsevier Ltd. All rights reserved.

1. Introduction

Fungi of the *Paracoccidioides* genus are the causative agents of paracoccidioidomycosis (PCM) – a prevalent systemic mycosis in Latin America (Restrepo and Tobon, 2005). These fungi present thermal dimorphism, growing in the environment as mycelium, the saprobic form, in temperatures below 28 °C, and as yeast cells at 36 °C in human host tissues (Restrepo, 1985). The mycelia form produces conidia that act as infectious propagules, which, when inhaled, suffer dimorphic transition in the lungs, resulting in the pathogenic yeast form (Brummer et al., 1993; Borges-Walmsley

et al., 2002). The disease evolution and the manifestation of clinical forms depend on immunological factors (Franco et al., 1987), the virulence levels of the fungus isolates (San-Blas and Niño-Vega, 2001), and the host gender (Restrepo et al., 1984).

The *Paracoccidioides* genus is currently subdivided into five species, namely *Paracoccidioides lutzii*, *Paracoccidioides brasiliensis*, *Paracoccidioides americana*, *Paracoccidioides restrepensis* and *Paracoccidioides venezuelensis* (Turissini et al., 2017), based on genotypic studies and geographic distribution. Diversity presented among isolates of the same genus has been explored with regard to various microorganisms, including *Paracoccidioides*. These studies have used various approaches in an attempt to characterize biochemical and molecular differences that can reflect on the virulence of isolates that cause the same disease (Kurokawa et al., 2005; Carvalho et al., 2005; Pigozzo et al., 2013; Siqueira et al., 2016).

Many of the virulence factors of medically-important pathogenic fungi are related to extracellular proteins. These act on the

* Corresponding author. Laboratório de Biologia Molecular, Instituto de Ciências Biológicas II, Universidade Federal de Goiás, Campus II, 74900-000, Goiânia, Goiás, Brazil. Fax: +55 62 3521 1110.

E-mail address: cibluz2@gmail.com (C.L. Borges).

¹ These authors have contributed equally to this work.

Insights of hypoxia-responsive genes in *Paracoccidioides* species: a genome analysis

Lucas Nojosa Oliveira^{a,b}, Santiago Aguiar Espellet Soares^a, Danielle Silva Araújo^{a,b}, Marielle Garcia Silva^{a,b}, Juliana Santana De Curcio^{a,b}, Célia Maria de Almeida Soares^{a,*}

^aLaboratório de Biologia Molecular, Instituto de Ciências Biológicas, ICB II, Campus II,
Universidade Federal de Goiás, Goiânia, Goiás, Brazil;

^bPrograma de Pós-graduação em Patologia Molecular, Faculdade de Medicina, Universidade
de Brasília, 70910-900, Brasília, Distrito Federal, Brazil;

*Corresponding author

Célia Maria de Almeida Soares
Laboratório de Biologia Molecular
Instituto de Ciências Biológicas II
Câmpus Samambaia
Universidade Federal de Goiás
74690-900, Goiânia, Goiás – Brazil
Tel/Fax: +55 62 3521 1110
E-mail address: cmasoares@gmail.com

Unveiling protein-protein interactions related to oxygen limitation in *Paracoccidioides brasiliensis*

Lucas Nojosa Oliveira^{a,b,†}, Kleber Santiago Freitas e Silva^{a,†}, Marielle Garcia Silva^{a,b}, Lilian Cristiane Baeza^{a,c}, Maristela Pereira^a, Célia Maria de Almeida Soares^{a,*}

^aLaboratório de Biologia Molecular, Instituto de Ciências Biológicas, ICB II, Campus II,
Universidade Federal de Goiás, Goiânia, Goiás, Brazil;

^bPrograma de Pós-graduação em Patologia Molecular, Faculdade de Medicina, Universidade
de Brasília, 70910-900, Brasília, Distrito Federal, Brazil;

^cCentro de Ciências Médicas e Farmacêuticas, Universidade Estadual do Oeste do Paraná,
Cascavel, Brazil.

[†]These authors have contributed equally to this work.

*Corresponding author

Célia Maria de Almeida Soares
Laboratório de Biologia Molecular
Instituto de Ciências Biológicas II
Câmpus Samambaia
Universidade Federal de Goiás
74690-900, Goiânia, Goiás – Brazil
Tel/Fax: +55 62 3521 1110
E-mail address: cmasoares@gmail.com

Key-words: hypoxia, BN-PAGE,

Analysis of the siderophores biosynthesis pathway in *Paracoccidioides* sp.

Marielle Garcia Silva^{a,b}, Lucas Nojosa Oliveira^{a,b}, Mirelle Garcia Silva Bailão^a, Aparecido Ferreira de Souza^a, Raisa Melo de Lima^a, Sônia Nair Báo^c, Maristela Pereira^a, Alexandre Melo Bailão^a, Célia Maria de Almeida Soares^{a,*}

^aLaboratório de Biologia Molecular, Instituto de Ciências Biológicas, ICB II, Campus II, Universidade Federal de Goiás, Goiânia, Goiás, Brazil;

^bPrograma de Pós-graduação em Patologia Molecular, Faculdade de Medicina, Universidade de Brasília, 70910-900, Brasília, Distrito Federal, Brazil;

^cLaboratório do Microscopia, Departamento de Biologia Celular, Instituto de Ciências Biológicas, Universidade de Brasília, Brasília, Distrito Federal, Brazil

*Corresponding author

Célia Maria de Almeida Soares
Laboratório de Biologia Molecular
Instituto de Ciências Biológicas II
Câmpus Samambaia
Universidade Federal de Goiás
74690-900, Goiânia, Goiás – Brazil
Tel/Fax: +55 62 3521 1110
E-mail address: cmasoares@gmail.com

Key-words: Iron, siderophore, FOB, *Paracoccidioides* sp.

Proteomic analysis of *Paracoccidioides lutzii* upon copper overload reveals metabolic changes and melanization induction

Igor Godinho Portis¹; Patrícia de Sousa Lima^{1, 2}; Rodrigo de Almeida Paes³; Lucas Nojosa Oliveira^{1,4}; Juliana Alves Parente Rocha¹; Joshua D. Nosanchuk⁵; Célia Maria de Almeida Soares¹.

1 – Laboratório de Biologia Molecular, Instituto de Ciências Biológicas II, Campus II, Universidade Federal de Goiás, Goiânia, Goiás, Brazil.

2 – Laboratório Interdisciplinar de Biologia, Universidade Estadual de Goiás, Itapuranga, Goiás, Brazil.

3 – Serviço de Micologia, Instituto de Pesquisa Clínica Evandro Chagas (IPEC), Fundação Oswaldo Cruz, Rio de Janeiro, RJ, Brazil.

4 – Programa de Pós-graduação em Patologia Molecular, Faculdade de Medicina, Universidade de Brasília, 70910-900, Brasília, Distrito Federal, Brazil.

5 – Department of Medicine, Albert Einstein College of Medicine, New York City, NY, USA.

*Corresponding author

Célia Maria de Almeida Soares

Laboratório de Biologia Molecular

Instituto de Ciências Biológicas II

Câmpus Samambaia, s/n

Universidade Federal de Goiás

74690-900, Goiânia, Goiás – Brazil

Tel/Fax: +55 62 3521 1110

E-mail address: cmasoares@gmail.comkl.l.nnnnnbby